(12) INTERNATIONAL APPLICATION PUBLISHED UNDER THE PATENT COOPERATION TREATY (PCT)

(19) World Intellectual Property Organization
International Bureau

(43) International Publication Date
18 May 2007 (18.05.2007)

PCT

(10) International Publication Number
WO 2007/056560 A2

(51) International Patent Classification:
C12Q 1/00 (2006.01) *G06F 19/00* (2006.01)
C12Q 1/70 (2006.01) *G01J 3/44* (2006.01)
C12Q 1/68 (2006.01)

(21) International Application Number:
PCT/US2006/043755

(22) International Filing Date:
9 November 2006 (09.11.2006)

(25) Filing Language: English

(26) Publication Language: English

(30) Priority Data:
60/735,062 9 November 2005 (09.11.2005) US
11/269,596 9 November 2005 (09.11.2005) US

(71) Applicant *(for all designated States except US)*: **CHEMIMAGE CORPORATION** [US/US]; 7301 Market Street, Pittsburgh, PA 15208 (US).

(72) Inventors; and

(75) Inventors/Applicants *(for US only)*: **MAIER, John, S.** [US/US]; 622 S. Lang Avenue, Pittsburgh, PA 15208 (US). **COHEN, Jeffrey** [US/US]; 5815 Wilkins Avenue, Pittsburgh, PA 15217 (US). **McCLELLAND, Lindy** [US/US]; 120 Weldon Street, Apt. #2, Rochester, NY 14611 (US). **STEWART, Shona** [US/US]; 357 Stratford Avenue, Apt. #1, Pittsburgh, PA 15232 (US).

(74) Agent: **GOLUB, Daniel, H.**; 1701 Market Street, Philadelphia, PA 19103 (US).

(81) Designated States *(unless otherwise indicated, for every kind of national protection available)*: AE, AG, AL, AM, AT, AU, AZ, BA, BB, BG, BR, BW, BY, BZ, CA, CH, CN, CO, CR, CU, CZ, DE, DK, DM, DZ, EC, EE, EG, ES, FI, GB, GD, GE, GH, GM, GT, HN, HR, HU, ID, IL, IN, IS, JP, KE, KG, KM, KN, KP, KR, KZ, LA, LC, LK, LR, LS, LT, LU, LV, LY, MA, MD, MG, MK, MN, MW, MX, MY, MZ, NA, NG, NI, NO, NZ, OM, PG, PH, PL, PT, RO, RS, RU, SC, SD, SE, SG, SK, SL, SM, SV, SY, TJ, TM, TN, TR, TT, TZ, UA, UG, US, UZ, VC, VN, ZA, ZM, ZW.

(84) Designated States *(unless otherwise indicated, for every kind of regional protection available)*: ARIPO (BW, GH, GM, KE, LS, MW, MZ, NA, SD, SL, SZ, TZ, UG, ZM, ZW), Eurasian (AM, AZ, BY, KG, KZ, MD, RU, TJ, TM), European (AT, BE, BG, CH, CY, CZ, DE, DK, EE, ES, FI, FR, GB, GR, HU, IE, IS, IT, LT, LU, LV, MC, NL, PL, PT, RO, SE, SI, SK, TR), OAPI (BF, BJ, CF, CG, CI, CM, GA, GN, GQ, GW, ML, MR, NE, SN, TD, TG).

Published:
— *without international search report and to be republished upon receipt of that report*

For two-letter codes and other abbreviations, refer to the "Guidance Notes on Codes and Abbreviations" appearing at the beginning of each regular issue of the PCT Gazette.

(54) **Title:** SYSTEM AND METHOD FOR CYTOLOGICAL ANALYSIS BY RAMAN SPECTROSCOPIC IMAGING

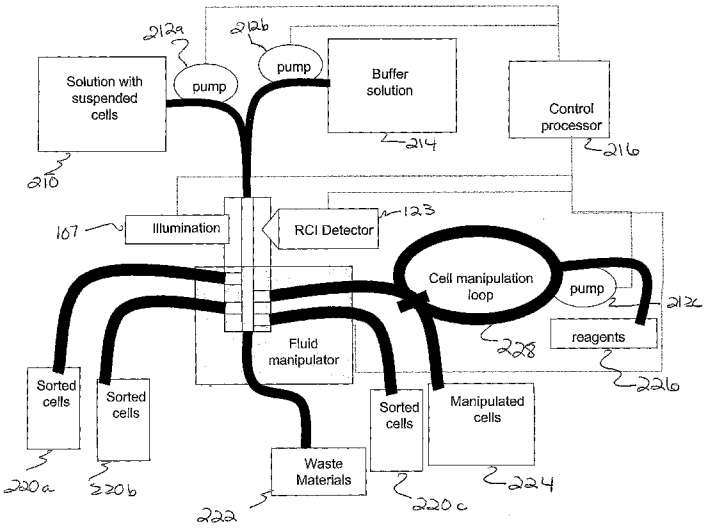

(57) **Abstract:** A method and system of differentially manipulating cells where the cells, suspended in a fluid, are irradiated with substantially monochromatic light. A Raman data set is obtained from the irradiated cells and where the data set is characteristic of a disease status. The data set is assessed to identify diseased cells. A Raman chemical image of the irradiated cells is also obtained. Based on the assessment and the Raman chemical image, the fluid in which the cells are suspended is differentially manipulated. The diseased cells are directed to a first location and other non-diseased cells are directed to a second location as part of the differential manipulation. The diseased cells may be treated with a physical stress, a chemical stress, and a iological stress and then returned to a patient from whom the diseased cells were obtained prior to the irradiation.

WO 2007/056560 A2

SYSTEM AND METHOD FOR CYTOLOGICAL ANALYSIS BY RAMAN SPECTROSCOPIC IMAGING

RELATED APPLICATIONS

This application claims the benefit of U.S. Provisional Appl. No. 60/735,062, filed November 9, 2005, entitled "Cytological Analysis by Raman Spectroscopic Imaging" which is incorporated herein by reference in its entirety. This application is also a continuation-in-part of U.S. Patent Appl. No. 11/269,596, filed November 9, 2005, entitled "Cytological Methods for Detecting a Disease Condition Such as Malignancy By Raman Spectroscopic Imaging" which is incorporated herein by reference in its entirety.

FIELD OF THE DISCLOSURE

This application generally relates to cytological analysis, immunization, modification and treatment of diseased cells enabled by the use of Raman spectroscopic techniques.

BACKGROUND OF THE DISCLOSURE

The disclosure relates generally to the field of mammalian cellular evaluation and to correlation of cellular physiological status and diagnosis of disease based on such evaluation. In one embodiment the disclosure relates to methods for facilitating the detection of disease conditions by detection methods that use Raman molecular imaging (RMI). In an exemplary embodiment the disclosure provides Raman spectroscopic methods of detecting malignant conditions, for example bladder cancer.

Cells are a basic unit of life. The body of an individual human is made up of many trillions of cells, the overwhelming majority of which have differentiated to form tissues and cell populations of various discrete types. Cells in a healthy human often exhibit physical and biochemical features that are characteristic of the discrete cell or tissue type. Such features can include the size and shape of the cell, its motility, its mitotic status, its ability to interact with certain chemical or immunological reagents, and other observable characteristics.

The field of cytology involves microscopic analysis of cells to evaluate their structure, function, formation, origin, biochemical activities, pathology, and other characteristics. Known cytological techniques include fluorescent and visible light microscopic methods, alone or in conjunction with use of various staining reagents (e.g., hemotoxylin and eosin stains), labeling reagents (e.g., fluorophore-tagged antibodies), or combinations thereof.

Cytological analyses are most commonly performed on cells obtained from samples removed from the body of a mammal. In vivo cytological methods are often impractical owing, for example, to relative inaccessibility of the cells of interest and unsuitability of staining or labeling reagents for in vivo use. Cells are commonly obtained for cytological analysis by a variety of methods. By way of examples, cells can be obtained from a fluid that contacts a tissue of interest, such as a natural bodily fluid (e.g., blood, urine, lymph, sputum, peritoneal fluid, pleural fluid, or semen) or a fluid that is introduced into a body cavity and subsequently withdrawn (e.g., bronchial lavage, oral rinse, or peritoneal wash fluids). Cells can also be obtained by scraping or biopsying a tissue of interest. Cells obtained in one of these ways can be washed, mounted, stained, or otherwise treated to yield useful information prior to microscopic analysis.

Information obtained from cytological analysis can be used to characterize the status of one or more cells in a sample. By way of example, the size, shape, and approximate number and proportions of cell types observed in a blood sample can yield information about a variety of diseases and other physiological states of the patient from whom the blood was obtained. Information obtained from other cell types can also reveal the disease or other physiological status of particular cells and tissues in a patient.

Some diseases are caused by exogenous infectious or chemical agents which induce adverse cellular effects when the agents are contacted with cells in the body. Other diseases (e.g., diseases wholly or partially of hereditary origin, such as sickle cell anemia) can arise in the absence of harmful exogenous agents. Some disease states are readily discernable from cytological analysis, such as diseases in which cells assume a characteristic shape or reactivity and disease in which an infectious agent can be observed in an infected tissue. However, other disease states (including many physiological states which precede or indicate a predisposition to develop a disease state) cannot be readily detected by ordinary cytological methods.

A further shortcoming of many cytological methods is that, even when cytological identification of a disease state is possible, the time, expense, and expertise necessary to perform the cytological analysis can make it impractical or impossible to perform that analysis. Some cytological methods rely on qualitative judgments made by a cytologist, and those judgments can vary among cytologist, conferring subjectivity to the analysis. In many instances, objective analyses would be preferable.

The apparatus and methods described herein overcome many of the shortcomings of known cytological methods and complement many of the advantages of such methods.

Cancer Diagnosis

Cancer is the second leading cause of death in the United States, with more than 1.2 million new cancers being diagnosed annually. Cancer is significant, not only in terms of mortality and morbidity, but also in terms of the cost of treating advanced cancers and the reduced productivity and quality of life achieved by advanced cancer patients. Despite the common conception of cancers as incurable diseases, many cancers can be alleviated, slowed, or even cured if timely medical intervention can be administered. A widely recognized need exists for tools and methods for early detection of cancer.

Cancers arise by a variety of mechanisms, not all of which are well understood, from evidently normal tissue. Cancers, called tumors when they arise in the form of a solid mass, characteristically exhibit decontrolled growth and/or proliferation of cells. Cancer cells often exhibit other characteristic differences relative to the cell type from which they arise, including altered expression of cell surface, secreted, nuclear, and/or cytoplasmic proteins, altered antigenicity, altered lipid envelope (i.e., cell membrane) composition, altered production of nucleic acids, altered morphology, and other differences. Typically, cancers are diagnosed either by observation of tumor formation or by observation of one or more of these characteristic differences. Because cancers arise from cells of normal tissues, cancer cells usually initially closely resemble the cells of the original normal tissue, often making detection of cancer cells difficult until the cancer has progressed to a stage at which the differences between cancer cells and the corresponding original normal cells are more pronounced. Depending on the type of cancer, the cancer can have advanced to a relatively difficult-to-treat stage before it is easily detectable.

Early definitive detection and classification of cancer is often crucial to successful treatment. Diagnosis of cancer must precede cancer treatment. Included in the diagnosis of many cancers is determination of the type and grade of the cancer and the stage of its progression. This information can inform treatment selection, allowing use of milder treatments (i.e., having fewer undesirable side effects) for relatively early-stage, non- or slowly-spreading cancers and more aggressive treatment (i.e., having more undesirable side effects and/or a lower therapeutic index) of cancers that pose a greater risk to the patient's health.

When cancer is suspected, a physician will often have the tumor or a section of tissue having one or more abnormal characteristics removed or biopsied and sent for histopathological analyses. Typically, the time taken to prepare the specimen is on the order of one day or more. Communication of results from the pathologist to the physician and to the patient can further slow the diagnosis of the cancer and the onset of any indicated treatment. Patient anxiety can soar during the period between sample collection and diagnosis.

A recognized need exists to shorten the time required to analyze cells in order to determine whether or not the cells indicate the presence of cancer. Furthermore, it would be beneficial to reduce the number and/or volume of cells required for such determination, in order to minimize patient discomfort and improve patient acceptance of biopsy.

Although certain immunohistology techniques can be performed without the need for microscopic visualization of cells, almost all histopathological analysis of suspected cancer cells and tissues involves microscopic examination of the suspect cells or tissue. Optical microscopy techniques are most common, owing to their relative simplicity and the wealth of information that can be obtained by visual examination of cells and tissues.

A suspension of cells (e.g., cells in urine, blood, sputum, semen, or a peritoneal or bronchial lavage) can be visually examined, with or without staining the suspended cells. A tissue biopsy obtained from a patient can be directly observed; stained and observed; embedded, sectioned, stained, and observed; or some combination of these.

In order to diagnose cancer, the cell or tissue preparation is analyzed by a trained pathologist who can differentiate between normal cells and malignant or benign cancer cells based on cellular morphology, tissue structure, staining characteristics, or some combination of these. Because of the tissue preparation required, this process is relatively slow. Moreover, the differentiation made by the pathologist is based on subtle morphological and other differences among normal, malignant, and benign cells, and such subtle differences can be difficult or time-consuming to detect, even for highly experienced pathologists. Such differences are even more difficult for relatively inexperienced pathologists to detect.

Clinicians typically classify cancer lesions by assigning a grade and a stage to the lesion after superficial examination of the lesion and microscopic analysis of a biopsy taken from the lesioned tissue or organ. Grading and staging of cancers is performed by analyzing

the bodily location, morphology, and extent of tissue invasion of cancer cells. The definitions of the various grades and stages of tumors vary with the type of cancer.

Grade describes the aggressiveness of the tumor cells, referring to their growth rate and likelihood of invading surrounding or distant (i.e., by metastasis) tissues. Grading is determined by microscopic analysis of tumor cells, whereby a pathologist examines how differentiated the tumor cells are from normal (non-tumorous) tissues of the same type. Tumors that resemble the corresponding normal tissue (i.e., low grade tumors) tend to grow and spread relatively slowly. In contrast, high grade tumors (i.e., those which do not resemble the corresponding normal tissue) tend to grow and spread more quickly. Patient survival is also correlated with cancer grade, higher grade corresponding to lower likelihood of survival. There are multiple systems for describing the grade of a tumor. Common systems rely on a three- or four-point grading system, the higher numbers referring to higher cancer grade. The grading system used is indicated in the grade designation, for example "I/III" referring to grade I on a three point scale and "II/IV" referring to grade II on a four-point scale. Stage describes the anatomical progression of a tumor. A variety of staging systems have been described for various tumor types.

The apparatus and methods described herein can be used to enhance or replace current cancer diagnostic methods.

Sickle Cell Trait

Red blood cells (RBCs) transport oxygen through the bloodstream from the lungs to other tissues in the body. The oxygen is bound to a protein called hemoglobin, which normally exists in the form of a tetramer of protein subunits. The bodies of some individuals are capable of making both normal and altered hemoglobin protein subunits. The altered hemoglobin subunits confer to hemoglobin that trait that, under certain circumstances, hemoglobin can polymerize. When hemoglobin polymerizes, the normal disk shape of RBCs is distorted such that RBCs take on a curved, elongated ("sickle") shape. Sickle-shaped RBCs are not able to pass through narrow blood vessels as easily as normal RBCs. As a result, sickle RBCs can obstruct blood flow, causing damage to blood vessels and tissues that depend on those vessels for oxygen and nourishment.

The adverse effects of sickle RBCs are often not noticed until significant tissue damage has been done. Furthermore, individuals who make both normal and altered hemoglobin are often not identified, because they suffer few or no adverse effects. Children

of two individuals, each of whom makes both normal and altered hemoglobin are at increased risk for sickle cell diseases such as sickle cell anemia, thalassemia, stroke, and damage to multiple organs. It is useful to identify individuals who make both normal and altered hemoglobin so that those individuals can make informed decisions regarding childbearing.

Currently, electrophoretic techniques are used to identify individuals who make altered forms of hemoglobin. Nucleic acid-based tests can also be used to diagnose individuals. However, once an individual has been diagnosed with sickle cell disease or as a carrier of the sickle cell trait, medical interventions are limited. Administration of hydroxyurea, for example, can enhance production of a fetal form of hemoglobin that inhibits RBC sickling. A method of identifying abnormal RBCs prior to sickling can identify individuals at risk for developing sickle cell disease or passing the sickle cell trait. Cytological methods for identifying RBCs expressing altered forms of hemoglobin can also permit treatment and/or manipulation of individual RBCs. Apparatus and methods of using them for these purposes are disclosed herein.

Heart Diseases

The heart pumps blood throughout the body and is responsible for providing oxygen and nourishment to substantially all tissues. Cardiac muscle cells of the heart can be adversely affected by a variety of disease states including, for example angina; coronary artery disease and atherosclerosis; inflammatory diseases; neoplasia; viral, bacterial, protozoan, and parasitic infections; cardiac insufficiency and failure; inherited myopathies; and myocardial deterioration attributable to mineral deficiency. Because cardiac muscle tissue is not easily accessible, the effects of these disease states on cardiac muscle tissue cannot be easily observed. For this reason, diagnostic methods which rely on observations of cardiac muscle tissue have not been widely used.

Apparatus and methods useful for direct analysis of cardiac muscle tissue would hasten and simplify diagnosis of heart disease states and permit earlier and more efficacious treatment. Apparatus and methods of using them for these purposes are disclosed herein.

Raman Spectroscopy

Raman spectroscopy provides information about the vibrational state of molecules. Many molecules have atomic bonds capable of existing in a number of vibrational states. Such molecules are able to absorb incident radiation that matches a transition between two

of its allowed vibrational states and to subsequently emit the radiation. Most often, absorbed radiation is re-radiated at the same wavelength, a process designated Rayleigh or elastic scattering. In some instances, the re-radiated radiation can contain slightly more or slightly less energy than the absorbed radiation (depending on the allowable vibrational states and the initial and final vibrational states of the molecule). The result of the energy difference between the incident and re-radiated radiation is manifested as a shift in the wavelength between the incident and re-radiated radiation, and the degree of difference is designated the Raman shift (RS), measured in units of wavenumber (inverse length). If the incident light is substantially monochromatic (single wavelength) as it is when using a laser source, the scattered light which differs in wavelength from the incident light can be more easily distinguished from the Rayleigh scattered light.

Because Raman spectroscopy is based on irradiation of a sample and detection of scattered radiation, it can be employed non-invasively or to analyze biological samples in situ. Thus, little or no sample preparation is required. In addition, water exhibits very little Raman scattering, and Raman spectroscopy techniques can be readily performed in aqueous environments.

Others have performed Raman spectroscopic analysis of biological tissues. Descriptions of such analyses can be found in the following publications: Petrich, 2001, Appl. Spectrosc. Rev. 36:181; Naumann, 2001, Appl. Spectrosc. Rev. 36:239; Manoharan et al., 1998, Photochem. Photobiol. 67:15; Frank et al., 1995, Anal. Chem. 67:777; Redd et al., 1993, Appl. Spectrosc. 47:787; Haka et al., 2002, Cancer Res. 62:5375; Utzinger et al., 2001, Appl. Spectrosc. 55:955; Liu et al., 1992, Lasers Life Sci. 4:257; Frank et al., 1994, Anal. Chem. 66:319; Bakker-Schut et al., 2002, J. Raman Spectrosc. 33:580; Notingher et al., 2003, Biopolymers(Biospectroscopy) 72:230-240; international patent application publication No. WO 93/03672; international patent application publication No. WO 97/30338; U.S. Patent No. 6,697,665; U.S. Patent No. 6,174,291; U.S. Patent No. 6,095,982; U.S. Patent No. 5,991,653; and U.S. patent application publication No. 2003/0191398. These investigators used traditional Raman sampling approaches in which tissues are analyzed by collecting a Raman spectrum from a narrowly focused point in a sample.

Still other investigators (e.g., international publication No. WO 2004/051242; Krafft et al., 2003, Vibr. Spectrosc. 32:75-83; Kneipp et al., 2003, Vibr. Spectrosc. 32:67-74)

used a Raman mapping approach wherein Raman spectra were obtained using a scanning sample holder or light source to generate a spectroscopic map of the sample. To implement this scanning strategy, there is an inherent trade off between acquisition time and the spatial resolution of the spectroscopic map. Each full spectrum takes a certain time to collect. The more spectra collected per unit area of a sample, the higher the apparent resolution of the spectroscopic map, but the longer the data acquisition takes. Performing single point measurements on a grid over a field of view will also introduce sampling errors which makes a high definition image difficult or impossible to construct. Moreover, the serial nature of the spectral sampling (i.e., the first spectrum in a map is taken at a different time than the last spectrum in a map) decreases the internal consistency of a given dataset, making the powerful tools of chemometric analysis more difficult to apply.

An apparatus for Raman Chemical Imaging (RCI) has been described by Treado in U.S. Patent No. 6,002,476 and U.S. Patent No. 6,788,860 which are incorporated herein by reference in their entirety. Treado disclosed that Raman chemical imaging can be used to distinguish breast cancer tissue from normal breast tissue, but did not disclose how or whether any similar method might be applicable to diagnosis, grading, or staging of bladder cancers or other cancer diagnostic methods and protocols.

The disclosure alleviates or overcomes the limitations of prior art tools and methods for cancer diagnosis, grading, and staging and permits diagnosis of a variety of disease states. Due to the nature of this method it also allows differential manipulation at a cellular level that enables novel vectored treatment of the diseased state.

The vectoring of therapy to specific cells is an effective way to provide therapy, however it has been difficult due to problems in finding or separating just the afflicted cells. Antibody markers applied in the blood stream or through local injections have been used so that photosensitized agents which when irradiated can release local therapeutic agents. Such phototerapies have been limited to soft tissues external that can be readily irradiated. Metastasis and local regions where particular metastisis has occurred will have an affinity to the circulating cancerous cells, and when treated cells return they can effect the local metastatic regions, directly or by attracting immune response to these treated cells.

BRIEF SUMMARY OF THE DISCLOSURE

The present disclosure provides for a method of differentially manipulating cells where the cells, suspended in a fluid, are irradiated with substantially monochromatic light.

A Raman data set is obtained from the irradiated cells where the data set is characteristic of a disease status. The data set is assessed to identify diseased cells. A Raman chemical image of the irradiated cells is also obtained. Based on the assessment and the Raman chemical image, the fluid in which the cells are suspended is differentially manipulated. The diseased cells are directed to a first location and other non-diseased cells are directed to a second location as part of the differential manipulation.

In one embodiment, the cells are selected from the group consisting of breast cells, ovary cells, kidney cells, prostate cells, lung cells, colon cells, bone marrow cells, brain cells, red blood cells, and cardiac muscle cells. In another embodiment, the diseased cells are cancer cells.

In accordance with another aspect of the disclosure, the diseased cells may be treated by killing the diseased cells, contacting the diseased cells with a pharmaceutical agent, a label, a cytotoxic agent or an expressible vector.

The disclosure provides for another method to differentially manipulate cells where the cells, suspended in a fluid, are irradiated with substantially monochromatic light. A Raman data set is obtained from the irradiated cells where the data set is characteristic of a disease status. The data set is assessed to identify diseased cells. Based on the assessment, the fluid in which the cells are suspended is differentially manipulated. The diseased cells are directed to a first location and other non-diseased cells are directed to a second location as part of the differential manipulation. The diseased cells are treated with one or more of the following stresses: a physical stress, a chemical stress, and a biological stress.

In one embodiment, the treated cells are returned to a patient from whom the diseased cells were obtained prior to the irradiation.

The present disclosure further provides for a system including a monochromatic illumination source, a spectroscopic device, an imaging device, a fluid manipulating device, a machine readable program code containing executable program instructions and a processor. The processor is operatively coupled to the monochromatic illumination source, the spectroscopic device, the imaging device and the fluid manipulating device and configured to execute the machine readable program code to perform a series of steps. The system may further include a flow cytometer which includes a detector for detecting a Raman chemical image.

BRIEF SUMMARY OF THE SEVERAL VIEWS OF THE DRAWINGS

The accompanying drawings, which are included to provide further understanding of the disclosure and are incorporated in and constitute a part of this specification, illustrate embodiments of the disclosure and, together with the description, serve to explain the principles of the disclosure.

Figure 1 is a schematic diagram of an exemplary system used to carry out the methods of the present disclosure.

Figure 2 illustrates an exemplary flow cytometer which may be used in the system or used to carry out the methods of the present disclosure.

Figure 3 is a graph of Raman scattering intensity over a range of Raman shift values for bladder cells obtained from a healthy patient (thin solid and dotted lines) and for bladder cells obtained from a patient afflicted with bladder carcinoma (thick solid line). The baselines of the spectra are offset to facilitate comparison. As shown in Table 2 the peaks in the Raman spectra are indicative of the molecular species present in the cells.

Figure 4 is a graph of Raman scattering intensity over a range of Raman shift values for normal (i.e., non-cancerous) bladder tissue (dotted lines) and grade 3 transitional cell carcinoma bladder tissue (solid line).

Figure 5 comprises Figures 5A, 5B, 5C, and 5D. Figure 5A is a graph of Raman scattering intensity over a range of Raman shift values for bladder cells collected from urine of a healthy patient (thin solid line), bladder cells collected from urine of a patient afflicted with low grade (grade 1) bladder cancer (dotted line), and bladder cells collected from urine of a patient afflicted with high grade (grade 3) bladder cancer (thick solid line). The baselines of the spectra are offset to facilitate comparison. The baselines of the spectra are offset to facilitate comparison. Figures 5B, 5C, and 5D are digital micrographs of the bladder cells from which the spectra were derived (respectively a bladder cell collected from urine of a healthy patient (4B), a bladder cell collected from urine of a patient afflicted with low grade (grade 1) bladder cancer (4C), and a bladder cell collected from urine of a patient afflicted with high grade (grade 3) bladder cancer (5D).

Figure 6 contains a scatterplot of the Raman spectra obtained from cells from 150 patients with different grades of bladder cancer (50 G0, 50 G1, 50 G3) in one projection of the Principle Component space. The scatterplot of these spectra is in PC2-PC3 space and has a J3 criterion of 4.2.

Figure 7 contains the raw Raman images for bladder cancer cells wherein each pixel contains a high resolution spectrum.

Figure 8 contains Raman molecular images of bladder cancer cells generated using objective multivariate methods as described herein to assign a value for each spectral component at each pixel in the image.

Figures 9 and 10 contain digitally stained bladder cancer cells produced from Raman molecular images wherein color is digitally applied thereto based on the intensity of the Raman molecular image.

Figure 11 contains a Raman image scatterplot which shows the distribution of spectra from the Raman image on the space defined by Mahalanobis Distance calculations for dispersive spectra corresponding to normal (G0), and cancerous (G1 and G3) bladder epithelial cells. It can be seen on inspection that the image spectral points in the vicinity of the G3 points correspond to the small region identified as a G3 component in the spectral unmixing.

Figure 12 shows a field of view (FOV) on low magnification brightfield mode of operation which shows the highlighting of approximately 10 cells of diagnostic interest during Raman imaging.

Figure 13 shows schematically a sequence of steps developed for targeting cells during Raman imaging.

Figure 14 is a graph of averaged Raman scattering intensity over a range of Raman shift values for normal red blood cells (RBCs; solid line) and for RBCs (including at least one sickled RBC) obtained from a patient with sickle cell disease (dashed line). The Raman spectra for these cells were obtained within 100 milliseconds of the onset of illumination of the cells. Spectra obtained from 16 fields of view, each including 3-5 RBCs, were averaged to produce these data.

Figure 15 is a graph of averaged Raman scattering intensity over a range of Raman shift values for normal RBCs (solid line) and for RBCs (including at least one sickled RBC) obtained from a patient with sickle cell disease (dashed line). The Raman spectra for these cells were obtained after illuminating the cells for a sufficient period (about 2-5 seconds) that the Raman spectral response of the cells remained stable over time. Spectra obtained from 16 fields of view, each including 3-5 RBCs, were averaged to produce these data.

Figure 16 is a graph of averaged Raman scattering intensity over a range of Raman shift values for normal RBCs that had been illuminated for analysis of Raman scattering for not more than 100 milliseconds (solid line). The Raman scattering intensity is also shown (dashed line) for the same RBCs that had been illuminated for a sufficient period (about 2-5 seconds) that their Raman spectral response remained stable over time. Spectra obtained from 16 fields of view, each including 3-5 RBCs, were averaged to produce these data.

Figure 17 is a graph of averaged Raman scattering intensity over a range of Raman shift values for RBCs (including at least one sickled RBC) obtained from a patient with sickle cell disease. The RBCs had been illuminated for analysis of Raman scattering for not more than 100 milliseconds (solid line). The Raman scattering intensity is also shown (dashed line) for the same samples that had been illuminated for a sufficient period (about 2-5 seconds) that their Raman spectral response remained stable over time. Spectra obtained from 16 fields of view, each including 3-5 RBCs, were averaged to produce these data.

Figure 18 is a graph of averaged Raman scattering intensity over a range of Raman shift values for connective tissue fibers in cardiac tissue samples obtained from patients afflicted with either idiopathic heart failure (solid line) or ischemic heart failure (dashed line). The graphs represents averaged Raman scattering intensity data obtained from five patients afflicted with idiopathic heart failure and averaged Raman scattering intensity data obtained from five patients afflicted with ischemic heart failure.

Figure 19 is a graph of averaged Raman scattering intensity over a range of Raman shift values for cardiac muscle cell bundles in cardiac tissue samples obtained from patients afflicted with either idiopathic heart failure (solid line) or ischemic heart failure (dashed line). The graphs represents averaged Raman scattering intensity data obtained from five patients afflicted with idiopathic heart failure and averaged Raman scattering intensity data obtained from five patients afflicted with ischemic heart failure.

Figure 20 is a comparison of averaged Raman scattering intensity between cardiac muscle cell bundles (solid line) and connective tissue fibers (dashed line) in cardiac tissue samples obtained from patients afflicted with idiopathic heart failure.

Figure 21 is a comparison of averaged Raman scattering intensity between cardiac muscle cell bundles (solid line) and connective tissue fibers (dashed line) in cardiac tissue samples obtained from patients afflicted with ischemic heart failure.

Figure 22, comprising Figures 22A and 22B, is a comparison of averaged Raman scattering intensities between prostate tissue samples obtained from 64 patients diagnosed with prostate cancer (solid line) and prostate tissue samples obtained from 32 patients whose prostate tissue was determined to be benign (dashed line). Figure 22B is a magnified portion of the graph in Figure 22A.

Figure 23 is a comparison of Raman scattering intensity among various types of normal and cancerous kidney cells. The line styles corresponding to the kidney cell spectra obtained are shown in the figure.

DETAILED DESCRIPTION OF THE DISCLOSURE

The disclosure relates to methods of assessing the disease state of a mammalian cell using a Raman spectroscopic approach. In a preferred embodiment the disclosure relates to the use of Raman Molecular Imaging (RMI) to analyze cell samples in order to aid in the diagnosis of disease conditions, especially neoplastic disorders (cancers), inflammatory disorders, autoimmune and other immune disorders, blood diseases, infectious diseases, et al. In a particularly preferred embodiment the present disclosure uses RMI to facilitate the diagnosis or detection of diseases characterized by the presence of diseased cells in the urine, e.g., bladder cancer.

The methods are useful for assessing cells known or suspected of being cancerous, for purposes of cancer diagnosis, grading, and/or staging. The methods are useful for cancer assessment of cells of at least bladder, prostate, lung, colon, kidney, breast, and brain. The methods are also useful for assessing disease states not necessarily associated with cancer, such as infection, inflammation, autoimmune attack, cardiac dysfunction, and hemoglobinopathies. The methods can be used to detect cells affected by congenital defects, such as sickling of red blood cells (RBCs) and cardiac muscle and connective tissues affected by a hereditary cardiomyopathy.

Raman spectroscopic data will suffice in some instances to identify occurrence of a disease state. However, it is often preferable to assess the disease state present at discrete locations within a cell sample (e.g., to assess the disease state of individual cells), such as when the cells are assessed in vivo. In such instances, Raman spectral data is simultaneously collected at a plurality of discrete locations within the sample, and the Raman data so generated can be assembled to form an image of the sample that reflects the Raman spectral properties of the discrete portions of the sample. Raman spectral data can

be combined with other spectroscopic information, such as a visible light microscopic image of the sample, to generate data representations (e.g., images) of the sample that are more informative than either the Raman data or the other spectroscopic data alone.

The methods described herein involve irradiating a sample including one or more mammalian cells with substantially monochromatic light and assessing Raman light scattering from the cell(s), preferably at many points on the cells in the sample or from entire areas of the sample (e.g., from an area that includes multiple cells). The intensity of Raman light scattering at one or more Raman shift values can be assessed by itself. However, a more information-rich image can be made by combining the Raman scattering data with visual microscopy data to make a hybrid image. Such a hybrid image can be formed using the Raman scattering data directly, or by first processing the Raman scattering data leading to a Raman Molecular Image which is then integrated in the hybrid image. A Raman Molecular Image is an image which depicts molecular differences within a field of view as determined through measurements of Raman scattered radiation. The generation of a Raman Molecular Image from measurements of Raman scattered radiation can be achieved through established techniques traditionally used in spectroscopic analysis including, for example: principle component analysis (PCA), Cosine correlation analysis (CCA), Euclidian distance (ED), spectral unmixing. Mahalanobis Distance, (MD) Euclidian Distance (ED), Band Target Energy Minimization (BTEM), and Adaptive Subspace Detector (ASD). In a hybrid image generated either from direct Raman scattered radiation imagery, or from a Raman molecular image derived from such measurements combined with a standard reflectance or transmission digital image, visual clues to the disease and/or metabolic state of the cell(s) in the sample can be derived from morphological and structural information derived from the visual microscopic image data, from the Raman scattering data, and from the superposition and/or integration of the two data sets.

In particular the subject imaging methods may combine Raman scattering detection methods, a well known analytical technique for analyzing molecular specificity, with high fidelity digital imaging to enable measurement of discrete molecular and structural differences in cellular samples. Consequently this technique does not target a specific molecule but instead uses RMI to produce an image corresponding to a sample cellular environment, e.g., a urine sample, which image is compared to reference images, e.g., those corresponding to cellular samples corresponding to reference cellular samples (e.g., urine

derived) known to contain diseased or normal cells, or mixtures thereof. Therefore, unlike conventional disease detection methods that detect disease by cytological methods, RMI does not depend on the use of specific reagents, e.g., affinity reagents such as antibodies or the introduction of exogenous moieties that permit detection of specific cells or antigens, e.g., stains. However, the disclosure further contemplates the subject Raman detection methods as an adjunct to other disease detection methods, including antibody, nucleic acid and other affinity probe -based disease.

The methods described herein allow quantitative evaluation of cell and tissue samples with little or no necessary sample preparation. Because the methods require relatively little cellular material, they can be performed in a non-invasive or minimally invasive manner. The methods are also suitable for in vivo or in situ use, such as with a probe inserted into a tissue or body cavity.

Definitions

As used herein, each of the following terms has the meaning associated with it in this section.

"Bandwidth" means the range of wavelengths in a beam of radiation, as assessed using the full width at half maximum method.

"Bandpass" of a detector or other system means the range of wavelengths that the detector or system passes through itself, as assessed using the full width at half maximum intensity method.

The "full width at half maximum" ("FWHM") method is a way of characterizing radiation including a range of wavelengths by identifying the range of contiguous wavelengths that over which the magnitude of a property (e.g., intensity or detection capacity) is equal to at least half the maximum magnitude of that property in the radiation at a single wavelength.

"Spectral resolution" means the ability of a radiation detection system to resolve two spectral peaks.

"Raman Molecular Imaging" is an analytical technique that uses Raman scattered radiation recorded in a spatially accurate wavelength resolved image to generate an image (a Raman molecular image) which depicts aspects of the molecular composition in a particular scene or field of view including a sample of interest, e.g., a cell or cell containing sample, e.g, one obtained from urine or other bodily derived fluid or tissue sample. Images

produced by this technique may be used to identify measures of discrete molecular and/or structural differences in an imaged moiety, e.g., a cell, tissue, organ or cell containing sample. This imaging technique can be performed ex vivo or in situ, e.g., probe tissue sample in vivo during diagnosis or treatment of a particular individual.

A Raman molecular image can be merged to a digital image of the scene using standard techniques used in color image processing to, for instance, highlight the molecular distinctions in the scene using the intensity of a specific color to indicate the presence of a molecular distinctive component.

Detailed Description

Raman Spectroscopic Analysis for Assessment of Disease State

The disclosure is based, in part, on the discovery that diseased cells, when irradiated with radiation having a wavelength in the range from 220 to 695 nanometers (the wavelength preferably being greater than 280 nanometers, such as radiation having a wavelength in the range from 500 to 695 nanometers), exhibit Raman scattering of the applied radiation, and that the wavelength of the Raman scattered light emitted by those irradiated cells is shifted by amounts characteristic of the diseased cells. That is, cells which are diseased exhibit a different Raman spectrum than do cells of the same type that are not diseased. The differences in the spectra can include, for example, changes in the intensity of Raman scattered light at certain RS values, changes in the shape of the Raman scattering spectrum over a range of RS values, changes in the ratio of the intensity of Raman scattered light at two RS values, and combinations of these. These differences can be used to assess the disease status of a mammalian cell, the tissue from which the cell is obtained, or the tissue in which the cell is located. This disclosure is also in part based on Applicant's discovery that Raman scattering when combined with high fidelity digital imaging provides for the production of images which facilitate the detection of discrete molecular and structural differences in cells and samples, wherein such cells may be isolated, or may be comprised in tissue samples or cell mixtures, or may be comprised in an individual.

Particularly, the disclosure in part overcomes the limitations of non-imaging Raman spectroscopy, as it extends beyond single-point measurements to high-definition RMI. Depending on the number of spectra obtained during RMI per unit of sample, a higher "resolution" may be obtained of the resultant spectroscopic map. In contrast to single point-scanning techniques, collection of a full field image at a series of points in spectral space

yields a two-dimensional image, each pixel of which is a spectrum extending into a third dimension. RMI uses this pixel-by-pixel Raman spectral information to characterize a molecular species in a sample.

Figure 1 schematically represents an exemplary system 100 used to perform the methods of the present disclosure. System 100 includes, in a single platform, an imaging device in the form of a microscope objective 106, a spectroscopic device in the form of an imaging spectrometer 117 or a dispersive spectrometer 121, a processor 127, a database 125, a device to manipulate cells 128, a microscope stage 103 and machine readable programmable code 129. System 100 further includes a monochromatic light source 107, white light source 105, bandpass filter 109 to remove SiO_2 bands arising from a laser excitation fiber optic. The laser light is directed to a band reject optical filter 110 and propagated through an imaging objective 106 to illuminate the sample 101 with substantially monochromatic light. Objective 106 collects photons emanating from the sample 101. Notch filters 112 and 113 reject light at the laser wavelength. In one embodiment, sample 101 includes cells suspended in a fluid. The cells may include diseased cells and disease free cells. Dispersive spectrometer 121 and imaging spectrometer 117 function to generate a Raman data set produced by the irradiated cells of the sample. The Raman data set may be characteristic of a disease status of the cells. In one embodiment, imaging spectrometer 117 functions to generate a spatially accurate wavelength resolved image, Raman chemical image, of the irradiated cells.

Device 128 functions to differentially manipulate fluid in which the cells are suspended. Device 128 also functions to direct diseased cells to a first location and non-diseased cells to a second location based on the assessment of the Raman data set and the Raman chemical image. Device 128 may include known cell cytometry devices that are used or adapted in the cell-analysis and -sorting methods described herein. In one embodiment, the cell cytometry device may also include a detector 123 for detecting the Raman chemical image. An exemplary cell cytometer device 128 is illustrated in Figure 2. Device 128 includes an input side including a reservoir for suspended cells 210, pumps 212a and 212b, reservoir for buffer solution 214 and a processor 216 to control pumps 212a and 212b. The suspended cells are flowed through a region where the suspended cells are illuminated with illumination source 107 and the Raman data set and/or Raman image are detected. The device 128 also includes an output side including reservoirs 220a, 220b and

220c for sorted cells and reservoir 224 for manipulated cells. The cells directed to reservoirs 220a, 220b and 220c were identified based on the assessment of the Raman data set and the Raman image. The material in waste reservoir 222 did not meet the criteria used in assessment of the Raman data set and the Raman image. Device 128 further includes a cell manipulation loop 228, pump 212c and reagents 226. The cell manipulating loop 228 functions for the addition of reagents to treat the sorted cells with a reagent such as an antibiotic or chemotherapy agent. The movement of cells into the cell manipulation loop is based on the assessment of the Raman data set and the Raman image.

Device 128 may also take the form of microfluidic device which is described in co-pending U.S. Patent Application No. 10/920,320, filed by ChemImage Corporation on 18 August 2004, the disclosure of which is incorporated herein by reference in its entirety.

Processor 127 is operatively coupled to the illumination source 107, spectroscopic device 117 or 121, imaging device 106 and the device to manipulate cells 128. Processor 127 is configured to execute the machine readable program code 129 so as to perform the methods of the present disclosure. The machine readable program code 129 contains executable program instructions to configure illumination source 107, spectroscopic device 117 or 121, imaging device 106 and device 128. The machine readable code also functions to assess Raman data sets obtained from the irradiated cells which are characteristic of a disease status of the diseased cells. The assessment of the Raman data set and the Raman images is based on spectroscopic and imaging data for various disease conditions as discussed below.

Though the discussion herein focuses on the system illustrated in Figure 1, the practice of the method of this disclosure is not limited to such a system. An alternative system with the ability to deliver digital images and spectroscopic data sets is described in US Patent No. 7,046,359 entitled "System and Method for Dynamic Chemical Imaging" which is incorporated herein by reference in its entirety.

In order to detect Raman scattered light and to accurately determine the Raman shift of that light, a sample, e.g., a cell or tissue sample should be irradiated with substantially monochromatic light, such as light having a bandwidth not greater than about 1.3 nanometers, and preferably not greater than 1.0, 0.50, or 0.25 nanometers. Suitable sources include various lasers and polychromatic light source-monochromator combinations. It is recognized that the bandwidth of the irradiating light, the resolution of the wavelength

resolving element(s), and the spectral range of the detector determine how well a spectral feature can be observed, detected, or distinguished from other spectral features. The combined properties of these elements (i.e., the light source, the filter, grating, or other mechanism used to distinguish Raman scattered light by wavelength; and the detector) define the spectral resolution of the Raman signal detection system. The known relationships of these elements enable the skilled artisan to select appropriate components in readily calculable ways. Limitations in spectral resolution of the system (e.g., limitations relating to the bandwidth of irradiating light) can limit the ability to resolve, detect, or distinguish spectral features. The skilled artisan understands that and how the separation and shape of Raman scattering signals can determine the acceptable limits of spectral resolution for the system for any of the Raman spectral features described herein.

In general, the wavelength and bandwidth of light used to illuminate the sample is not critical, so long as the other optical elements of the system operate in the same spectral range as the light source. For a diffraction grating, the spectral resolution is defined as the ratio between the wavelength of interest and the separation, in the same units as the wavelength, required to distinguish a second wavelength. By way of example, an apparatus described in the examples herein can distinguish a Raman shift band at 1584 cm^{-1} from a separate peak that differs by about 12 cm^{-1}. Therefore, the Raman peak resolving power is 1584/12, or about 132, for the apparatus described in the examples. With a broader source (or a source filter enabling passage of light exhibiting an intensity profile characterized by a greater full width half maximum), greater peak separation would be required, because the Raman peaks would be more blurred on account of the greater variety of irradiating wavelengths that are shifted. Such a system would have a lower Raman peak resolving power.

By way of example, a suitable Raman peak resolving power can be determined as follows. If the lower limit of performance for a peak of interest at 1584 cm^{-1} is distinguishing a peak at 1650 cm^{-1}, then this represents a separation of 66 wavenumbers. This indicates that the lower limit of Raman peak resolving power is about 1584/66 = 24 for these peaks. Similar calculations can be performed to determine the minimum resolving power required for distinguishing other Raman peaks described herein.

The source of substantially monochromatic light is preferably a laser source, such as a diode pumped solid state laser (e.g., a Nd: YAG or Nd:YVO_4 laser) capable of delivering

monochromatic light at a wavelength of 532 nanometers. Other lasers useful for providing substantially monochromatic light having a wavelength in the range from about 280 to 695 nanometers include HeNe (which can be used to supply irradiation at any of several spectral lines, at about 543, 594, 612, and 633 nanometers), argon ion (532 nanometers), argon gas (360 nanometers), HeCd (442 nanometers), krypton (417 nanometers), and GaN (408 nanometers, although doped GaN lasers can provide 350 nanometers). Other lasers can be used as well, such as red diode lasers (700-785 nanometers) and eximer lasers (200-300 nanometers). Use of ultraviolet irradiation can permit use of resonance Raman techniques, which can yield more intense signals and simplified spectral peaks. However, lasers capable of ultraviolet irradiation tend to be very costly and complex to use, limiting their desirability.

Because Raman scattering peaks are independent of the wavelength of the illumination source (i.e., the RS value does not depend on the incident wavelength), the wavelength of light used to irradiate the cells is not critical. However, the illumination wavelength influences the intensity of the Raman peaks and the fluorescent background signals detected. Others have believed that irradiating cells with light having a wavelength less than those commonly used (i.e., light having a wavelength greater than about 700 nanometers is commonly used) would harm cells in the illuminated sample, owing to energy absorption by the cells.

As described herein, it has been discovered that wavelengths at least as low as about 500 nanometers (e.g., from 350 to 695 nanometers), and likely as low as 280 nanometers or even 220 nanometers, can be used without causing significant cell damage, especially if wide-field illumination techniques are employed and the intensity of the illuminating radiation is carefully controlled. Because the intensity of scattered light is known to be dependent on the fourth power of the frequency (i.e., inverse wavelength) of the irradiating light, and only proportional to the intensity of the irradiating light, lowering the wavelength of the irradiating light has the effect of increasing scattering signal output. Thus, a Raman scattering signal of equal intensity can be obtained by irradiating a sample with light having a higher wavelength and by irradiating the sample with a lower (irradiation) intensity of light having a shorter wavelength. Even under constant illumination, cells can survive irradiation with light having a wavelength as short as 500 nanometers if the intensity of the irradiating light is controlled. Irradiation using even shorter wavelengths can be performed

without harming the illuminated cells if intermittent or very short duration irradiation methods are employed. Irradiating cells with sub-700 nanometer wavelength light significantly boosts the Raman scattering signal obtained from the cells, leading to greater intensity and resolution of the Raman spectra of the cells and permitting more sensitive assessment of the disease state of the cells than was possible using previous methods.

An appropriate irradiation wavelength can be selected based on the detection capabilities of the detector used for assessing scattered radiation. Most detectors are capable of sensing radiation only in a certain range of frequencies, and some detectors detect frequencies in certain ranges less well than they do frequencies outside those ranges. In view of the Raman shift values that can be expected from tumor tissue samples, as disclosed herein, many combinations of light sources and detectors will be appropriate for use in the systems and methods described herein. By way of example, front- and back-illuminated silicon charge coupled device (CCD) detectors are useful for detecting Raman scattered light in combination with irradiation wavelengths described herein.

A sample including one or more cells can be irradiated by the light source in a diffuse or focused way, using ordinary optics. In one embodiment, light from the source is focused on a portion of a single cell of the sample and Raman scattering from that portion is assessed. A limitation of this approach is that the power input on the illuminated area must not be so great that the cell is harmed or significantly altered, at least prior to assessment of Raman scattering. Preferably, the amount of energy transferred to the cell during illumination is not sufficient to alter the morphology, Raman spectral characteristics, or other characteristics of the cell relevant for assessment of its state.

In another embodiment, the light used to irradiate the cells is focused on a larger (i.e., whole cell or multi-cell) portion of the sample or the entire sample. Use of such wide-field illumination can diffuse the irradiation power density across the sample, reducing the rate of energy transfer to the cells therein and protecting their function and viability. Wide-field illumination allows the acquisition of data and assessment of Raman scattering across the illuminated field or, if coupled with wide-field parallel detectors, can permit rapid Raman scattering analysis across all or part of the illuminated field. This facilitates presentation of Raman scattering data in the form of an image of all or part of the illuminated field, either alone or in combination with data obtained from the field using

other spectroscopic methods. In contrast, scanning spot methods to detect Raman scattering require high laser power densities focused into a small region.

The maximum useful power density of irradiation depends on the need for post-Raman scattering assessment of the cells and the anticipated duration of irradiation. The duration and power density of irradiation must not combine to render the irradiated cells unsuitable for any desired post-assessment use. For example, when cells are irradiated in vivo, it is important that the irradiation not significantly impair the viability or biological function of the cells. In vivo irradiation should also not significantly alter the chemical signature, composition, or biological integrity of the irradiated cells and tissues. The skilled artisan is able to select irradiation criteria sufficient to avoid these effects. When prolonged irradiation of the sample is anticipated (e.g., an irradiation period of minutes or hours, corresponding to a reasonable estimate of the duration of pathologist examination), the power density of illumination should be sufficiently low that the sample is not appreciably altered during the period of illumination.

If desired, the intensity of irradiation can be deliberately selected to harm or kill illuminated cells. It can be desirable to kill diseased cells that are detected in vivo. By way of example, if a portion of the bladder epithelium of a patient is imaged using the methods described herein and portions of the epithelium are identified which harbor cancerous cells, those portions can be subjected to intense or prolonged irradiation in order to kill the cancerous cells. Alternatively, the Raman imaging methods described herein can be used to identify undesirable cells in vivo, and those undesirable cells can be ablated using a separate system which optionally employs the optics used for Raman imaging (or separate optics). Owing to the high resolution of the Raman scattering methods described herein, small tissue lesions can be precisely killed, even if those lesions are surrounded by or interspersed with regions of healthy tissue. Thus, for example, these methods can be used to direct destruction of cancerous cells in an epithelium. Similarly, the methods can be used to identify portions of an in vitro sample that contain diseased cells, so that those portions can be selected, discarded, or treated in desired ways.

Imagographic analysis of Raman scattering (RMI) on a cellular scale can be performed using known microscopic imaging components. High magnification lenses are preferred, owing to their higher light collection relative to low magnification lenses. The numerical aperture of the lens determines the acceptance angle of light into the lens, so the

amount of light collected by the lens varies with the square of the numerical aperture. By way of example, a 100 x objective lens will typically have a numerical aperture value of about 0.9, and most 20 x objective lenses will have a numerical aperture of about 0.4. Thus, the amount of light collected by the 100 x lens will be about five times greater than the amount of light collected by the 20 x lens. In view of the fact that Raman scattered light can have a relatively low magnitude, selection of a high magnification lens can improve low level signal detection.

Raman scattered radiation can be assessed on a cell-by-cell basis, by comparing regions of a single cell, or by comparing regions that contain multiple cells, for example. The cell or cells from which Raman scattering is assessed can be single cells, multiple cells of substantially a single type, or multiple cells of mixed types, e.g., tissue samples e.g. from biopsies of patients being tested for a specific disease such as a malignancy. When cells of mixed types are assessed, the Raman spectral data can be assessed on an averaged (over all cells present) basis or by extracting spectral information specific to one or more cell types from the raw data. Spectral unmixing techniques for extracting spectral information from data obtained from complex systems are known. Suitable spectral unmixing techniques are described, for example, in U.S. Patent No. 7,072,770 which is incorporated herein by reference in its entirety. The suitability of averaged spectral data depends on the extent to which non-diseased cells present in a mixture are known or expected to obscure a Raman spectral characteristic of a normal or diseased cell of a desired type in the mixture. For example, in a mixture of cell types, if a diseased cell of the type one wishes to assess exhibits a characteristic Raman spectral feature (e.g., a peak at a particular RS value) that is distinguishable from the Raman signals exhibited by all other cell types in the mixture, then the diseased cells can be detected without resolving the spectra of the cell types in the mixture.

Raman spectral data can be collected in the form of a two- or three-dimensional image that maps Raman scattering with position in a sample, as described herein. Such imaging methods can be used to produce Raman images (displayed alone or in combination with other spectroscopic data such as a visible light reflectance microscopic image) of individual cells, subcellular regions thereof, or intercellular regions (e.g., extracellular matrix). The cells can be isolated cells, such as individual blood cells or cells of a solid tissue that have been separated from other cells of the tissue. When the imaged cells are

ordered (e.g., cells aligned by shape or cells arrayed in a solid tissue matrix), Raman spectral data can be collected at various positions relative to the cells and the polarization characteristics of the Raman scattered light can be assessed, each in order to derive position- and orientation-related information about the Raman scattering entities of the cells.

As discussed supra, RMI can be used to collect a full field image at a series of points in spectral space to yield a two-dimensional image wherein the pixel-by-pixel Raman spectral information may be used to characterize the molecular species in a cell sample. A high fidelity image may be obtained where each pixel represents a Raman spectrum. The spectral information may be used to generate images of specific constituents in a sample, e.g., a cell or cell containing sample.

Contrast may be present in the images based on the relative amounts of Raman scatter that is generated by the different species within a sample. Since a spectrum is generated for each pixel location, multivariate statistical analysis (i.e., chemometric analysis) tools such as Spectral Mixture Resolution, as Correction Analysis, Principle Component Analysis (PCA) or Multivariate Curve Resolution (MCR) can be applied to the image data to extract pertinent information that may be missed by univariate measures. Additionally, there are many other multivariate data reduction techniques that are known to those in this field that can be applied to Raman imaging data.

RMI provides very good resolution of samples. For example, a spatial resolving power of better than 250nm has been observed using visible laser wavelengths. This resolution is almost two orders of magnitude better than conventional infrared imaging, wherein diffraction is typically limited to 20,000 nm. Moreover, image definition (based on the total number of imaging pixels) can be very high for RMI when high pixel density detectors are used (e.g., 1 million plus detector elements).

As noted previously, different laser sources may be used in the subject disclosure. Particularly, Raman imaging may utilize laser sources not typically used for Raman spectroscopy of biomaterials. For example, a Nd:YVO4 solid state laser may be used which operates at 532 nm as a typical light source. That this laser is suitable is surprising because of the potentially anticipated susceptibility to background fluorescence. More typically, laser used for biomaterial analysis operate at 785 nm. However, while not required, red laser sources alternatively may be used in RMI. It has been found that when implementing spatially resolved Raman analysis (imaging), that fluorescence background is not a

pervasive background interferent and is not homogeneously distributed, but rather localized. Moreover, when laser excitation at 532 nm is used, the ν^4 dependence (4^{th} power dependence on excitation frequency) of Raman coupled with improved detection efficiency of the CCD detector combines to make 532 nm excitation a preferred wavelength. However other light (radiation) wavelengths may also be used if desired.

As described herein, RMI methods are enhanced by the use of a tunable optical filter called a Liquid Crystal Tunable Filter (LCTF). An LCTF can be electronically controlled to pass through a very narrow wavelength band of light. The spectral resolving power of 8 cm^{-1} (0.25 nm) is appropriate to perform Raman spectroscopy, and the resultant image fidelity is sufficient to exploit fully the resolving power of a light microscope, yielding a resolution of better than 250nm.

In the present disclosure, RMI is preferably used to analyze cells, cell samples and tissues in vitro or in vivo as a means of facilitating disease detection. However, RMI is a highly versatile method that can be used to analyze other materials as well such as other complex heterogeneous materials such as polymer blends, semiconductor materials, et al. Assessment of Raman scattered light can be measured using any known detector appropriate for sensing radiation of the expected wavelength (generally about 5 to 200 nanometers greater than the wavelength of the irradiating radiation). In view of the relatively low intensities of many Raman scattered light signals, a highly sensitive detector may be preferred or required, such as one or more cooled charge-coupled device (CCD) detectors. For parallel operation, CCD detectors having multiple pixels corresponding to discrete locations in the field of illumination can be used to enable simultaneous capture of spectroscopic data at all pixel locations in the CCD detector.

Raman scattered light can be assessed at individual points in a sample, or an optical image of the Raman scattered light can be generated using conventional optics. The Raman data or image can be visually displayed alone or in combination with (e.g., superimposed upon) a microscopic image of the sample. The Raman data or image can be processed to generate a molecular image which can be visually displayed alone or in combination with (e.g., superimposed upon) a microscopic image of the sample. Conventional methods of highlighting selected Raman data, or data derived from Raman data (e.g., by color coding or modulating the intensity of Raman scattered light) can be used to differentiate Raman signals arising from various parts of the sample. By way of example, the intensity of

Raman scattered light having a Raman shift of 1584 cm^{-1} can be displayed in varying shades or intensity of green color, superimposed on a brightfield optical microscopic image of the sample. In this way, Raman scattering can be correlated with microscopic landmarks in the sample.

If the cells are irradiated using light having a wavelength in the range from about 500 to 700 nanometers, then an RS value in the range 1000 to 1650 cm^{-1} can be assessed using a detector capable of detecting radiation having a wavelength of about 550 to 785 nanometers, and an RS value in the range 2750-3200 cm^{-1} can be assessed using a detector capable of detecting radiation having a wavelength of about 650 to 890 nanometers. Selection of an appropriate detector can be performed by a skilled artisan in view of the irradiation light and the anticipated Raman shifts.

Raman scattering intensity values assessed at one or more RS values can be correlated with the disease state of the corresponding cell(s) by observing the existence (or non-existence) of increased RS intensity relative to a normal (i.e., non-diseased) cell or to a cell exhibiting a lower grade or severity of the disease. This assessment can be performed using raw intensity values, by comparing intensities at different parts of a sample (e.g., portions that exhibit distinct morphological appearances), by comparing intensity at multiple RS values, by combining analysis of an RS value with light microscopy information, by comparing the shape of Raman spectra assessed over a defined range, or by other methods apparent to one skilled in Raman spectroscopy, pathology, visible light microscopy, or some combination of these disciplines.

The ratio of Raman scattering intensities at two RS values can vary at different irradiation wavelengths, but will normally exhibit similar trends. This variation is attributable to the nature of Raman scattering. Raman scattering at a particular RS value depends on both the electronic and vibrational structure of the illuminated molecule. Ordinarily, the electronic state of the molecule does not affect Raman scattering, and electronic and vibrational structures are often considered independent of one another to simplify understanding. Sometimes, however, the energy of illuminating radiation can be used to shift the electronic state of the illuminated molecule, and the transition of the molecule between electronic states resonantly enhances vibration of the molecule. The result of these processes is a very significant (e.g., 100- to 1000-fold) increase in the intensity of the scattered radiation. This enhanced scattering intensity is commonly called

resonance Raman scattering and can greatly simplify signal detection, especially in noisy backgrounds. By varying the wavelength of light used to illuminate a cell, resonance Raman effects can be avoided or taken advantage of (e.g., depending on whether the resonating molecule corresponds to an RS value that is informative regarding the disease state of a cell or not).

The methods described herein can be used by assessing the intensity of light scattered from a portion of the sample and subtracting out the intensity of light scattered from a different, reference portion of the sample that is known or believed to correspond to normal (i.e., non-diseased) tissue or from a separate sample of non-diseased cells of the same type. For example, RS data from different cells or from different areas of a single bladder tissue sample (or urine cytology slide or urine with cells suspended in it) can be compared. A difference of scattered light intensity between the analyzed and reference portions of the sample indicates a difference in cancerous state of bladder cells.

Cells include many chemical species, and irradiation of cells can result in Raman scattering at a variety of wavelengths. In order to determine the intensity of Raman scattered light at various RS values, scattered light corresponding to other RS values must be filtered or directed away from the detector. A filter, filter combination, or filter mechanism can be interposed between the irradiated sample and the detector to accomplish this. The system (i.e., taking into account the bandwidth of the irradiating radiation and the bandpass of any filter or detector) should exhibit relatively narrow spectral resolution (preferably not greater than about 1.3 nanometers, and more preferably not greater than about 1.0, 0.5, or 0.25 nanometers) in order to allow accurate definition and calculation of RS values for closely spaced Raman peaks. If selectable or tunable filters are employed, then they preferably provide high out-of-RS band rejection, broad free spectral range, high peak transmittance, and highly reproducible filter characteristics. A tunable filter should exhibit a spectral resolving power sufficient for Raman spectrum generation (e.g., a spectral resolving power preferably not less than about 12-24 cm^{-1}). Higher and lower values can be suitable, depending on the bandwidth of irradiating radiation and the Raman shift values desired to be distinguished.

A tunable filter is useful when Raman scattering measurements are simultaneously made at multiple locations in the illuminated field and when a Raman spectrum (i.e., assessments at multiple RS values) is to be obtained using the detector (e.g., for collecting

2-dimensional RS data from a sample). A variety of filter mechanisms are available that are suitable for these purposes. For example, an Evans split-element liquid crystal tunable filter (LCTF) such as that described in U.S. Patent No. 6,002,476 is suitable. Another suitable filter is a multi-conjugate liquid crystal tunable filter described in U.S. Patent No. 6,992,809 which is incorporated herein by reference in its entirety. An LCTF can be electronically controlled to pass a very narrow wavelength band of light. The spectral resolving power of 8 cm^{-1} (0.25 nanometer) is suitable to perform Raman spectroscopy, and the image fidelity is sufficient to take full advantage of the resolving power of a light microscope, yielding a spatial resolution better than 250 nanometers. Other suitable filters include Fabry Perot angle-rotated or cavity-tuned liquid crystal (LC) dielectric filters, other LC tunable filters (LCTF) such as Lyot Filters and variants of Lyot filters including Solc filters, acousto-optic tunable filters, and polarization-independent imaging interferometers such as Michelson, Sagnac, Twynam-Green, and Mach-Zehnder interferometers. Also, Raman image data can be obtained by use of a Computed Tomography Imaging Spectrometer (CTIS) or Fiber Array Spectral Translator (FAST). This list of suitable filters is not exhaustive.

Accommodation for Tissue Fluorescence

Tissues sometimes exhibit localized fluorescence which, if not accounted for, can complicate Raman spectral analysis. If such fluorescence occurs at a wavelength of interest for assessing the disease state of a cell in a sample, then a subtractive method can be used to correct for tissue fluorescence and prevent fluorescent emissions from obscuring relevant Raman scattering data.

In general, fluorescent emission is spectrally much broader than Raman scatter. For instance a typical Raman band in a cell sample will have a bandwidth of about 20 cm^{-1}. In contrast, the fluorescence spectrum (which can be tens to hundreds of nanometers in breadth) of the same cell sample irradiated with the same light will have a bandwidth of thousands of wavenumbers. Because of this, strategic choices of where in Raman shift space measurements are made (i.e., choice of which RS values are used for scattered light intensity measurements) permit correction for fluorescent emissions. By way of example, two image frames can be assessed in Raman space, one at 1584 cm^{-1} (an RS value at which the cells scatter radiation) and another at 2600 cm^{-1}. If the cells exhibit substantially no Raman scattering at 2600 cm^{-1}, then the radiation detected in the frame assessed at 2600 cm^{-1} will consist essentially only of radiation fluorescently emitted from the sample. The

radiation detected in the frame assessed at 1584 cm^{-1} will include both i) Raman scattered radiation and ii) fluorescently emitted radiation having substantially the same intensity as radiation fluorescently emitted at 2600 cm^{-1}. Subtracting the intensity of emissions assessed at 2600 cm^{-1} from the intensity of emissions at 1584 cm^{-1} will yield an intensity value essentially equal to the intensity of Raman scattered light at 1584 cm^{-1}. This is one example of a way by which the intensity of Raman scattered light from a sample can be assessed even if the sample also fluorescently emits light having the same wavelength as the Raman shifted light.

Materials present in cell and tissue samples obtained from humans or other mammals can interfere with Raman scattering of the cells of interest in the samples. These materials are preferably removed prior to Raman scattering analysis of the cells. By way of example, red blood cells (RBCs) exhibit strong Raman scattering at RS values including or overlapping 1581 cm^{-1}, and debris such as that which commonly occurs in bodily fluids or in excised samples can exhibit Raman scattering at a wide variety of RS values. RBC and debris can be removed from samples in relatively straightforward ways using known methods, such as gently rinsing cell samples with distilled, deionized water, normal saline, or dilute phosphate buffer. If RBCs are the cells being examined, then white blood cells (WBCs) and/or debris can be removed from the sample, using known methods (e.g., rinsing with distilled water or with an acetic acid solution), if Raman scattering by the WBCs and/or debris interferes with RBC Raman signals of interest.

Cells and Tissues

The methods described herein can be used to assess Raman scattering from substantially any cell for which a Raman scattering spectrum can be obtained. Use of the methods for assessment of the disease state of mammalian cells - especially human cells - is an important embodiment of the disclosure. However, the method can be used to assess Raman scattering from cells of plants, non-mammalian animals, fungi, protists, and monera. Samples containing cells of multiple types (e.g., a human tissue sample containing mycoplasma cells or a human kidney tissue sample including multiple cell types) can also be assayed, and Raman scattering data for the various cell types can be mapped together with microscopic image data, for example, to differentiate the cells.

The cells can be isolated cells, such as individual blood cells or cells of a solid tissue that have been separated from other cells of the tissue (e.g., by degradation of the

intracellular matrix). The cells can also be cells present in a mass, such as a bacterial colony grown on a semi-solid medium or an intact or physically disrupted tissue. By way of example, blood drawn from a human can be smeared on the surface of a suitable Raman scattering substrate (e.g., an aluminum-coated glass slide) and individual cells in the sample can be separately imaged by light microscopy and Raman scattering analysis. Similarly a slice of a solid tissue (e.g., a piece of fresh tissue or a paraffin-embedded thin section of a tissue) can be imaged on a suitable surface.

The cells can be cells obtained from a subject (e.g., cells obtained from a human blood or urine sample, tissue biopsy, or surgical procedure). Cells can also be imaged where they naturally occur, such as by imaging the cells in an accessible location, imaging cells in a remote location using a suitable probe, or by revealing cells (e.g., surgically) that are not normally accessible.

Cells that are imaged can be alive or dead. Non-living extracellular matter, such as extracellular matrix and connective tissue fibers can also be imaged. Cells and other materials from which Raman spectral data are collected should not be treated in any way known to obscure a Raman spectral characteristic that is to be observed. By way of example, cells and other materials can be imaged in place, by assessing Raman-shifted light scattered from a tissue illuminated in situ in a living mammal. Such analysis can identify the disease state of a cell in the tissue. Analogous posthumous analysis of a cell or tissue can identify a disease state that led or contributed to mortality of the organism from which it was obtained.

Cells obtained from an organism can reflect exposure of the organism to a compound detectable by Raman spectroscopy (i.e., if the compound is associated with a tissue of the organism) or exposure to an environmental condition which influences the Raman spectrum of a cell or tissue type in the organism. By assessing these factors, the Raman imaging methods described herein can be used to differentiate individual organisms, to assess their exposure to Raman-active compounds, or to assess their exposure to certain environmental conditions.

Raman Scattering by Bladder Cancer Cells

In one embodiment, the disclosure includes the discovery that normal and cancerous bladder cells can be differentiated from one another by their Raman spectral features.

Normal, non-cancerous ladder cancer cells exhibit significant Raman scattering at an RS value of about 1584 cm^{-1}, relative to non-cancerous bladder cells. The intensity of Raman scattering at this RS values increases with increasing grade of bladder cancer. Other RS values at which Raman scattering is associated with the cancerous state of bladder cells include about 1000, 1100, 1250, 1370, and 2900 cm^{-1}. This list of values is not exhaustive. Furthermore, there is a generalized increase in Raman scattering at RS values in the range from about 1000 to 1650 cm^{-1} and in the range from about 2750 to 3200 cm^{-1} in bladder cancer cells, relative to non-cancerous bladder cells, and this generalized increase is more pronounced in the range of RS values from about 1530 to 1650 cm^{-1}. These RS values and ranges are useful for assessing the cancerous state of bladder cells.

Raman Scattering by Sickled Red Blood Cells

In another embodiment, the disclosure includes the discovery that normal and sickled red blood cells (RBCs) can be differentiated from one another by various Raman spectral features.

RBCs exhibit a dynamic Raman spectral response to illumination. The initial Raman spectrum of an RBC (i.e., the spectra observable in about the first 100 milliseconds after the onset of illumination) changes as illumination continues until a stable (i.e., substantially unchanging) Raman spectrum occurs within a few seconds after the onset of illumination (e.g., after one to two seconds or less, depending on the intensity of the illuminating radiation). Normal and sickled RBCs exhibit Raman spectral differences in both their initial and stable Raman spectra. Changes in both initial and stable spectra of normal and sickled RBCs, as well as differences in the dynamic changes in the Raman spectra of both cell types upon illumination can be used to differentiate normal and sickled RBCs.

The Raman spectral features of sickled RBCs can be detected regardless of whether the RBC has assumed the characteristic crescent shape that RBCs of patients afflicted with sickle cell anemia assume under certain physiological conditions (e.g., low oxygen tension). The Raman spectral features of sickled RBCs can be used to identify RBCs from a patient who is homozygous for the sickle cell trait gene or a patient who is heterozygous for that gene. In heterozygotes, both normal and sickled hemoglobin are produced. For RBCs obtained from a heterozygote, an averaged Raman spectrum intermediate between the Raman spectra disclosed herein for normal and sickled RBCs can be expected, the

intensities of the characteristic features depending on the proportions of normal and sickled hemoglobin produced by the patient.

Figures 14-16 show the initial and stable spectra of RBCs obtained from an individual whose genome does not include an allele of the sickle cell trait gene and from another individual who is homozygous for the sickle cell trait gene. The spectra are averaged spectra obtained from 16 fields of view, each of which fields included 3-5 RBCs. Spectra corresponding to sickled RBCs are averaged spectra from fields which included at least one RBC that had the characteristic crescent shape.

In the initial spectra (i.e., spectra obtained not more than 100 milliseconds following the onset of illumination), sickled RBCs exhibit at least three Raman spectral peaks that are shifted relative to the corresponding peaks in normal RBCs. The first is a peak that occurs at about 1086 cm^{-1} in normal RBCs, but at about 1070 cm^{-1} in sickled RBCs. The second is a peak that occurs at about 996 cm^{-1} in normal RBCs, but at about 991 cm^{-1} in sickled RBCs, and a difference in the peak width can also be seen, with the 991/996 cm^{-1} peak being broader for normal RBCs. The third is a peak that occurs at about 671 cm^{-1} in normal RBCs, but at about 666 cm^{-1} in sickled RBCs. Other differences in the initial spectra of normal and sickled RBCs can be seen in the spectra shown in Figure 14.

In the stable spectra (i.e., spectra after at least 2-5 seconds following the onset of illumination), the intensities of at least two Raman spectral peaks exhibited by sickled RBCs differ from the intensities of the corresponding peaks exhibited by normal RBCs. The first is a peak that occurs at about 1366 cm^{-1}, and the second is a peak that occurs at about 1389 cm^{-1}, as can be seen in Figure 15. Other differences in the stable spectra of normal and sickled RBCs can be seen in the spectra shown in Figure 15.

Normal and sickled RBCs can also be distinguished by the dynamic response of Raman-shifted light scattered by the respective cells. As indicated in Figure 16, normal RBCs do not exhibit a significant dynamic shift in the RS value of the peak at about 1082 cm^{-1} or the peak at about 676 cm^{-1}. Comparing Figures 16 and 17, it can be seen that both normal and sickled RBCs exhibit a dynamic loss of the peak at about 706 cm^{-1}, and a shift in the RS value of a peak that initially occurs at about 1629 cm^{-1} to about 1636 cm^{-1}. Similarly, dynamic decreases in peak heights are observed at RS values of about 1366 cm^{-1}, 1385 cm^{-1}, and 1437 cm^{-1} for both normal and sickled RBCs, but the dynamic changes are

greater at the peaks at RS values of about 1366 cm^{-1}, 1385 cm^{-1} in sickled RBCs than in normal RBCs.

The differences disclosed herein regarding the Raman spectral characteristics of normal and sickled RBCs can be used to differentiate the two cell types, or to confirm such differentiation by other methods (e.g., by microscopic observation of RBC morphology). The devices and methods used herein can be coupled with a device to sort, ablate, or otherwise treat normal and sickled RBCs, to achieve differential treatment of such cells.

Raman Scattering by Cardiac Tissue

In another embodiment, the disclosure includes the discovery that Raman spectral characteristics of regions of cardiac tissue can be used to differentiate cardiac tissue having different disease states. For example, cardiac tissues of patients afflicted with idiopathic heart failure can be distinguished from patients afflicted with ischemic heart failure.

At least two types of tissue structures can be distinguished in cardiac tissues. First, bundles of muscle cells form a contractile fibrous matrix which provides the pumping impetus to the cardiac tissue. Second, connective tissues in the heart provide structure and support for the contractile cardiac muscle tissue, connect cardiac muscle fibers to one another, and form valves and other internal barriers within the heart.

Figures 18-21 show Raman spectral characteristics of cardiac muscle and connective tissues of patients afflicted with idiopathic or ischemic heart failure. As expected, based on the differential composition of cardiac muscle and connective tissues, the two tissue types exhibit different Raman spectra. However, these figures also demonstrate that the Raman spectra of the two tissue types can be used to distinguish cardiac tissues of patients afflicted with idiopathic heart failure (presumably including at least some patients with genetically-encoded defects in cardiac tissue components) from cardiac tissues of patients afflicted with ischemic heart failure.

The Raman spectral characteristics of cardiac tissues described herein can be used to diagnose a condition in a patient, to confirm a diagnosis made by other means, to predict susceptibility to cardiac disease, or to assess the cause of death of an individual post mortem. Because the methods described herein are able to identify the type cardiac tissue (e.g., connective tissue or cardiac muscle tissue) associated with heart failure, they can be used to assess the likely efficacy of various forms of therapy. By way of example, some forms of idiopathic heart failure are believed to arise from loss of structural integrity of

connective tissues, such as in patients whose genomes include certain genetically-encoded forms of collagen that are less stable or strong than others. Identification of loss of connective tissue integrity in a patient's heart suggests that therapeutic options contributing to the physical geometric support of the heart may be preferable to options which improve cardiac muscle contractility, at least in that patient.

The Raman spectral features of cardiac tissues disclosed herein for patients afflicted with ischemic heart failure are not believed to be exhibited exclusively by patients with ischemic heart failure. Ischemic heart failure is attributable to physiological defects other than cardiac muscle and cardiac connective tissue defects. For example, many instances of ischemic heart failure are attributable to vascular pathologies. For that reason, the Raman spectral data described herein for cardiac tissue samples obtained from patients afflicted with ischemic heart failure can be expected to be exhibited by ischemic cardiac tissue, regardless of the cause of the ischemia. Because cardiac ischemia attributable to vascular disease can be a local phenomenon (i.e., only affecting certain areas of the heart), the samples obtained from patients afflicted with ischemic failure may represent relatively normal cardiac tissues, albeit under the conditions of global ischemia caused by a poorly functioning heart. At least some Raman spectral features of such tissue can be exhibited by patients who are afflicted with other forms of cardiac ischemia, such as myocardial infarction and angina pectoris.

As can be seen from examining Figure 17, the Raman spectrum of cardiac connective tissue from patients afflicted with idiopathic heart failure can be differentiated from the Raman spectrum of the same tissue from patients afflicted with ischemic heart failure. For example, Raman spectral peaks at 747 cm^{-1}, 1080 cm^{-1}, 1125 cm^{-1}, 1309 cm^{-1}, and 1358 cm^{-1} differ. The width of Raman peaks at 1584 cm^{-1} and 1665 cm^{-1} can also be used as a basis for differentiating the tissues. Because cardiac ischemia, is not expected to significantly alter the structure of cardiac connective tissue in patients in which it occurs (other than at foci of ischemic insult, at which scar tissues can form), the Raman spectrum of the connective tissue from patients afflicted with ischemic heart failure can be expected to be substantially the same as that of tissue in patients with non-diseased cardiac tissue. Thus, the Raman spectral characteristics disclosed herein for cardiac connective tissue from patients afflicted with idiopathic heart failure can be used to diagnose, predict, or confirm

(e.g., by autopsy) occurrence in a patient of a connective tissue defect associated with heart failure.

The data shown in Figure 18 indicate that fewer Raman spectral differences are evident between cardiac muscle tissue from patients afflicted with idiopathic heart failure and cardiac muscle tissue from patients afflicted with ischemic heart failure. This is as expected, because cardiac muscle tissue from most patients afflicted with heart failure (of whatever etiology) can be expected to show evidence of ischemia. Nonetheless, the differences between the Raman spectral characteristics of cardiac muscle tissues from patients of the two types indicate differences in cardiac muscle tissue that can account for at least some of the heart failure that is otherwise considered "idiopathic." Comparing the spectra in Figure 18, differences can be seen in the widths of Raman spectral peaks at RS values of about 1584 cm^{-1} and 1665 cm^{-1}. In addition, the RS value of the peak at 1080 cm^{-1} (in cardiac muscle tissue obtained from patients afflicted with ischemic heart failure) is narrower in spectral data corresponding to patients afflicted with idiopathic heart failure and is proportionally less intense (relative to the ischemic heart failure samples) at slightly lower RS values, such as 1078 cm^{-1}. The Raman spectral characteristics disclosed herein for cardiac muscle tissue can be used to diagnose, predict, or confirm (e.g., by autopsy) occurrence in a patient of a cardiac muscle tissue defect associated with heart failure.

As shown in Figures 20 and 21, there are significant Raman spectral differences between spectra obtained from cardiac muscle tissue and cardiac connective tissue, whether the cardiac tissue was obtained from patients with ischemic or idiopathic heart failure. Examples of these differences include: better resolution of peaks at 831 cm^{-1} and 852 cm^{-1} in the muscle tissue; occurrence of a peak at 1168 cm^{-1} in muscle tissue; better distinction in the muscle tissue between the 1390 cm^{-1} and 1401 cm^{-1} peaks; sharper definition of the 1556 cm^{-1} in connective tissue; and occurrence in connective tissue of a broad underlying band between about 800 cm^{-1} and 1200 cm^{-1}. These spectral differences demonstrate that the methods described herein can be used to differentiate tissue sub-types within a broader tissue type (e.g., cardiac connective tissue can be differentiated in a microscopic image of a cardiac tissue sample from cardiac muscle tissue in the same sample.

Raman Scattering by Kidney Tissue

In another embodiment, the disclosure includes the discovery that Raman spectral characteristics of regions of prostate tissue can be used to differentiate normal, malignant, and benign kidney tissues, as well as kidney tissue afflicted with end stage renal disease. Figure 23 shows differences in Raman spectra obtained from various kidney tissue samples. These spectral differences evident in this figure demonstrate that the methods described herein can be used to differentiate normal and diseased kidney tissues.

Raman Scattering by Prostate Tissue

In another preferred embodiment, the disclosure includes the discovery that Raman spectral characteristics of regions of prostate tissue can be used to differentiate cancerous and benign prostate tissues.

Figure 22 shows differences in normalized Raman spectra obtained from cancerous and benign prostate tissue samples. For example, cancerous prostate tissue samples exhibit lower Raman scattering intensities at RS values of about 1080, 1300, and 1600 cm^{-1}. Other spectral differences are evident from the figure. These spectral differences demonstrate that the methods described herein can be used to differentiate cancerous and benign prostate tissues.

Raman Scattering by Diseased Cell Types

It was discovered that diseased cells exhibit enhanced Raman scattering at the RS values disclosed herein, relative to the corresponding non-diseased cells. Examples of diseased cells which can be differentiated from non-diseased cells of the same type using the methods described herein include cancerous kidney cells (e.g., cancerous renal tubular cells), cancerous prostate cells, cancerous colon cells, cancerous breast cells, cancerous lung cells, cancerous bone marrow cells, cancerous brain cells, cells of inflamed tissues, cells of tissues undergoing autoimmune attack, and cardiac muscle cells of diseased heart tissue (e.g., ischemic heart tissue). The methods described herein can be used to assess the diseased state of cells of at least these types by assessing Raman scattering by the cells at RS values in the range 280 to 1800 cm^{-1} and/or 2750-3200 cm^{-1} or at the particular RS values indicated herein. For instance, the range of RS values from 500 to 1800 cm^{-1} is informative for several disease types disclosed herein. Comparison of Raman scattering at those RS values with reference values or with non-diseased cells of the same type can indicate the diseased state of the sampled tissue.

Without being bound by any particular theory of operation, it is believed that tissues for which a diseased state can be detected using the methods described herein exhibit altered metabolic activity, relative to corresponding non-diseased cells of the same type. The altered metabolic activity is thought to be attributable to one or more disease processes occurring in the tissue. For instance, in an inflamed tissue or organ, an altered metabolic activity is required to mount the inflammatory response to the inciting event. This response drives the cells / tissues into a state of altered metabolic activity, further altering the biochemical makeup of the cell. These alterations are manifested in the Raman scattering characteristics of the cells or tissues. An implication of this theory of operation is that the methods disclosed herein should be useful for differentiating diseased and non-diseased tissue for many (and potentially all) diseases that are characterized by altered basal metabolism.

The methods described herein can also be used to determine the type and/or origin of cells found within the body by assessing Raman scattering characteristics of the cells and comparing them with the known Raman scattering characteristics of various cell types. In this way, the origin of a cancerous metastasis can be determined or migration of non-cancerous cells from a body location at which they normally occur to an abnormal body location can be detected.

The cells analyzed as described herein can be substantially any cells that can be obtained from, or accessed, in a mammal such as a human. Such cells can be cells obtained from a body fluid (e.g., urine, saliva, sputum, feces, blood, mucus, pus, semen, and fluid expressed from a wound or vaginal fluid), cells obtained by rinsing a body surface (e.g., a bronchial or peritoneal lavage), cells of a fresh tissue sample (e.g., scraped, biopsied, or surgically removed tissue), cells of paraffin-embedded or otherwise archived tissue samples, or cells that are examined in vivo in the mammal. The cells can be individual cells, clumps of cells, or cells that exist in a matrix of other cells and/or extracellular matrix.

Cells to be analyzed as described herein should be placed on and secured to a surface to prevent movement during analysis, unless the cells tend to adhere to the surface on their own. This is particularly important if Raman spectroscopy and light microscopy data are to be combined, because it is important to be able to correlate the microscopic characteristics of the cells, as directly or indirectly (e.g., using computer-processed or -stored image data) observed with the Raman scattering exhibited by the same cells. Cells can be secured or

fixed on a surface using substantially any known technique, and any reagents known to exhibit strong Raman scattering at the RS values disclosed herein should be avoided or accounted for in scattering intensity determinations. Cells can be secured or fixed as individual cells on a substrate, as a substantially flat layer or slice of cells on a substrate, or as a three-dimensional mass of cells. When a secured or fixed cell preparation includes cells at different elevations above the surface of the substrate, spatial analysis of the preparation is possible using known adaptations to light microscopy and Raman scattering methods. By way of example, Raman scattering can be correlated with height above the substrate by assessing Raman scattering using different planes of focus. Information obtained at the various planes can be reconstructed (e.g., using a computer for storage and display of the information) to provide a two- or three-dimensional representation of the sample.

Raman scattering analysis can be assessed for cells in vivo, for example using an insertable and removable fiber-optic probe (e.g., a fiberscope such as that described in U.S. Patent No. 6,788,860 which is incorporated herein by reference in its entirety). The probe can be fixed in place relative to the cells being assessed using known methods, and such fixation should be employed if reproducible accessing of the cells is desired. For example, if cells are to be assessed in vivo to determine their disease status and cells determined to be diseased are thereafter to be ablated by delivery thereto of intense laser illumination, then it is important that the probe not be displaced relative to the cells during the interval between determination of disease status and ablation.

Combined Raman Spectroscopic Analysis and Visible Light Microscopy

Cellular imaging based on optical spectroscopy, in particular Raman spectroscopy, can provide a clinician with important information. Such techniques can be performed ex vivo (e.g., on raw, fixed, or mounted body fluids, cells, tissues, or biopsies) or in vivo (e.g., using endoscopic techniques). Molecular imaging simultaneously provides chemical morphological information (i.e., size, shape and distribution) for molecular species present in the sample. Using Raman spectroscopic imaging, a trained clinician can determine the disease state of a tissue or cellular sample based on recognizable changes in chemical morphology without the need for sample staining or modification.

By contrast, visible light microscopy offers the trained clinician only physical morphological and structural clues regarding the disease state of the cells or tissue being

examined. Use of colored or fluorescent dyes can provide limited information regarding the cell surface or internal constituents of the cells, and can aid in determining the identity (i.e., cell or tissue type) or biochemical makeup of the cells. However, many staining reagents and methods can alter the morphology and/or structure of cells and tissue, thereby destroying useful information even as they reveal other information. Furthermore, many staining reagents and methods cannot practically be used for in vivo imaging or imaging of cells.

Combining Raman spectroscopy and visual light microscopy techniques enhances the usefulness of each by adding context to the information generated by the separate methods. Thus, physical morphological and structural information derivable from microscopic examination can be understood in the context of the biochemical makeup of the corresponding cellular materials and Raman scattering-based clues to the disease state and/or metabolic state of the cells being examined. If desired, staining or labeling reagents can be used in combination with Raman scattering and light microscopy in order to yield further information about the cells.

By way of example, the presence of micrometastases in lymph nodes draining bladder tissue provide important information regarding the stage and metastatic potential of a bladder tumor, which information can be used to select an appropriately aggressive anti-cancer treatment. However, differentiating between bladder cells and other cells which may occur in a lymph node can be difficult, as can differentiating between cancerous and non-cancerous bladder cells. Using the methods described herein, bladder cells in a lymph node can be identified using microscopic techniques (e.g., using a bladder cell-specific staining reagent such as a labeled monoclonal antibody) and Raman scattering spectroscopy can be used to assess the cancerous state of any bladder cells identified in the lymph node. Alternatively, Raman scattering techniques can be used both to identify cell type (i.e., by assessing characteristic Raman spectral properties of cells) and to determine the disease status of the cells that are present.

Substantially any Raman spectrometer capable of defining, detecting, or capturing data from cell- and tissue-scale samples can be used to generate the Raman scattering data described herein. Likewise, substantially any light microscopy instrument can be used to generate visible light microscopy information. In circumstances in which positions of cells in the sample can be correlated (e.g., by analysis of cell position and/or morphology or by

analysis of indicia on or shape of the substrate), it is not necessary that the Raman and microscope be integrated. In such circumstances, the data collected from each instrument can be aligned from separate observations. Preferably, however, a single instrument includes the Raman spectroscopy and light microscopy functionalities, is able to perform both analyses on a sample within a very short time period (e.g., less than one hour, preferably less than 10 minutes or 1 minute), and is able to correlate the spatial positions assessed using the two techniques. Information gathered using such an instrument can be stored in electronic memory circuits, processed by a computer, and/or displayed together to provide a depiction of the cell sample that is more informative than the separate depictions of the information obtained by the two techniques. A suitable example of equipment having these characteristics is the FALCON (RTM) RMI microscope available from ChemImage Corp. (Pittsburgh, PA). Suitable instruments are also described in U.S. Patent No. 6,002,476 and in co-pending U.S. patent application 09/619,371 which are incorporated herein by reference in their entirety.

A visible light microscope is not the only instrument which can be used in conjunction with a Raman spectrometer to analyze cells as described herein. Substantially any spectroscopic instrument can be used cooperatively with a Raman spectrometer, so long as at least some portion of the field of view of each instrument can be correlated with a portion of the field of view of the other. By way of example, a Raman spectrometer can be coupled with both a visible light microscope and a fluorescent spectrometer, using the same optics (e.g., as in the FALCON (TM) microscope system of ChemImage Corp.) or different optical paths. Data collected using the Raman and fluorescent spectrometers can be combined with visual data collected using the visible light microscope, for example by i) correlating the intensity of red shading of one or more portions of the visible microscopic field with the intensity of Raman scattered light at a selected RS value originating from the portion(s) and ii) correlating the intensity of green shading of one or more portions of the visible microscopic field with the intensity of fluorescent light at a particular wavelength emitted from the portion(s). By combining the information obtainable from multiple spectroscopic instruments, multiple optical properties of cells can be determined. A non-limiting list of such optical properties include absorbance, fluorescence, Raman scattering, and polarization characteristics. These devices and techniques can also be used to determine morphological and kinetic properties of cells, such as their shape and movement.

Each of the properties thus determined can be used to assess the disease state of the cell, for example by comparison with properties of cells known to be diseased or non-diseased.

An example of a probe suitable for in vivo analysis of cells in a mammal is described in co-pending U.S. Patent No. 6,965,793 which is incorporated herein by reference in its entirety). The tip of the probe can be inserted near or against a tissue of interest and Raman scattering and visible microscopic image data can be collected therefrom, optionally at various discrete depths using focusing techniques and/or at various RS values. Substantially any fiber optic or other optical probe that can deliver irradiation to a tissue in vivo and collect Raman light scattered therefrom can be adapted to an appropriate Raman spectrometer to perform the methods described herein. The probe preferably also includes an optical channel (e.g., a common optical fiber or a separate one) to facilitate microscopic imaging of the same tissue for which Raman spectroscopy is performed.

Information generated from Raman spectroscopy and/or light microscopy as described herein can be stored in electronic memory circuits, such as those of a computer, for storage and processing. A wide variety of data analysis software packages are commercially available. Suitable types of software include chemometric analysis tools such as correlation analysis, principle component analysis, factor rotation such as multivariate curve resolution, and image analysis software. Such software can be used to process the Raman scattering and/or visible image data to extract pertinent information that might otherwise be missed by univariate assessment methods.

Images of spectral information obtained from a single field of view of a sample can be combined in a straightforward manner if the images are obtained using the same optical path. For instance, a multimodal imaging instrument such as the FALCON (TM) Raman imaging microscope of ChemImage Corp. (Pittsburgh, PA) can be used to obtain Raman, fluorescent and visible light reflectance image data from a sample using the same field of view and substantially the same optical path). Spatial alignment of spectral images can be as simple as overlying the spectral images from a single field of view, optionally with minor automated or manual alignment of image features.

Differential Manipulation of Cells

In one embodiment, cells removed from the body of a patient are suspended in a fluid, analyzed individually or in clumps, optionally treated, and either discarded or returned to the patient's body. The cells may include breast cells, ovary cells, kidney cells, prostate

cells, lung cells, colon cells, bone marrow cells, brain cells, red blood cells, and cardiac muscle cells. In one embodiment, the diseased cells are cancer cells. The fluid can be a naturally-occurring body fluid (e.g., blood or serum or peritoneal fluid) or an artificially-introduced exogenous fluid (e.g., a peritoneal wash or dialysis fluid used to irrigate a body cavity). The suspended fluid can also be made by excising a clump of solid tissue from a patient and degrading it in a fluid to yield a cell suspension, for example. Using a device 128 analogous to an ordinary cell cytometer, cells (or clumps of small numbers of cells) are suspended in a fluid stream, irradiated with a monochromatic light source, and assessed individually by Raman spectroscopy for an indication of health or disease (e.g., cancerous state). A Raman chemical image of the cells is also obtained. Based on the assessment and/or the Raman chemical image, diseased cells are separated from non-diseased cells by directing the diseased cells to a location and directing the non-diseased cells to a different location. In one embodiment, the cells are suspended in independently manipulable aliquots of the fluid.

During analysis of an individual cell or clump of cells, one or more of the spectroscopic analytical techniques described herein can be performed with the cell or clump. By way of example, the cell or clump can be irradiated with monochromatic light and/or a broad band light source, and Raman-shifted scattered radiation can be collected and analyzed to yield a Raman spectrum (if multiple wavelengths of scattered light are analyzed) or the intensity of Raman scattered radiation at a pre-selected wavelength. Multiple spectroscopic methods can be applied to the cell to yield additional information. By way of example, an individual cell or clump can be analyzed to assess both its absorption at a pre-selected wavelength in the infrared region of the spectrum (e.g., to identify the cell as an ovary cell) and the intensity of Raman scattered radiation at a pre-selected wavelength (e.g., to identify the ovary cell as a cancerous ovary cell). A decision can be made (e.g., by an operator or by operation of a logic circuit) regarding how the cell or clump should be handled based on the information collected.

In one embodiment of these methods, cells that are identified as diseased are discarded, and cells that are not identified as diseased are returned to the body of the patient from whom they were obtained. Alternatively, the cells that are identified as diseased can be treated and returned to the body of the patient. The treatments may include a physical stress, a chemical stress or a biological stress. Such treatment can include contacting the

cell with a pharmaceutical agent intended to alleviate the diseased state of the cell and thereafter returning the treated cell to the body of the patient. Another suitable treatment is to contact the cell with a label suitable for imaging or other detection in the body (e.g., a fluorescent dye or a tomography contrast agent) and thereafter return the labeled cell to the body of the patient, wherein the location or behavior of the cell can be detected. A third example of a suitable treatment is to treat the cells that are identified as diseased with an agent which kills or lyses them, and returning the killed cells or fragments thereof to the body of the patient, wherein the cells and fragments can induce or enhance an immune response that selectively kills other diseased cells in the patient's body. Adjuvants or immune-enhancing agents can be co-administered with the killed/lysed cells if desired. Yet a fourth example of a suitable treatment of cells that are identified as diseased is to load or saturate the diseased cells with a therapeutic or cytotoxic agent prior to returning the loaded/saturated cells to the patient's body. In the patient's body, the loaded/saturated diseased cells can migrate to body locations at which other diseased cells are found and release their therapeutic or cytotoxic agents, alleviating the disease. The cells in this fourth example can be supplemented with an expressible vector such that the supplemented cells manufacture a therapeutic or cytotoxic product.

The device 128 useful for performing the cell-analysis and -sorting methods are suitable for miniaturization, such that an operable device can be implanted within a patient or carried by a patient in a mobile device that accompanies the patient (i.e., permitting treatment to continue outside a clinical setting). Such devices 128 can include a reservoir for containing an agent with which certain cells identified with the device are to be treated. Such devices 128 can also include a reservoir in which cells to be collected or discarded are stored for an interim period, such as the period during which the device is implanted or the period between patient visits to a clinic.

Examples

The disclosure is now described with reference to the following Examples. These Examples are provided for the purpose of illustration only, and the disclosure is not limited to these Examples, but rather encompasses all variations which are evident as a result of the teaching provided herein.

Example 1

Raman Scattering Analysis of Bladder Cancer Cells.

Raman molecular imaging (RMI) was used to distinguish cancerous and non-cancerous bladder cancer cells to demonstrate that RMI is useful for detection of bladder cancer.

RMI is an innovative technology that combines the molecular chemical analysis capacity of Raman spectroscopy with the power of high definition digital image microscopic visualization. This platform enables physicians and their assistants to identify both the physical architecture and molecular environment of cells in a urine sample and can complement or be used in place of current histopathological methods.

The data presented in this example demonstrate that the Raman scattering signal from bladder cancer tissue and cells voided in the urine can be identified and be distinguished from normal bladder tissue and cells. Detectable differences between high and low grade tumor cells were observed. These data establish that RMI signatures of bladder cancer cells are viable for discriminating high and low grades of bladder cancer, so that the disease can be detected in its earliest stages. These results demonstrate that RMI can be used as a non-invasive screening tool for detection of bladder cancer, for example in high risk populations (e.g., smokers over 40 years of age).

The experimental data presented below were derived from measurements made using a FALCON (TM) RMI microscope obtained from ChemImage Corp. (Pittsburgh, PA). The FALCON (TM) system uses 532 nanometer laser light to illuminate a sample over a wide field and collects Raman image data at multiple Raman shift (RS) values using a liquid crystal tunable filter (LCTF) unit equipped with a cooled charge-coupled device (CCD) array detector. This system is capable of collecting Raman spectra of the entire field of view and simultaneously acquiring Raman imaging spectral data and dispersive spectral data, as described in U.S. Patent No. 6,717,768 which is incorporated herein by reference it its entirety. Those features permit selection between full-field imaging and full-field collection of spectral data using a single set of optics. Data was processed using the CHEMIMAGE ANALYZE (TM) 6.0 spectral image processing software obtained from ChemImage Corp., applying standard techniques for signal processing and multivariate spectral data reduction techniques.

Samples were derived from anatomical pathology specimens retained in a cryogenic tissue bank. Sections of tissue samples embedded in TISSUE-TEK OCT (RTM) (10.24% w/w polyvinyl alcohol; 4.26% w/w polyethylene glycol; 85.50% w/w non-reactive

ingredients; obtained from Saura Finetek USA., Torrence, CA) were cut using a cryomicrotome at a thickness of 10 micrometers and placed on optical quality fused silica microscope slides. Excess OCT was removed with deionized water, and slides were air dried.

Figure 2 shows the Raman spectra of bladder mucosal cells obtained from two patients not afflicted with bladder cancer (thin solid and dotted lines in Figure 2) and from one patient afflicted with bladder carcinoma (thick solid line in Figure 2).

The Raman spectra shown in Figure 2 indicate the reproducibility of spectra for normal (non-cancerous) mucosa. Significant differences between the Raman spectra of the normal samples and the mucosal sample obtained from the patient afflicted with bladder carcinoma can be seen, for example at Raman shift values in the range from about 1000 to 1650 cm^{-1}, and more pronounced in the region from about 1525 to 1650 cm^{-1}. These data indicate that bladder carcinoma cells can be differentiated from normal bladder mucosal cells by RMI.

The peaks in the Raman spectrum are indicative of the molecular species present within the cells. As may be seen from the Figure a striking spectroscopic difference between normal and cancerous tissue is a peak centered at 1584 cm^{-1}. This peak is believed by the inventors to correspond to a molecular species having cytochrome-like molecular moieties. This peak is observed due to partial resonance enhancement based on the selection of 532nm excitation for RMI.

Related thereto, recent literature assigns a peak observed at 1587cm to C=C stretching in olefinic lipids. Shen et al.,Vibrational Spectroscopy,37:225 (2005) Others attribute a peak in this region to in-plane ring vibrations of nucleic acid molecules.(Omberg et al., Applied Spectroscopy, 58:813(2005) Van der Sneppen assigns a band at 1584cm to C-C stretching of the pyrrole ring in studies of the cytochrome C molecule. (Van der Sneppen et al., Dissertation Thesis, Vrjie Universiteit Amsterdam (2003) Wood et al. points out a band at 1581cm observed in deoxygenated red blood cells.(J. Biomed. Optics Vol10 (2005).

The table below (Table 1) shows Raman Band assignments for some peaks observed in bladder cancer spectra.

Raman Shift (cm2)	Assignment	Biomolecular Class
1006	Phenyl ring breath	Amino Acid (Phenylanlanine)
1128	C-N stretch	Protein backbone
1249	Amide III stretch	Protein
1304	CH_2 twist	Protein lipid
1323	CH_2/ bend	Cholesterol
1340	Pyrole ring	Protein and DNA
1368	CH_3	Phospholipids
1450	CH_2 /CH_3 deformation	Protein
1584	Cytochrome-like moiety (resonance enhanced)	Unknown
1630-1650	Amide I	Protein
2935	CH stretch	Protein

Table 1: Raman Band Assignments for some peaks seen in bladder cancer spectra

Figure 3 shows the differences between the Raman spectra for three normal bladder mucosa tissue samples and a grade 3 transitional cell carcinoma (TCC) tissue. Significant Raman scattering intensity differences (between normal and TCC bladder mucosa tissues) were observed at Raman shifts of about 1000, 1250, 1370, and 1584 cm^{-1}. In this experiment tumor tissue was smeared onto a slide in order to mechanically separate cells from the tumor tissue.

More specifically, smears of cells from the grade 3 TCC bladder mucosa were prepared by manually pressing the tissue against the slide and dragging it across the aluminum surface. Raman spectra of the smears were obtained, and the spectra were found to be reproducible among the smears prepared. Furthermore, the Raman spectra obtained using smears were virtually identical to the Raman spectra obtained using intact tissue samples. These results indicate that the RMI method is not highly sensitive to the method used to prepare the cells for imaging, meaning that relatively simple cytological preparative

methods can be employed. More specifically, this suggests that cells shed into urine may potentially be analyzed by these methods in order to detect the presence of normal and cancerous cells, e.g., prostate cancer cells.

Accordingly, once the ability to recognize reproducible results from tissues had been established, single cell monitoring methods, investigating cells shed in urine, were used. Red blood cells (RBCs) and other suspended or soluble substances present in normal urine can interfere with RMI. For example, RBCs exhibit Raman scattering peaks at Raman shifts (wavenumber values) of 1380 cm^{-1} and 1590 cm^{-1}. It was found to be desirable to rinse cells (e.g., with distilled water) prior to RMI in order to avoid interference from RBCs, cell and tissue debris, and other potentially interfering substances in urine. (These methods result in lysis of any red blood cells present therein.) This was performed by collecting cells from urine samples by centrifugation, rinsing the collected cells with distilled, deionized water, again centrifuging, and re-suspending the cells. A drop of the cell suspension was placed on an aluminum-coated microscope slide and smeared using another slide. In tissue sections, paraffin should also be removed as thoroughly as possible.

Microscopic inspection of cells obtained from urine samples indicated that there were white blood cells (WBCs) present. Raman spectra of WBCs and transitional epithelium are distinguishable from the Raman spectra of normal bladder mucosal cells. Nonetheless, it is preferable to remove WBCs from urine samples prior to assessing Raman scattering data from the remaining cells. Even if WBCs are not removed from the sample, their morphology and Raman scattering characteristics can be used to distinguish them from other cells in the sample.

Particularly, epithelial bladder cells vary in diameter from 15microns for cancerous cells to around from 50 microns for normal cells. Also, with respect to the Raman spectra obtained, it is noted that while the cells contain a small amount of autofluorescence, that is burnt out by the laser before the spectrum is acquired. This takes about 30 seconds. The burning down of the fluorescence is seen on the dispersive spectrum by a reduction of the background and the subsequent increase in signal-to-background ratio of the Raman peaks.

It was demonstrated that Raman spectrum of normal bladder cells obtained from urine is significantly different from the Raman spectra of low and high grade malignant bladder cells obtained from urine. These results are shown in Figure 5.

Figure 6 contains a scatterplot of obtained from cells from 150 patients with different grades of bladder cancer (50 G0, 50 G1, 50 G3) in one projection of the Principle Component space. These spectra can be used as a basis for a model used to classify spectra using a Mahalanobis distance-based approach. Mahalanobis distance takes into account the distribution of a class of spectra in comparing it to the unknown.

The scatterplot contained in Figure 6 has a J3 criterion of 4.2. J3 criterion is a relative measure of variance between and within classes. A larger J3 criterion indicates that there is more between-class variance than within-class variance, pointing toward improved ability to separate members of classes.

The accuracy matrix of this set of data can be seen in TABLE 3 herein. The accuracy matrix indicates what fraction of the time a spectrum from a given grade falls within the bounds of that grade in the Principle Component Space.

Splitting the 50 spectra from each case into a model and the validation set allows the construction of a model-based classifier which can be tested with the validation data. The results of this exercise on these data are contained in Table 2 below.

Percent	G0	G1	G3
G0	100	0	0
G1	6	94	0
G3	0	2	98

Table : 2

The sensitivity for G1 or G3 cancer in this exercise is 92% and specificity is 82%. Positive predictive value was 94% and negative predictive value was 86%.

An alternative means to classify the spectral data with such distinct features is to quantify the peak height of distinctive bands. An example of this approach to scaling the spectra is normalization and measuring the height of the peak of interest. Using this approach and cutoff values for peak height of the feature at 1584 cm-1 a simple classification approach was developed. In the validation set of spectra this had a sensitivity of 82% and specificity of 92%, a PPV of 95% and a NPV of 71%.

Based on the foregoing automated spectral classification approach, experiments were conducted with the object of implementing an automated acquisition approach, which

does not require the expertise of a spectroscopist to acquire high quality spectral data. To enable automated, unbiased collection of Raman spectral data, an automated acquisition approach was developed within the acquisition software which only requires a cell of interest be placed and focused in the field of view of the microscope. This involves making an initial assessment of overall signal strength, selecting a time base for monitoring photobleaching, acquiring spectra during photobleaching until the sample is stable. Stable spectra are acquired when a specified Signal-to-Noise Ratio (SNR) is reached. Our results indicate that using a SNR ratio as a target, that high quality spectra can be obtained in about 1 to 3 minutes. This suggests that the methods herein can be performed by non-experts, e.g., bachelor-level technicians. These experiments further included the location of individual cells and acquisition and classification of a Raman spectrum (a single mouse click operation). In these experiments, a series of 30 cases demonstrated a sensitivity of 79% and a specificity of 87%.

Figure 7 shows the raw Raman image of a G3 bladder cancer cell. Figure 8 shows the Raman Molecular Image derived from the raw data shown. The raw data was reduced to the RMI through a chemometric procedure called spectral mixture resolution, which, for each pixel in the image, estimates the fraction of a selected set of reference spectra which contribute at that pixel. (In this experiment the mean G0, G1 and G3 spectra obtained previously were used as reference spectra to generate "concentration" images of those components in these cells.)

It can be seen from Figure 9 that the G0 cell has no significant G3 spectral contribution whereas the G3 cell has a localized region with a very strong G3 spectral contribution. This contribution is spatially located just outside one of the two nuclei in this cancerous epithelial cell.

These images were acquired with the operator establishing the instrument operating parameters. Alternatively, this mode of operation can be automated. Thereby the system can simultaneously obtain a Raman image and a dispersive Raman spectra. Thus for a single cell both a single spectra and an image comprising thousands of spectra over a chosen spectral range can be obtained automatically.

Figure 11 contains a Raman image scatterplot showing the distribution of spectra from the Raman image on the space defined by Mahalanobis Distance Calculations on dispersive spectra from G0, G1 and G3 bladder cells. The points in the Figure in the

vicinity of the G3 points correspond to the small region on the image identified as a G3 component in the spectral unmixing.

The foregoing experiments establish that RMI can distinguish structural and/or molecular differences between normal and cancerous bladder cells. For example, significant Raman scattering intensity differences (between normal and tumor cells) were observed at approximate Raman shift values of 2900, 1584, 1370, and 1250 cm^{-1}. The high and low grade cells have similar spectra, but they exhibit small differences in some spectral regions. Additionally, as shown in Figure 6, these differences appear to be significant at Raman shift values of about 2900, 1584, 1370, 1250, and 1100 cm^{-1}.

The results described above include Raman spectra which extend over both the so called "fingerprint region" (roughly 280-1800 cm^{-1}) and the "CH" region (roughly between 2750 and 3200 cm^{-1}). The CH region is often neglected in Raman spectroscopy of biological samples because of the purported lack of specificity and biological relevance of Raman spectral information obtained for this region. By contrast, the data presented herein demonstrate that the proportion of signal in the CH band relative to the fingerprint region varies between cancer and normal samples. Cancer samples tend to have proportionally more scatter in the fingerprint region. By normalizing the spectra such that the area under each curve is the same, this is evident by comparing the heights of the peaks in the fingerprint region to the peak in the CH region, as shown in Figures 3 and 4. The value of including the CH region in Raman analysis extends to the imaging paradigm where Raman images of a sample taken in the CH region can be used to ratiometrically standardize fingerprint region information to allow comparison of samples and distinction of signals which represent cancer.

The results herein further demonstrate that Raman scattering data generated as described herein can be used to differentiate bladder cancer cells of different grades. The methods described herein can therefore be used to assess cancer grade in patients and to inform treatment decisions. Combined with superficial and/or microscopic visual analysis, the tumor can be more accurately and thoroughly characterized than was previously possible. The grade determination can also be made more quickly than was previously possible.

The experimental results discussed in this example are representative of RMI signals obtained by the described methods. These results consistently show the signature spectrum

of G3 cells in urine samples with definitive diagnosis by other means. This spectrum does not appear in patients without bladder cancer, suggesting that these methods should not have "false positives"). Still further the experimental results discussed herein suggest the presence of a chemical entity responsible for the pronounced peak at 1584 cm-1. This entity is believed to be localized to the bladder cancer cell but not the nucleus thereof. Recently Raman spectroscopy was demonstrated to be capable of detecting protein concentrations as low as 1 fmol of protein and distinguishing proteins that differ by as few as 3 of 51 amino acids.

Therefore, the subject methods should be suitable for detecting and identifying the moiety that is selectively expressed in cancerous bladder cells and not normal cells. Also these methods can be used to detect whether the same chemical entity is preferentially expressed and correlates to other (non-bladder) cancer cell types.

While the foregoing experiments are evidence that the subject Raman spectroscopic methods may be used to identify and distinguish diseased from normal cells, other improvements are within the scope of the disclosure. For example, the sample preparation techniques potentially may be improved by the addition of acetoacetic acid to enhance red blood cell lysis, and an alcohol wash included to provide for some fixation of cells. Alternatively, the procedures may be modified to include the use of automated cytology preparation systems such as the Cytec ThinPrep system. ThinPrep for sample preparation has the advantage that it provides a validated, commercially available technology which is in wide use in the cytology field.

Still further, the inventive methods may be modified to enhance cell targeting. The inventors have observed that cell targeting is most accurate when a trained expert in uropathology uses a digital video capability of the microscope platform to identify a cell of diagnostic interest. Further, as the sample preparation approaches are improved, the cells become more evident on the preps allowing a technician to identify these cells. Figure 9 contains a field of view (FOV) on the low magnification brightfield mode of operation. Approximately 10 cells are highlighted in this FOV. These cells are intact and relatively separated from other debris in the field of view. They also have distinct spectroscopic features in terms of autofluorescence (cells have less debris) and Raman signal (characteristic spectra noted above). These cells can be targeted for evaluation by pointing at them with a mouse. The system is spatially aligned such that the operator can select

regions of interest (e.g., cells) at a low magnification and move to a higher magnification for further evaluation.

Figure 13 depicts schematically an exemplary sequence of steps useful for targeting cells.

A prepared sample on a microscope slide is a region of interest spot that is visible to the eye. Herein, brightfield (RGB) video imaging is used to create a large map containing a region of interest. As noted previously, epithelial bladder cells are large (on the order of 50m in diameter) and therefore are relatively easy to distinguish from other cellular materials contained in urine samples even at low magnification.

Based on the significant experience using the exemplified microscope system to acquire data on a series of contiguous FOVs and building a montage image, using a 1.24 x microscope objective in conjunction with a translating stage, a video image can be acquired at several adjacent sites on the field of view, and the frames can be montaged together to produce a large image containing the whole sample spot. This procedure takes relatively little time, approximately 4 minutes. Such image provides perspective over a whole region of interest, and highlights where target (epithelial) cells are found. The two criteria that best identify epithelial cells in urine samples are the size of the cells and their low fluorescence compared to other cellular components in urine.

Also, video imaging with white light illumination has been found to provide the best contrast for locating and targeting bladder cells in urine. In contrast to other biological materials, bladder cells exhibit very little autofluorescence, and using both UV and 532nm excitation highlights the other components in urine more than epithelial cells. Consequently, as shown in several of the earlier-discussed figures normal brightfield imaging may be used to target cells.

From the low magnification montaged image of the region of interest, a cell or number of cells that are of interest can be targeted. From there it is an easy exercise to locate the target cell and change to a higher magnification objectives used for Raman acquisition. This takes approximately 5 minutes to locate the sample spot and acquire the initial montaged image. Once this has been effected, it need not be repeated on the same microscope slide preparation, and targeting at higher objective magnifications is very fast, i.e., on the order of 20 seconds.

Another means for targeting cells of interest is to employ the Raman imaging capabilities of the instrument. Acquiring a band specific image targeted at the 1584 cm band will highlight cells that possess the strong features observed to date in clinical samples. Moreover, in addition to spectral properties, imaging allows the size and shape of objects in FOV to be assessed. This discrimination allows for the operator to target cells that possess the target, i.e., disease phenotype.

Another improvement involves data acquisition. As shown in Figure 13, once the targeting strategy has been implemented, acquisition of Raman spectra of each cell takes on average about 5 minutes, including targeting at a higher objective magnification and signal acquisition. This can be further optimized to determine the optimal laser power and acquisition time for maximum SNR without photodamaging the target cells. Sample time evaluation will preferably be held to 30 minutes or less.

Other improvements involve image based processing. It has been found that the CH stretching region correlates strongly with protein content in a cellular system. This fact can be exploited as a basis for normalizing other spectroscopic features within a cell. For example, in the case of bladder epithelial cancer the ratio of the integrated signal at the 1584 cm^{-1} peak to the integrated signal over the CH stretch region may be evaluated. This operation can be performed on a pixel-y-pixel basis leading to a new image where each pixel is in this ratio. This image may possess value for diagnostic purposes. Also, taking a mean value of the image will allow reduction to a discrete number. This number should represent a simple measure of molecular environment of the cell which integrates the structural and biochemical characteristics of the cell.

Additionally the disclosure embraces alternative data reduction approaches to parametering a Raman image in order to classify the spectrum at each pixel in terms of an established library of spectral features. A simple measure of spectral distance between a pixel spectrum and a library presented as an image. For example, a potential spectral library approach involves taking measurements of the Cosine Correlation between the spectrum at each pixel in an image and both the mean G3 and mean G0 spectrum from a data set. This mean value from the image provides for facile data reduction and this process may be repeated for a number of spectral library members yielding several parameters for a particular data set.

Also, hybrid models are within the scope of the disclosure, i.e., which bring together the reduced data from the afore-discussed approaches for use in identification of specific disease phenotypes.

Still further, the inventive methods include the development of algorithms that have a constant false alarm rate, which are adaptive and self-organizing to an environment. For example, Receiver Operator Characteristic Curve (ROC) curve formalism can be used to establish a threshold value. Another approach is to group the parameters in the form of a vector and use multivariate methods to classify a sample based on one of these vectors. These specific multivariate methods include by way of example Euclidian distance and Mahalanobis distance based calculations. These methods require a preliminary set of data which provides the true spectra. Also, a Matched Filter Minimum Distance classifier based on Mahalanobis Distance may be utilized. (See e.g., Manolakis et al., IEEE Signal Processing Magazine, January 2002 which contains research relating to this algorithm for data processing and applications thereof, in particular hyperspectral imaging applications.)

Example 2

Raman Scattering Analysis of Red Blood Cells.

Raman molecular imaging (RMI) was used to distinguish normal and sickled human red blood cells (RBCs).

Individual RBCs were obtained from two patients, one of whom was known to be afflicted with sickle cell disease (i.e., homozygous for the sickle cell trait gene) and the other of whom was known not to harbor an allele of the gene for the sickle cell trait. Prior to analysis, RBCs were treated by smearing onto an aluminum-coated glass slide and air dried.

For each RBC, a visual microscopic determination was made of whether the cell was normal (i.e., normally-shaped) or sickled (i.e., sickle-shaped) using a FALCON (TM) Raman imaging microscope obtained from ChemImage Corp. (Pittsburgh, PA). A single Raman spectrum was obtained from a field of view that included 3-5 RBCs using the Raman scattering channel of the FALCON instrument. For samples of sickled RBCs, each field included at least one RBC that exhibited the crescent shape characteristic of sickle cell disease. The substantially monochromatic illumination wavelength was 532.1 nanometers, and Raman-shifted scattered light was assessed for RS values in the range from about 600-1800 cm^{-1}. Raman spectral data obtained from the RBCs was base-line corrected and

smoothed using an Savitsky-Golay (5-2) algorithm. Baseline correction was performed by fitting a low order polynomial to the spectrum and iteratively adjusting the coefficients of the polynomial to optimize the Raman spectrum.

A succession of Raman spectra were obtained over time for individual RBCs. The first Raman spectrum was obtained within a period of time not exceeding 100 milliseconds after the cell was illuminated. Dynamic changes were observed in the Raman spectra until the cell had been illuminated for at least about 2-5 seconds. A commercial software package (CHEMIMAGE XPERT (TM) from ChemImage Corp., Pittsburgh, PA) was used to display, analyze, and compare the Raman spectra.

The data obtained from these experiments are shown in Figures 14-17.

Example 3

Raman Scattering Analysis of Cardiac Tissue.

Raman molecular imaging (RMI) was used to assess cardiac muscle tissue and connective tissue in cardiac tissue samples obtained from patients afflicted with either idiopathic heart failure or ischemic heart failure.

Human cardiac tissue samples were obtained from five patients afflicted with ischemic heart failure and from five other patients afflicted with idiopathic heart failure. The tissue samples were obtained in the form of small tissue fragments fractured from explanted hearts which were frozen immediately after removal. Approximately 5 millimeter square tissue fragments were embedded in OCT and sliced into 5-10 micron sections. Tissue slices were placed on an aluminum coated slide. Excess OCT was removed with distilled water. Samples were air-dried and evaluated using a FALCON (TM, ChemImage Inc., Pittsburg, PA) Raman microscope.

Each tissue sample was sighted by visible light microscopy a Raman spectrum was obtained from an approximately 25 micron by 25 micron area of the sample. The area from which Raman scattered light was collected included sections of approximately 2-5 cardiac muscle cells (when areas of cardiac muscle were analyzed) or about 625 square microns of intermuscular fibrous material when connective tissue was analyzed. Scarred portions of cardiac tissues obtained from ischemic heart failure patients were excluded from analysis. The visual sightings and Raman scattering determinations were made using a FALCON (TM) Raman imaging microscope obtained from ChemImage Corp. (Pittsburgh, PA). The substantially monochromatic illumination wavelength used for Raman analysis was 532.1

nanometers, and Raman-shifted scattered light was assessed for RS values in the range from about 600-1800 cm^{-1}. Observations were made on at least three non-contiguous areas representing muscle and intermuscular fiber for each sample. Raman scattered light was collected with a 100x objective.

Raman-shifted scattered light was collected from portions of cardiac tissue which were determined by visible light microscopy to contain substantially only cardiac muscle fibers or substantially only connective tissue. Spectra were obtained from each of these two sub-portions of cardiac tissue samples from the two disease groups. The data obtained from these experiments are shown in Figures 17-20.

Example 4

Raman Scattering Analysis of Kidney Tissue.

Raman molecular imaging (RMI) was used to assess kidney tissue samples of known types using substantially the methods described herein. The data obtained from these experiments are shown in Figure 22.

Example 5

Raman Scattering Analysis of Prostate Tissue.

Raman molecular imaging (RMI) was used to differentiate cancerous and benign samples of human prostate tissue.

Human prostate tissue samples were obtained from 64 patients afflicted with prostate cancer and from 32 patients not afflicted with prostate cancer. The tissue samples were obtained in the form of frozen surgically excised samples. Pieces of tissue approximately one centimeter square and several millimeters thick were embedded in OCT and sectioned using a cryomicrotome, generating slices which were from 5-10 microns thick. Slices were placed on an aluminum coated slide, and excess OCT was removed with distilled water.

Each tissue sample was sighted by visible light microscopy a Raman spectrum was obtained from an approximately 625 square micron area of the sample. The area from which Raman scattered light was collected included parts from approximately 2-10 prostate cells. The visual sightings and Raman scattering determinations were made using a FALCON (TM) Raman imaging microscope obtained from ChemImage Corp. (Pittsburgh, PA). The substantially monochromatic illumination wavelength used for Raman analysis was 532.1 nanometers, and Raman-shifted scattered light was assessed for RS values in the range from about 600-1800 cm^{-1}.

The data obtained from these experiments are shown in Figure 23.

While this disclosure has been disclosed with reference to specific embodiments, it is apparent that other embodiments and variations of this disclosure can be devised by others skilled in the art without departing from the true spirit and scope of the disclosure. The appended claims include all such embodiments and equivalent variations.

CLAIMS

What is claimed is:

1. A method comprising:

irradiating cells suspended in a fluid with substantially monochromatic light;

assessing a Raman data set obtained from said irradiated cells and characteristic of a disease status thereof to identify diseased cells;

obtaining a Raman chemical image of said irradiated cells; and

differentially manipulating the fluid in which the cells are suspended based on the assessment and said Raman chemical image, wherein said diseased cells are directed to a first location and other non-diseased cells are directed to a second location as part of said differential manipulation.

2. The method of claim 1, further comprising:

suspending the cells in independently manipulable aliquots of the fluid.

3. The method of claim 2, further comprising:

handling the fluid using a flow cytometer.

4. The method of claim 3, wherein the flow cytometer includes a detector for detecting the Raman chemical image.

5. The method of claim 1, further comprising:

killing the diseased cells.

6. The method of claim 1, further comprising:

contacting the diseased cells with a pharmaceutical agent.

7. The method of claim 1, further comprising:

contacting the diseased cells with a label.

8. The method of claim 1, further comprising:

contacting the diseased cells with a cytotoxic agent.

9. The method of claim 1, further comprising:

contacting the diseased cells with an expressible vector.

10. The method of claim 1, wherein the cells are selected from the group consisting of breast cells, ovary cells, kidney cells, prostate cells, lung cells, colon cells, bone marrow cells, brain cells, red blood cells, and cardiac muscle cells.

11. The method of claim 1, wherein the fluid is serum.

12. The method of claim 1, wherein the fluid is an exogenous fluid contacted with a tissue of a patient.

13. The method of claim 1, wherein the diseased cells are cancer cells.

14. A system comprising:

a monochromatic illumination source;

a spectroscopic device;

an imaging device;

a fluid manipulating device;

a machine readable program code containing executable program instructions; and

a processor operatively coupled to said monochromatic illumination source, said spectroscopic device, said imaging device and said fluid manipulating device and configured to execute said machine readable program code so as to perform the following:

configure said monochromatic illumination source to irradiate cells suspended in a fluid with substantially monochromatic light;

configure said spectroscopic device to obtain a Raman data set from said irradiated cells, wherein said Raman data set characterizes a disease status of said irradiated cells;

assess said Raman data set obtained by said spectroscopic device so as to identify diseased cells;

configure said imaging device to obtain a Raman chemical image of said irradiated cells; and

configure said fluid manipulating device to differentially manipulate the fluid in which the cells are suspended based on the assessment and said Raman chemical image, wherein said fluid manipulating device is further configured to direct said diseased cells to a

first location and other non-diseased cells to a second location as part of said differential manipulation.

15. The system of claim 14, wherein said fluid manipulating device comprises a flow cytometer.

16. The system of claim 15, wherein the flow cytometer comprises a detector for detecting the Raman chemical image.

17. A system comprising:

means to irradiate cells suspended in a fluid with substantially monochromatic light;

means to obtain a Raman data set from said irradiated cells, wherein said Raman data set characterizes a disease status of said irradiated cells;

means to assess said Raman data set obtained by said spectroscopic device so as to identify diseased cells;

means to obtain a Raman chemical image of said irradiated cells;

means to differentially manipulate the fluid in which the cells are suspended based on the assessment and said Raman chemical image; and

means to direct said diseased cells to a first location and other non-diseased cells to a second location as part of said differential manipulation.

18. A storage medium containing machine readable program code, which, when executed by a processor, causes said processor to perform the following:

configure a monochromatic illumination source to irradiate cells suspended in a fluid with substantially monochromatic light;

configure a spectroscopic device to obtain a Raman data set from said irradiated cells, wherein said Raman data set characterizes a disease status of said irradiated cells;

assess said Raman data set obtained by said spectroscopic device so as to identify diseased cells;

configure an imaging device to obtain a Raman chemical image of said irradiated cells; and

configure a fluid manipulating device to differentially manipulate the fluid in which the cells are suspended based on the assessment and said Raman chemical image; and

further configure said fluid manipulating device to direct said diseased cells to a first location and other non-diseased cells to a second location as part of said differential manipulation.

19. A method comprising:

irradiating cells suspended in a fluid with substantially monochromatic light;

assessing a Raman data set obtained from said irradiated cells and characteristic of a disease status thereof to identify diseased cells;

differentially manipulating the fluid in which the cells are suspended based on the assessment, wherein said diseased cells are directed to a first location and other non-diseased cells are directed to a second location as part of said differential manipulation; and

treating the diseased cells with one or more of the following stresses: a physical stress, a chemical stress, and a biological stress.

20. The method of claim 19, further comprising:

returning the treated cells to a patient from whom the diseased cells were obtained prior to the irradiation.

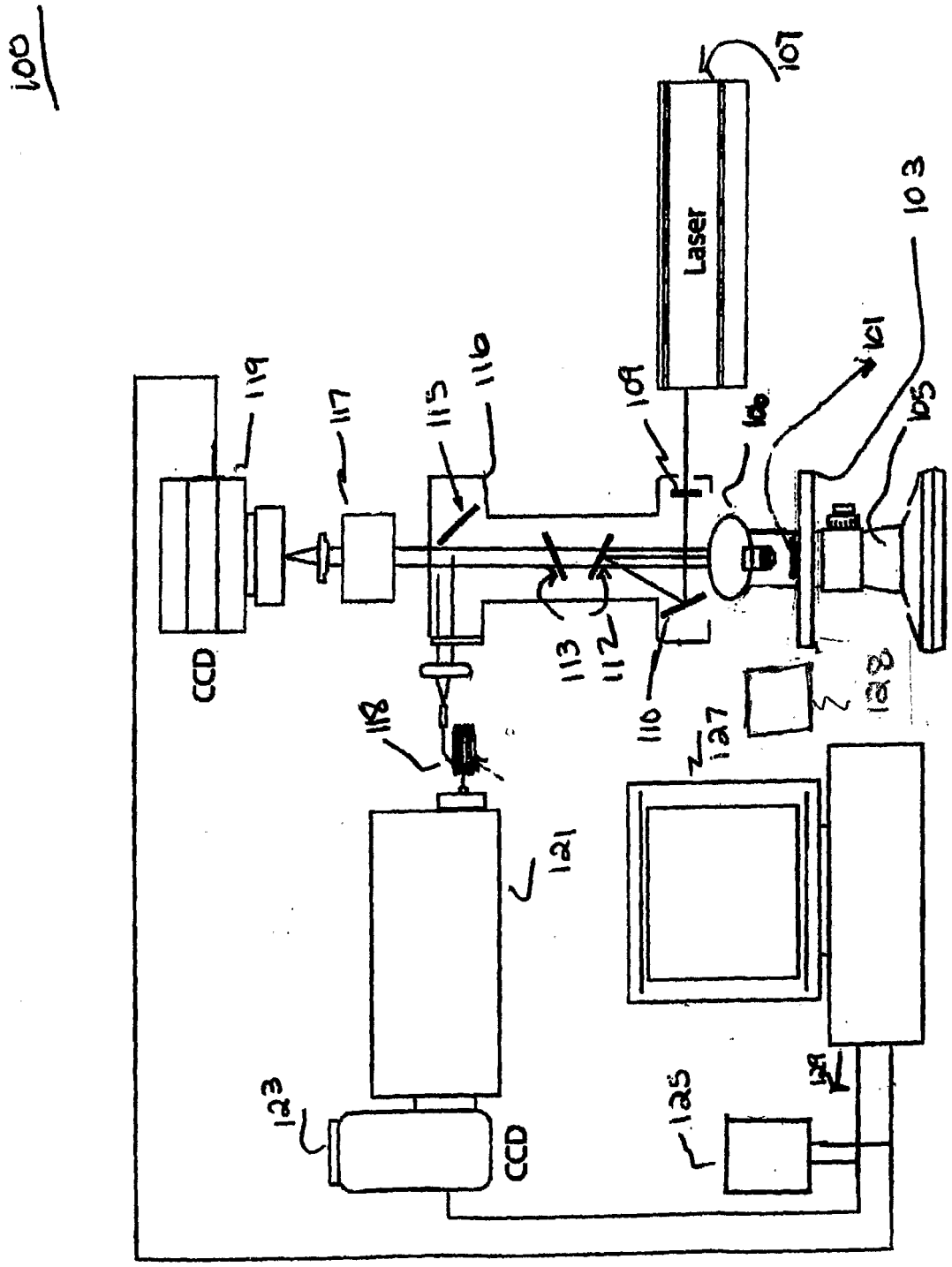
100
107
Laser
103
101
105
109
108
119
117
115
116
CCD
113
112
110
118
127
128
121
123
CCD
125
129

Figure 1

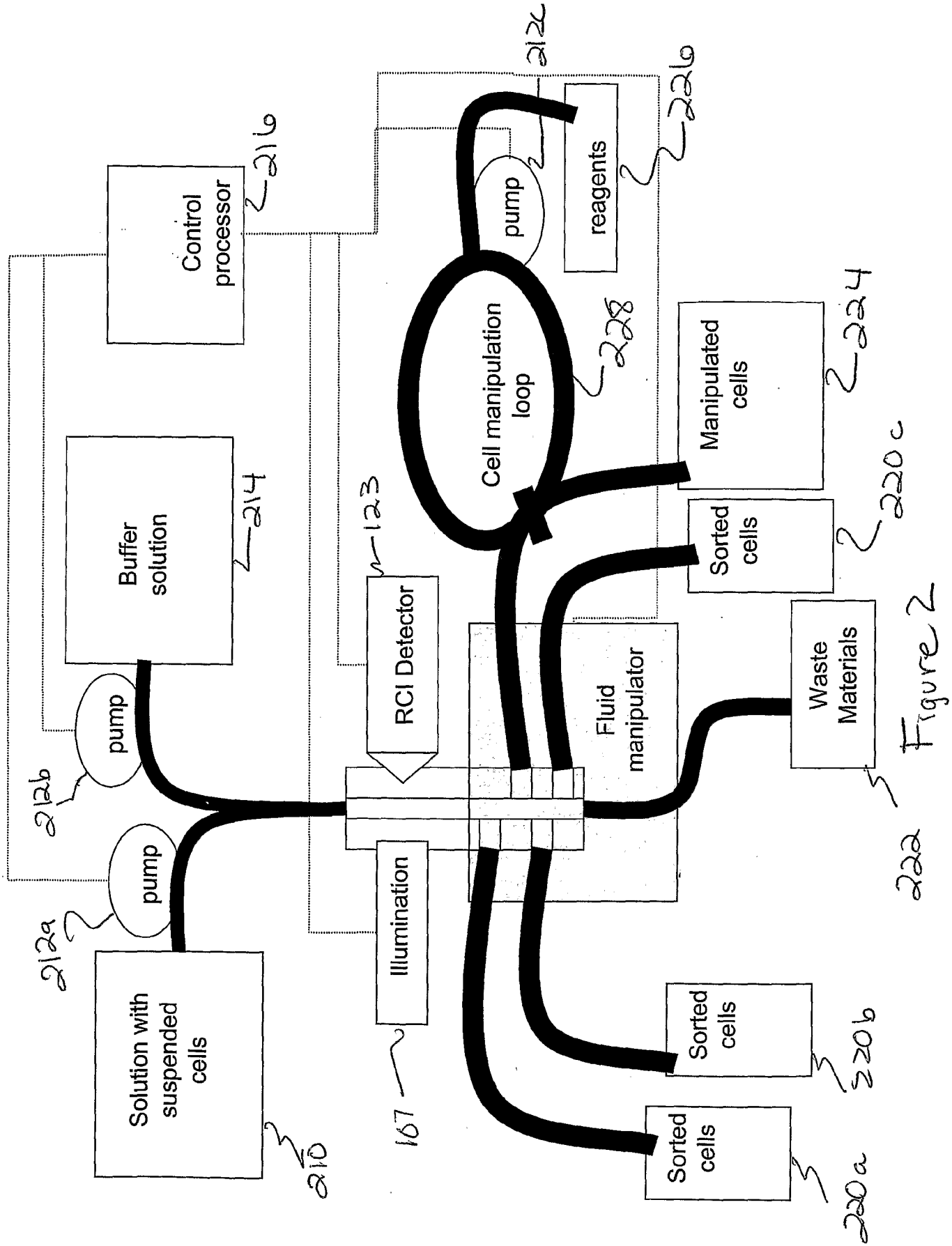
Control processor
216
Buffer solution
214
pump
212b
pump
212a
Solution with suspended cells
210
RCI Detector
123
Illumination
167
pump
212c
reagents
226
Cell manipulation loop
228
Manipulated cells
224
Sorted cells
220c
Fluid manipulator
Waste Materials
222
Sorted cells
220b
Sorted cells
220a

Figure 2

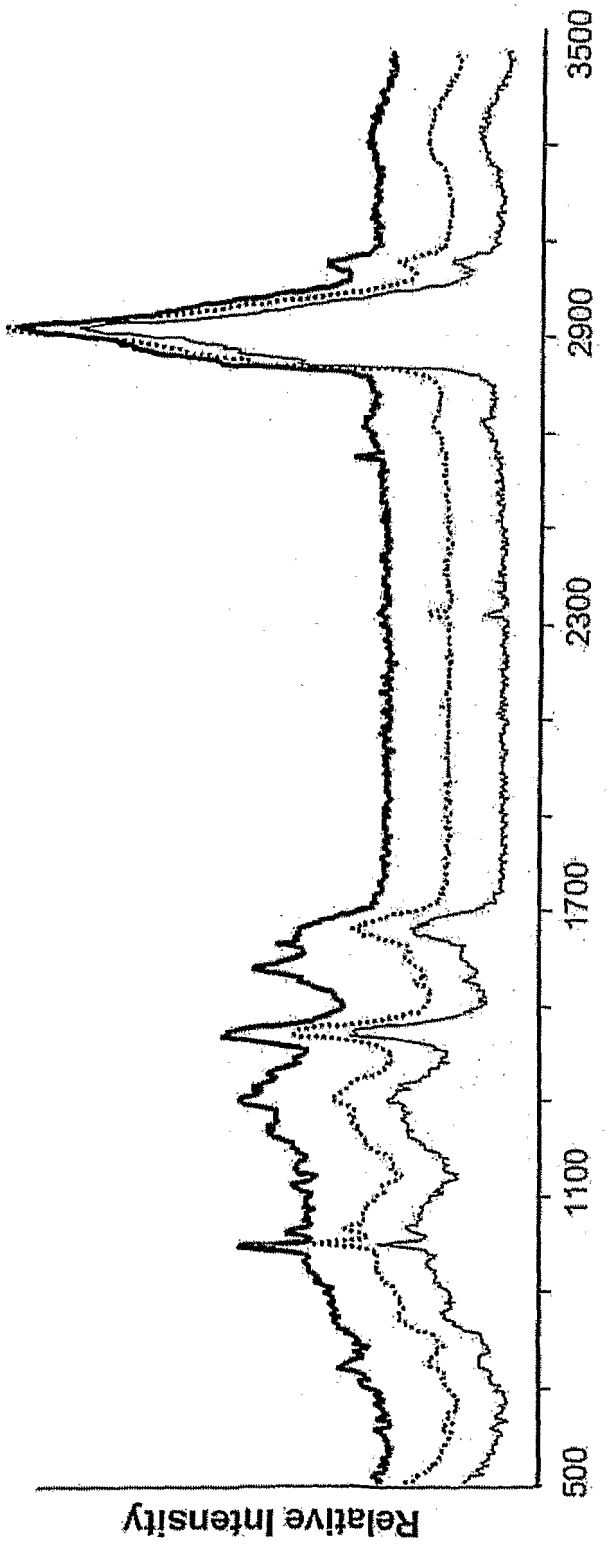
Relative Intensity
500
1100
1700
2300
2900
3500
Wavenumber (cm^-1)

Figure 3

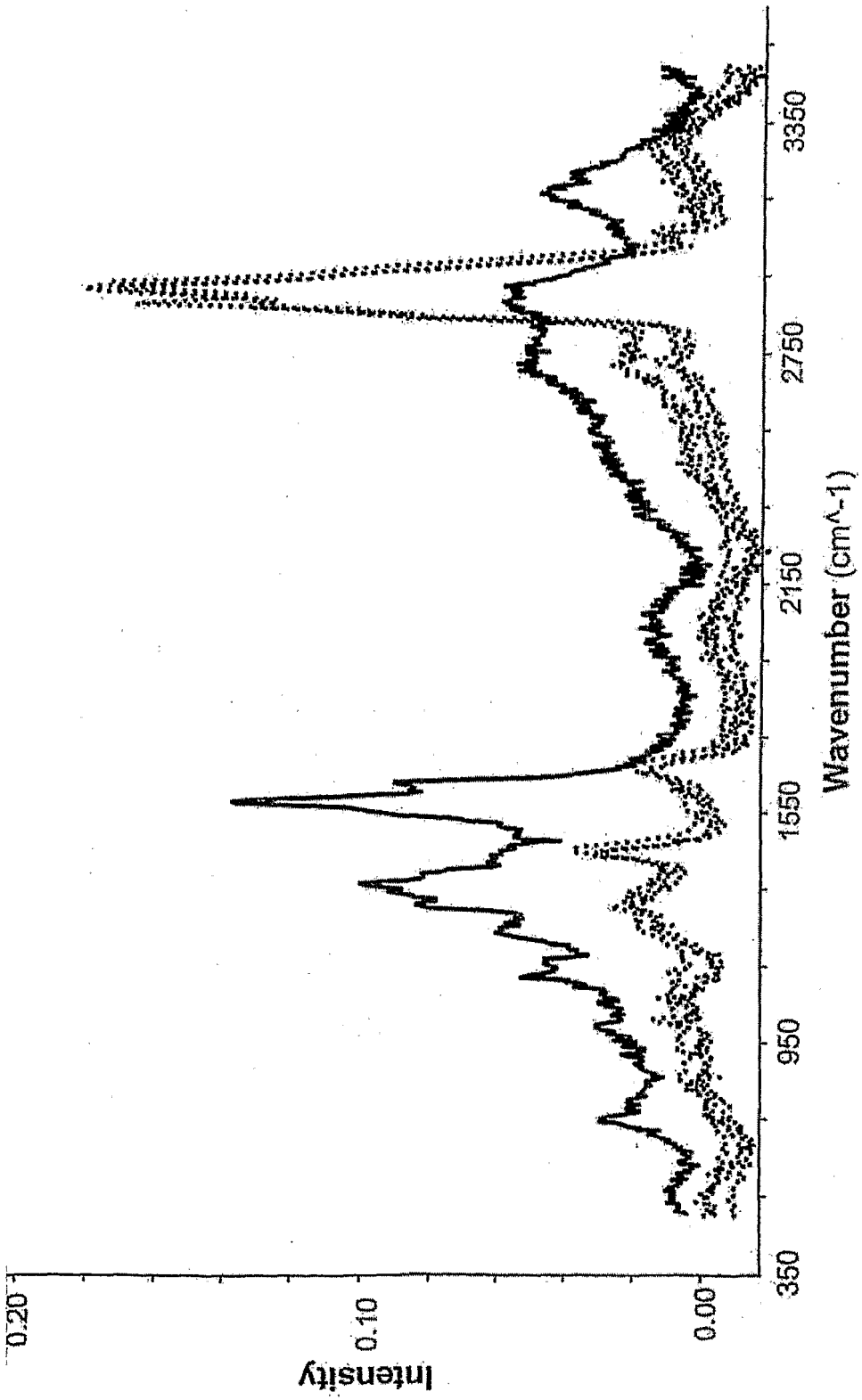
Intensity
0.20
0.10
0.00
350
950
1550
2150
2750
3350
Wavenumber (cm^-1)

Figure 4

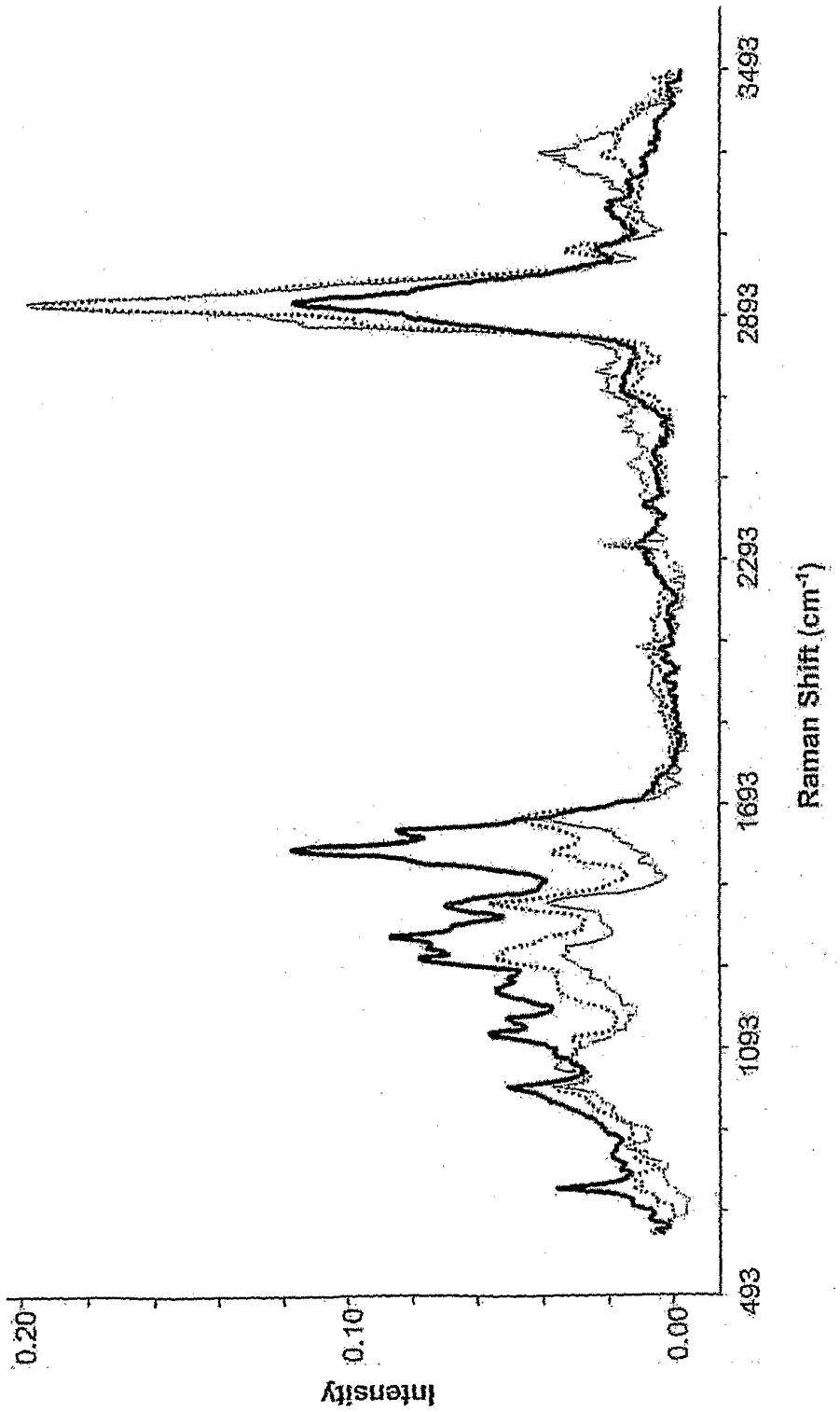
Intensity
0.20
0.10
0.00
493
1093
1693
2293
2893
3493
Raman Shift (cm-1)

Figure 5A

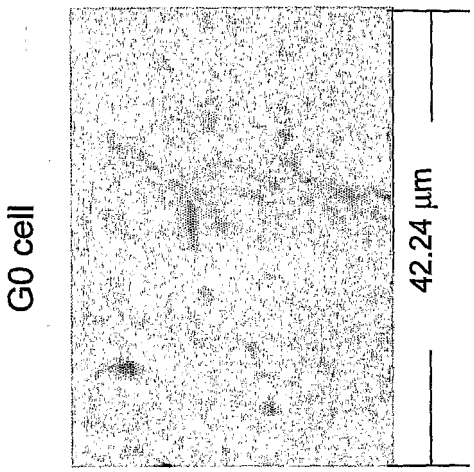

Figure 5B

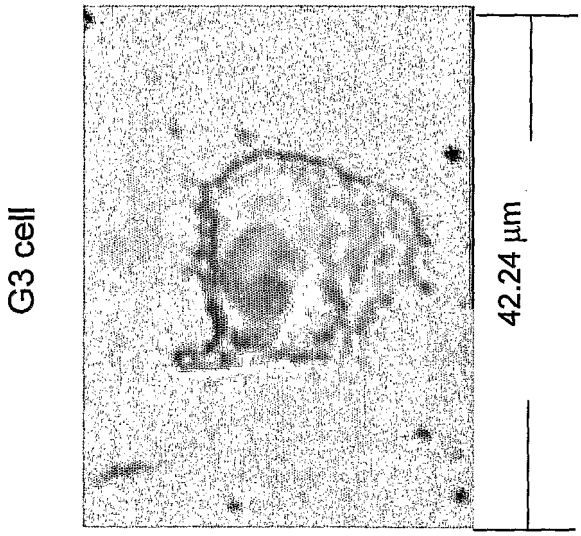

Figure 5C

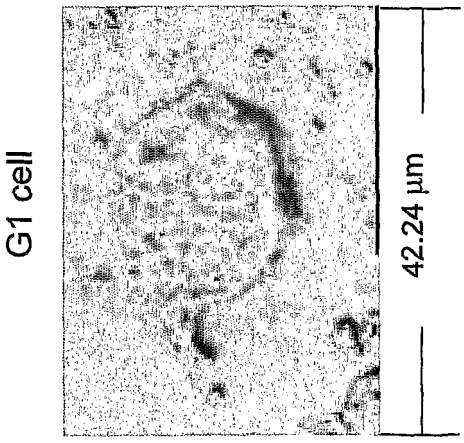

Figure 5D

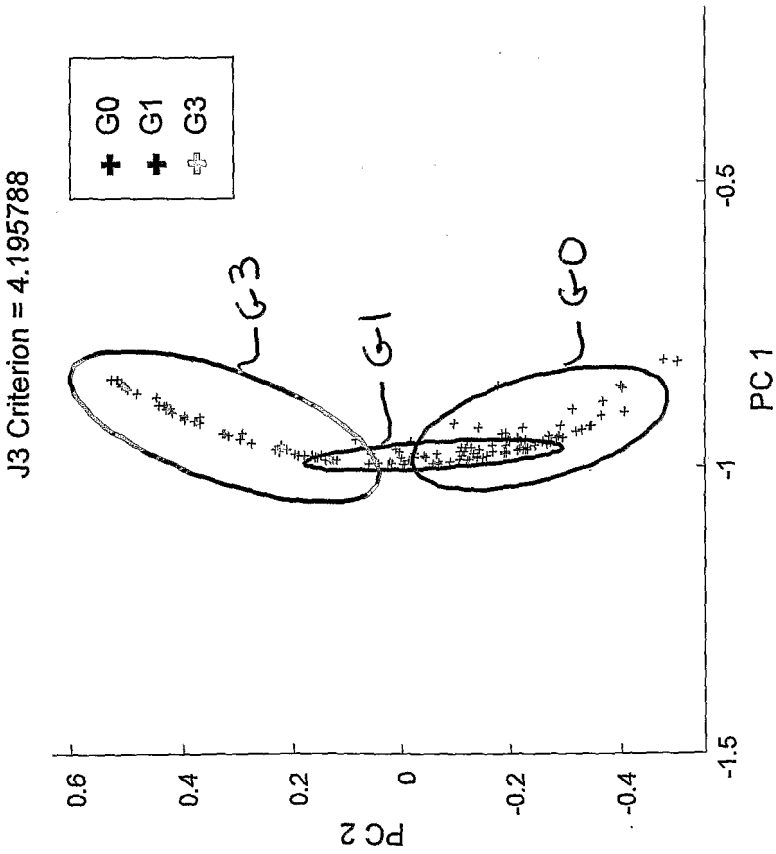
J3 Criterion = 4.195788
G0
G1
G3
G3
G1
G0
PC 2
0.6
0.4
0.2
0
-0.2
-0.4
PC 1
-0.5
-1
-1.5

Figure 6

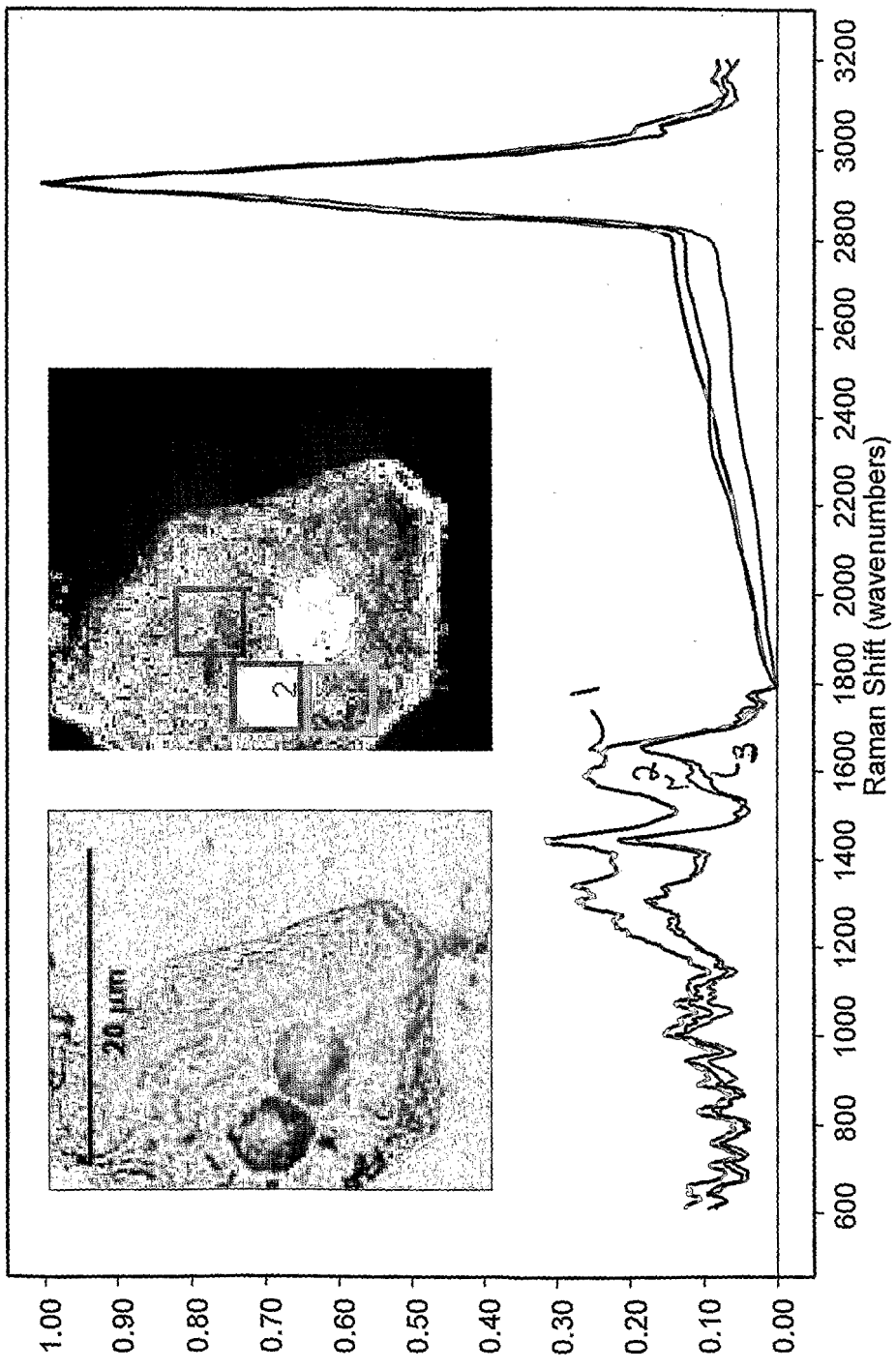
ROI 1
ROI 2
ROI 3
20 μm
1
2
3
1.00
0.90
0.80
0.70
0.60
0.50
0.40
0.30
0.20
0.10
0.00
600
800
1000
1200
1400
1600
1800
2000
2200
2400
2600
2800
3000
3200
Raman Shift (wavenumbers)

Figure 7

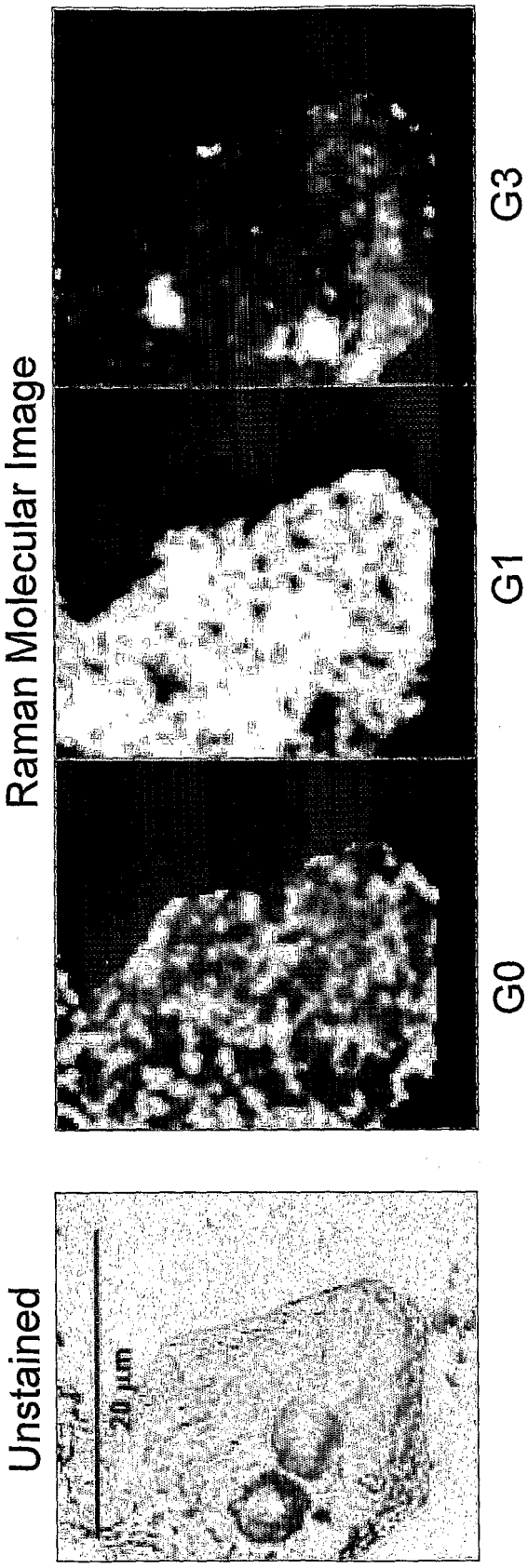

Figure 8

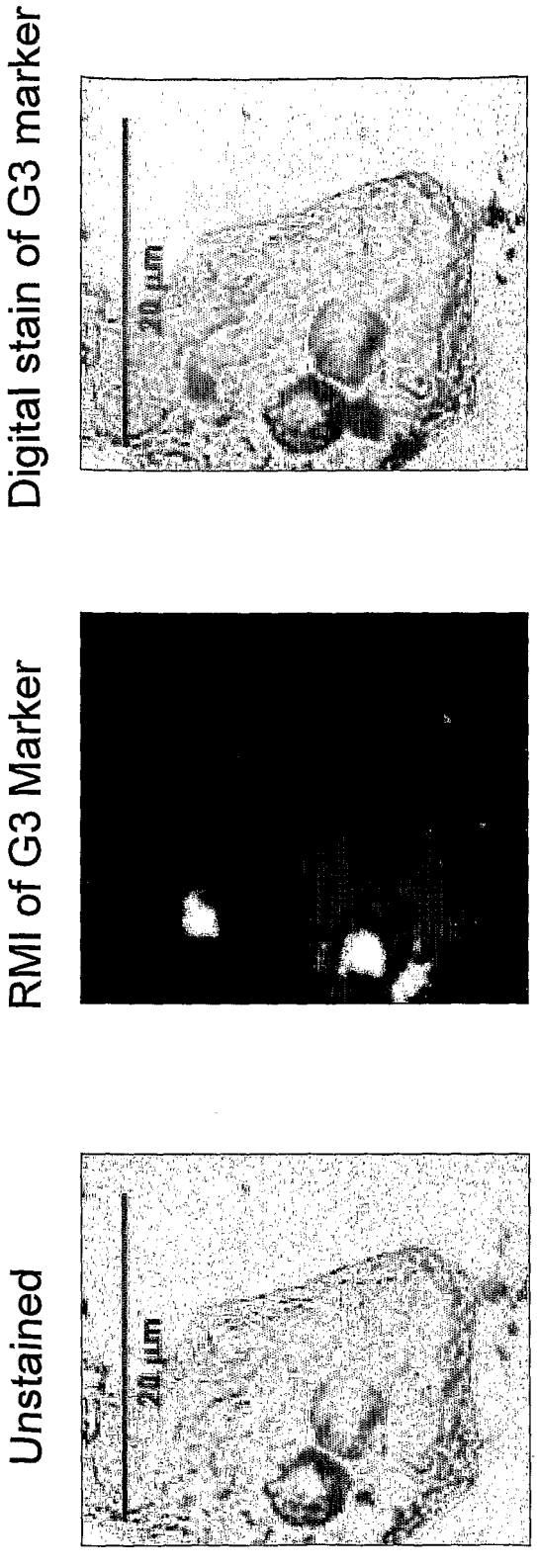
Digital stain of G3 marker
20 µm
RMI of G3 Marker
Unstained
20 µm

Figure 9

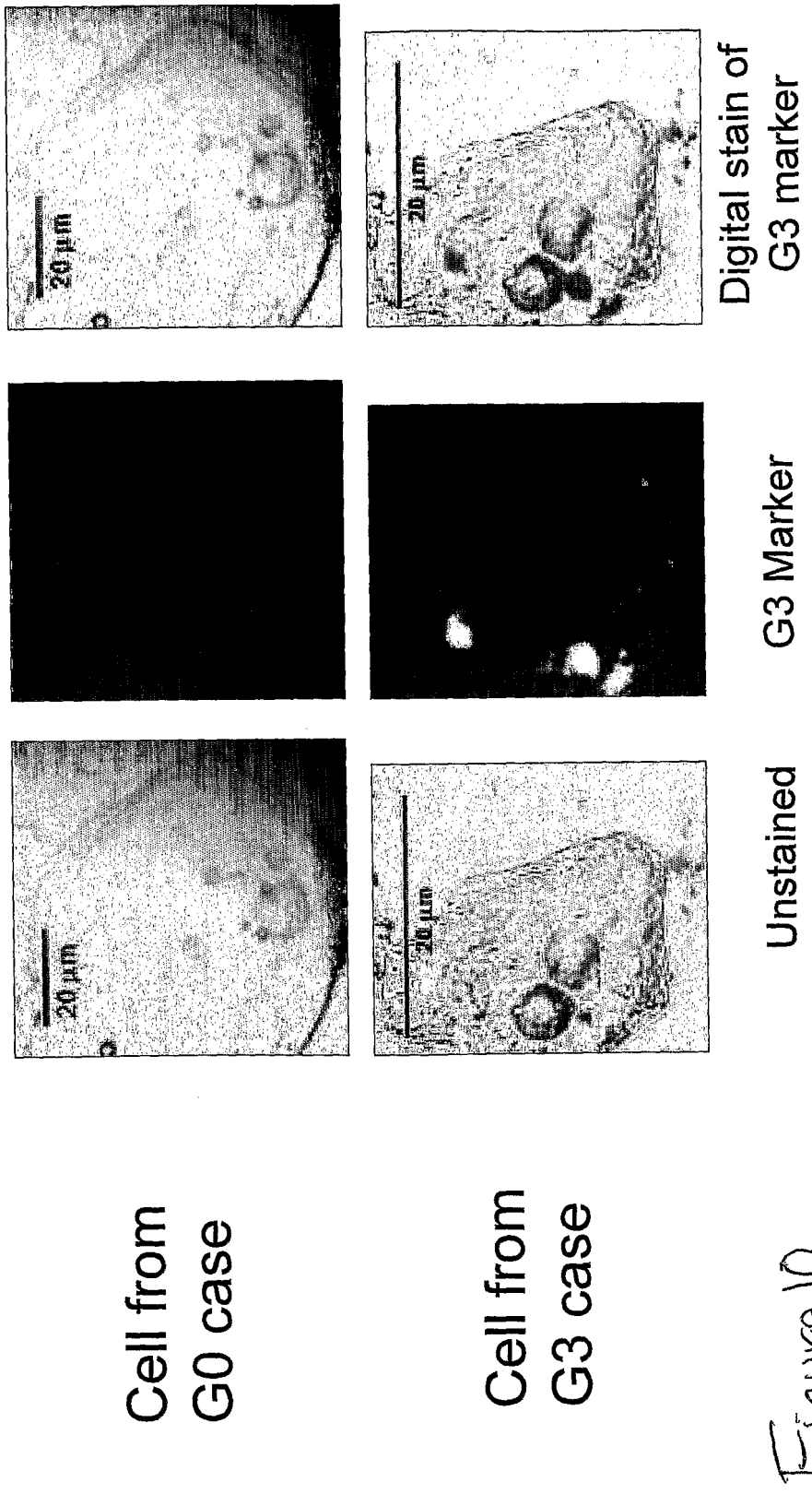
Unstained
G3 Marker
Digital stain of G3 marker
Cell from G0 case
Cell from G3 case
20 µm

Figure 10

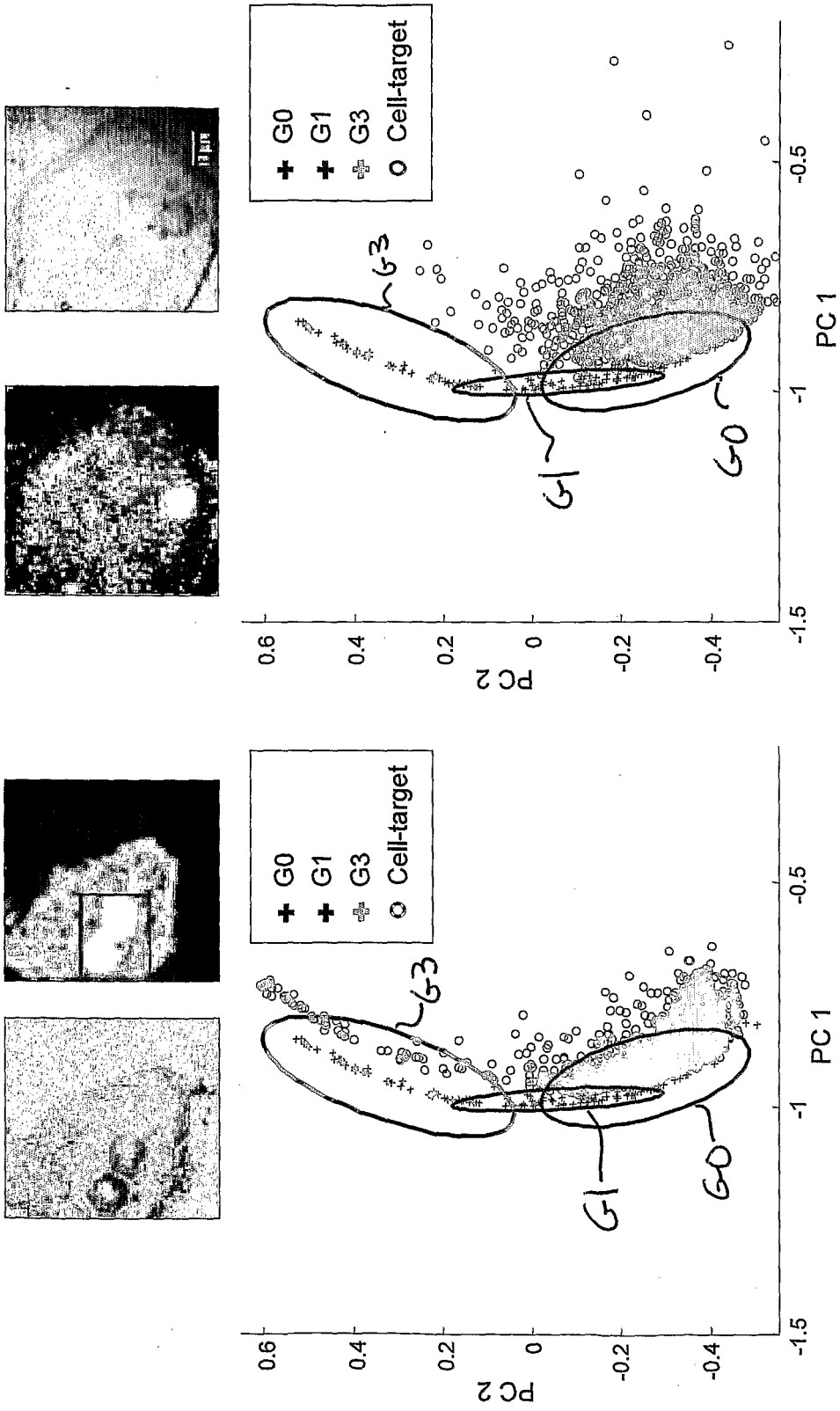

Figure 1L

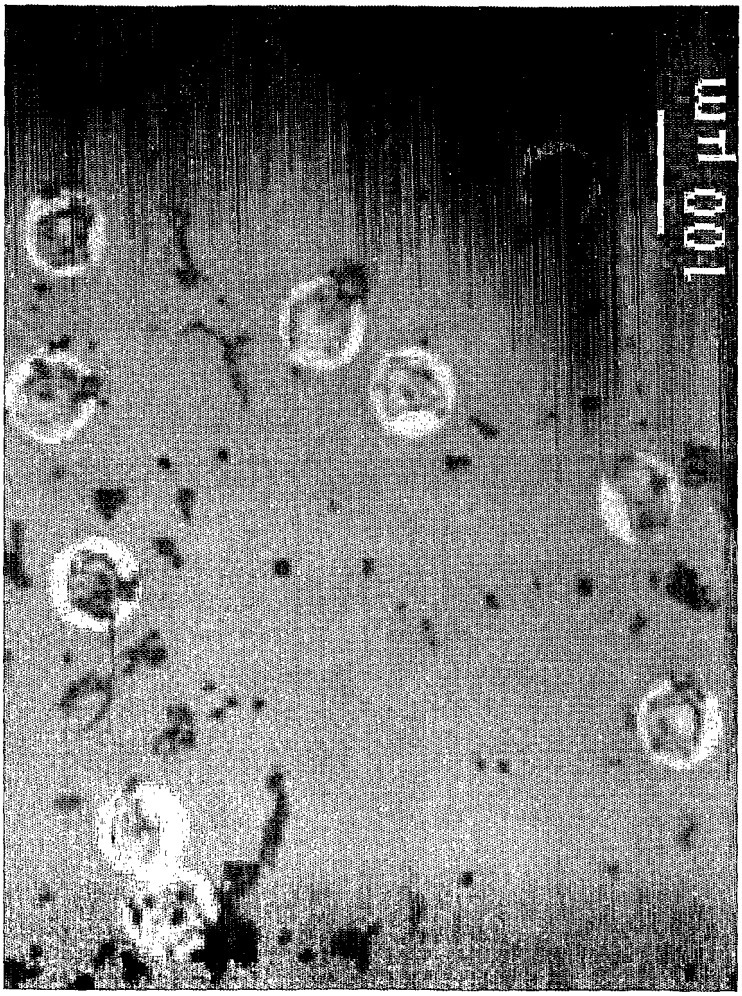

Figure 12

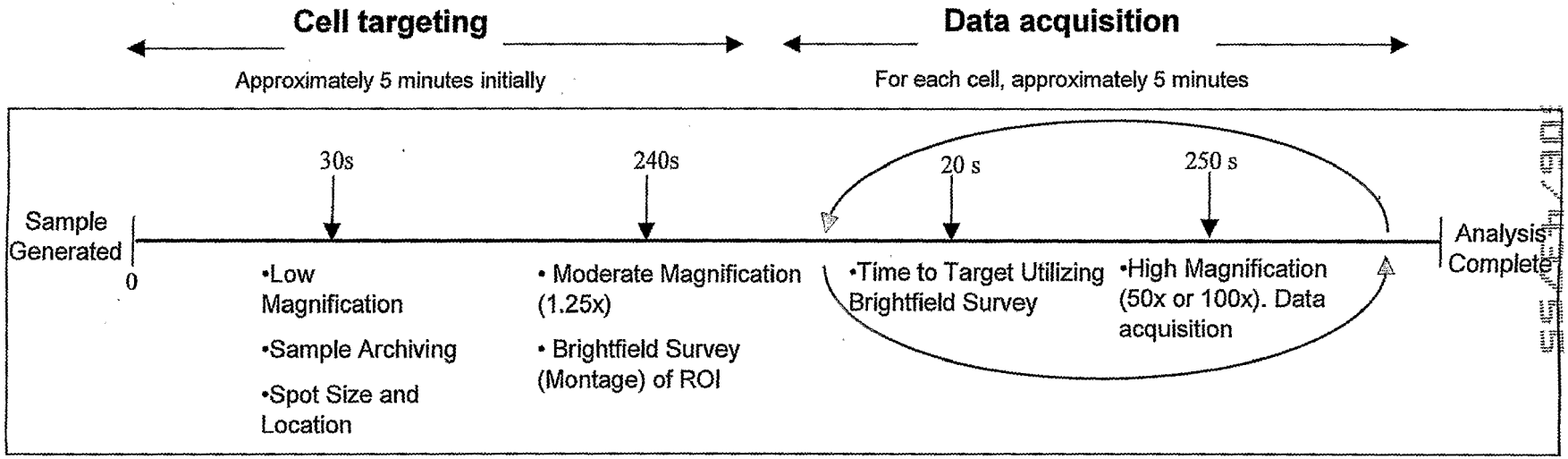

Digital Montage Image

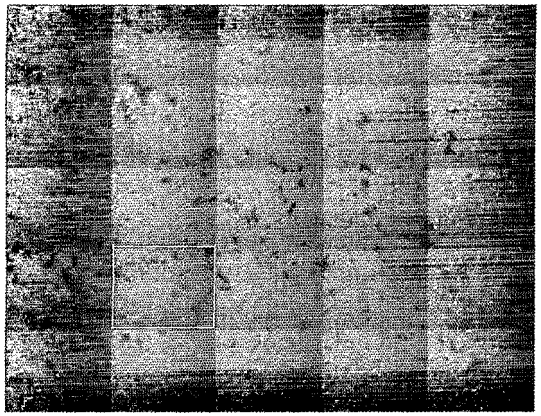

5x Brightfield

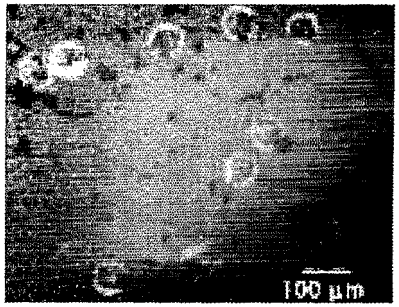

50x Brightfield image

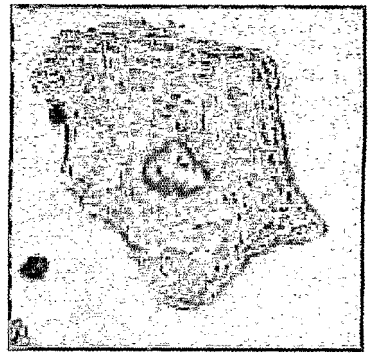

Macro Inspection	30 s
Time to Locate cells of interest	240 s
Time to select cells of interest	30 s
Time to Target initial cells	5 min
Time to Focus on a single cell	30 s
Time to Acquire spectrum and image	270 s
Time to Acquire Spectrum and image	5 min
Total time to Analyze one Sample	30 min

Figure 13

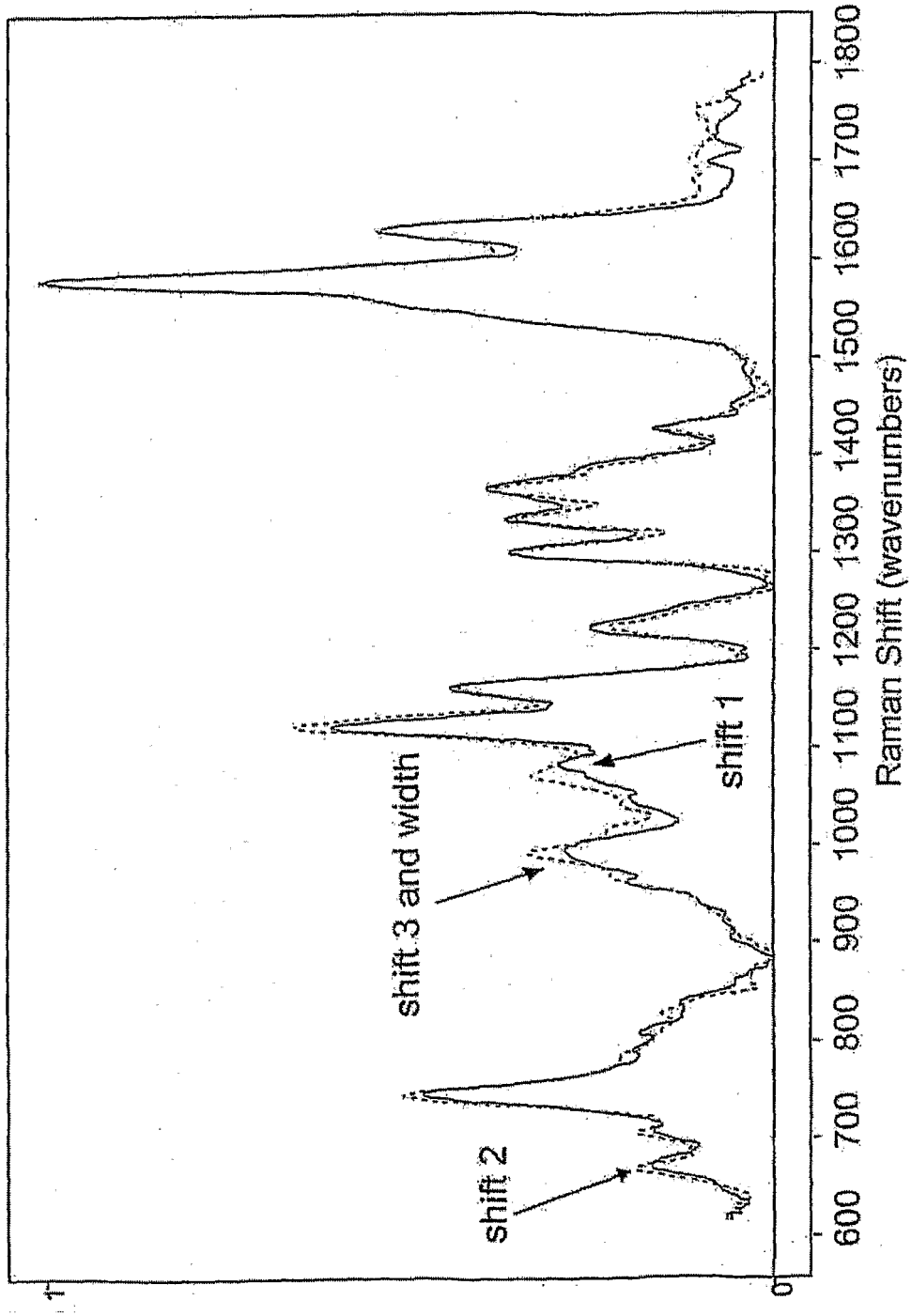
shift 2
shift 3 and width
shift 1
600
700
800
900
1000
1100
1200
1300
1400
1500
1600
1700
1800
Raman Shift (wavenumbers)
1
0

Figure 14

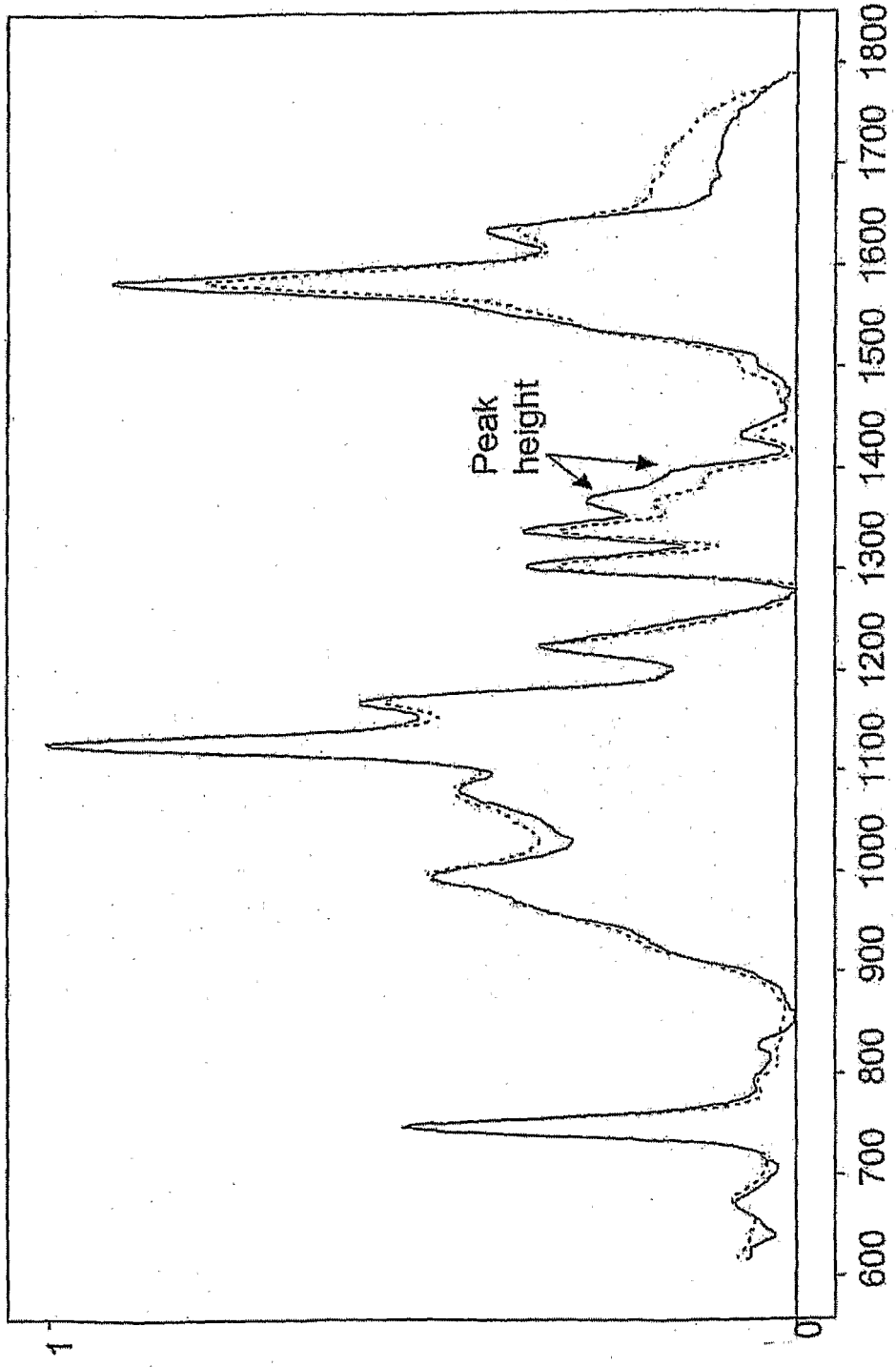
Peak height
600
700
800
900
1000
1100
1200
1300
1400
1500
1600
1700
1800
Raman Shift (wavenumbers)
1
0

Figure 15

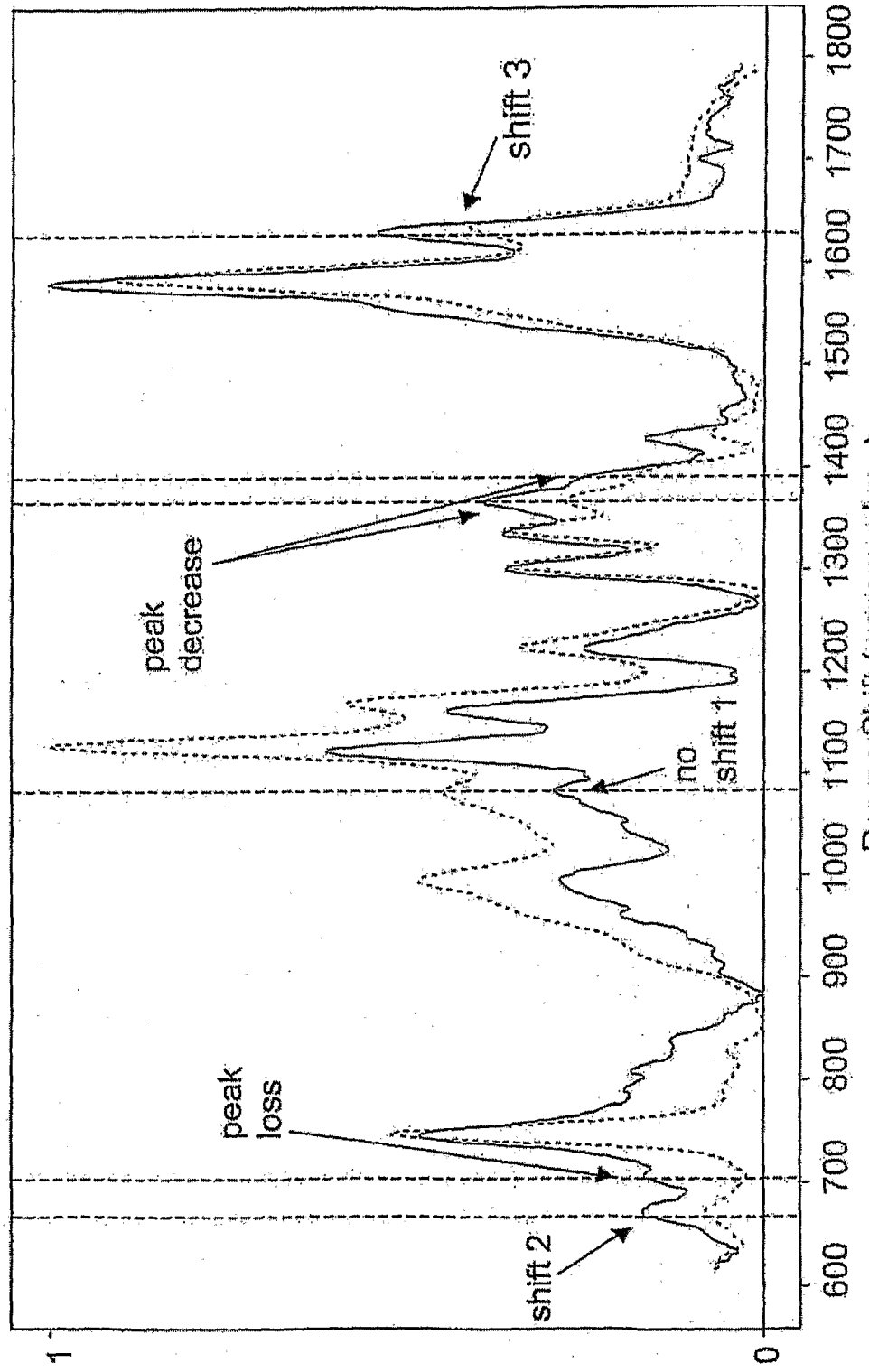
shift 3
peak decrease
no shift 1
peak loss
shift 2
1
0
600
700
800
900
1000
1100
1200
1300
1400
1500
1600
1700
1800
Raman Shift (wavenumbers)

Figure 16

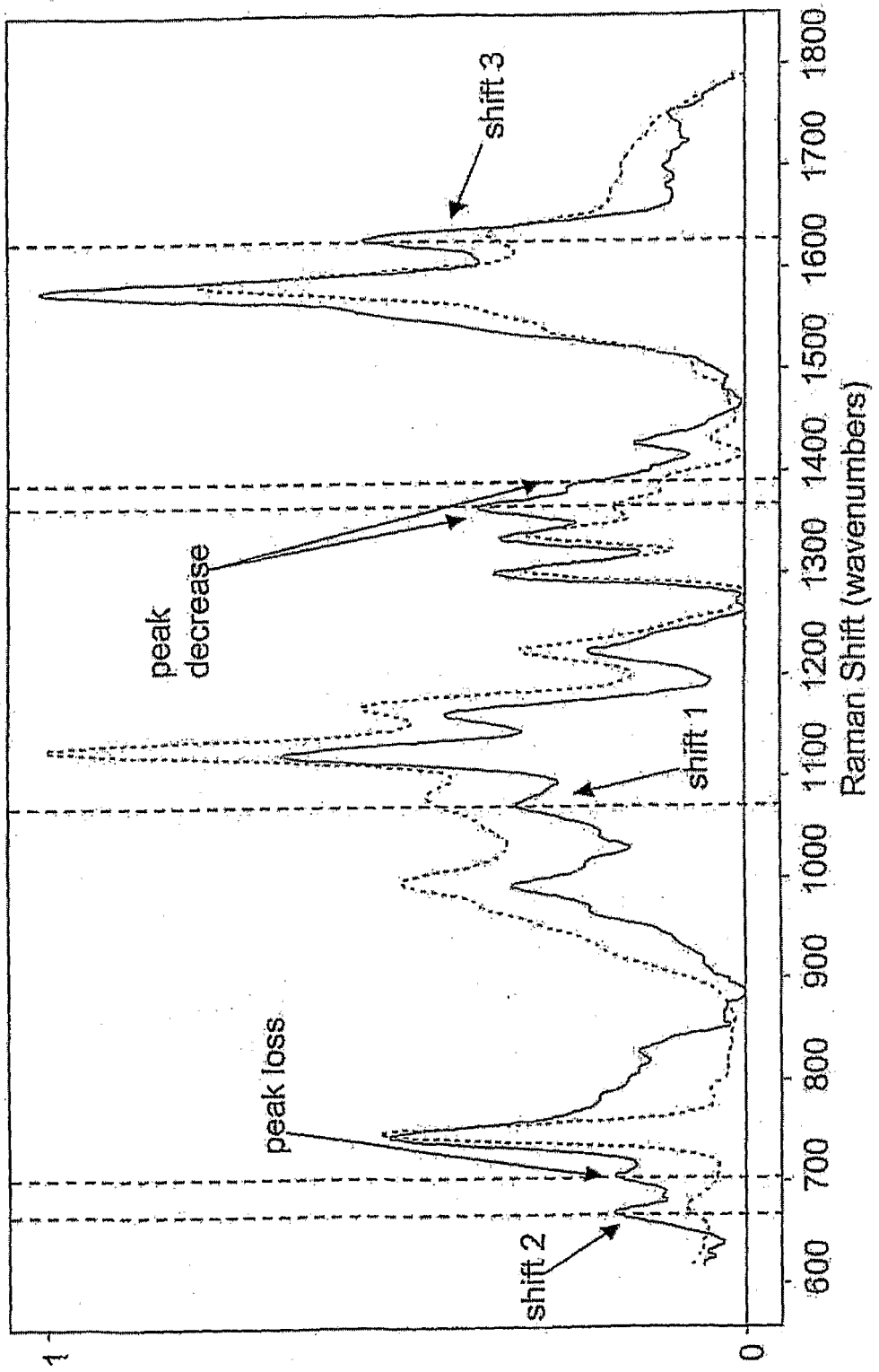
shift 3
peak decrease
shift 1
peak loss
shift 2
1
0
600
700
800
900
1000
1100
1200
1300
1400
1500
1600
1700
1800
Raman Shift (wavenumbers)

Figure 17

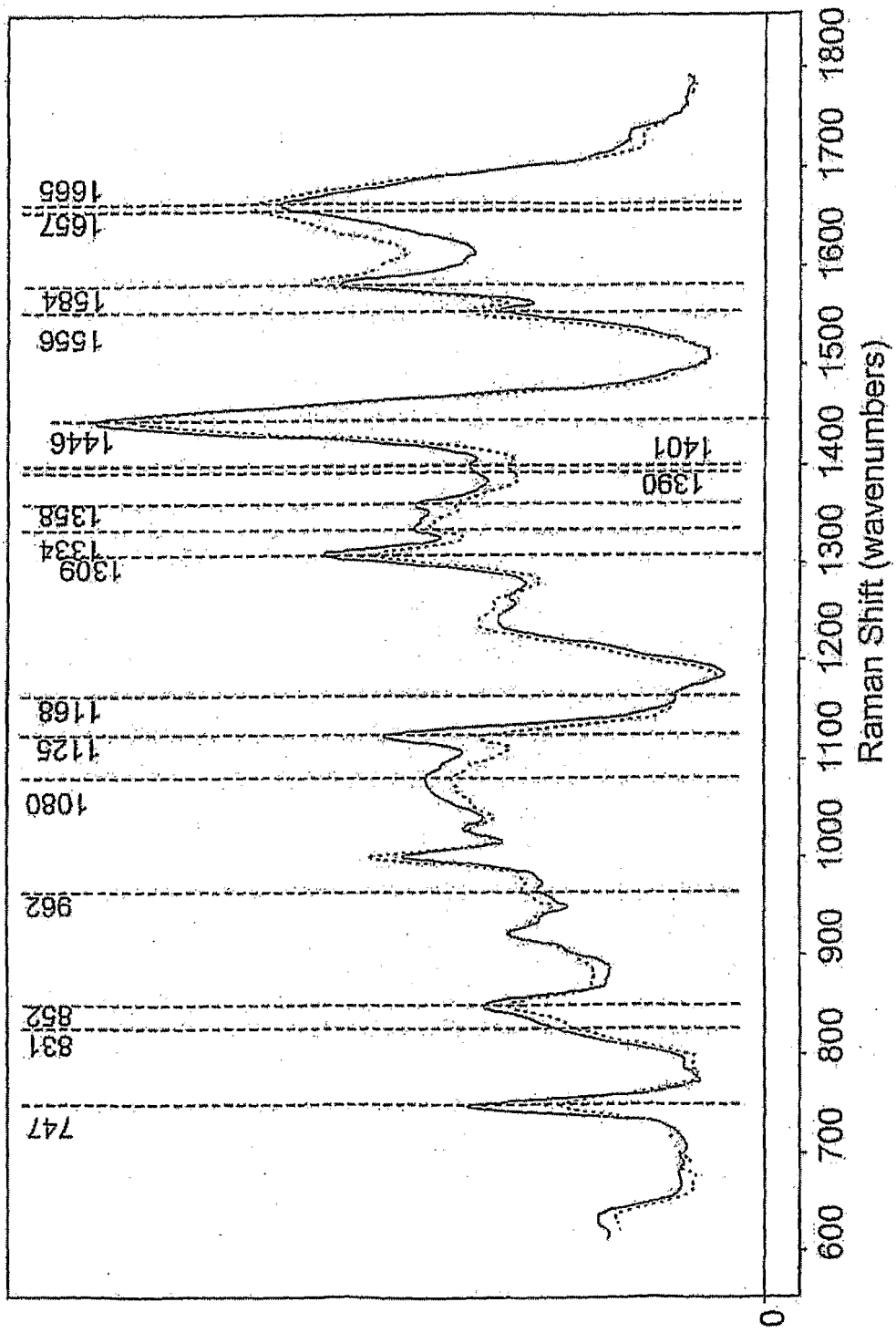
600
700
800
900
1000
1100
1200
1300
1400
1500
1600
1700
1800
Raman Shift (wavenumbers)
0
747
831
852
962
1080
1125
1168
1309
1334
1358
1390
1401
1446
1556
1584
1657
1665

Figure 18

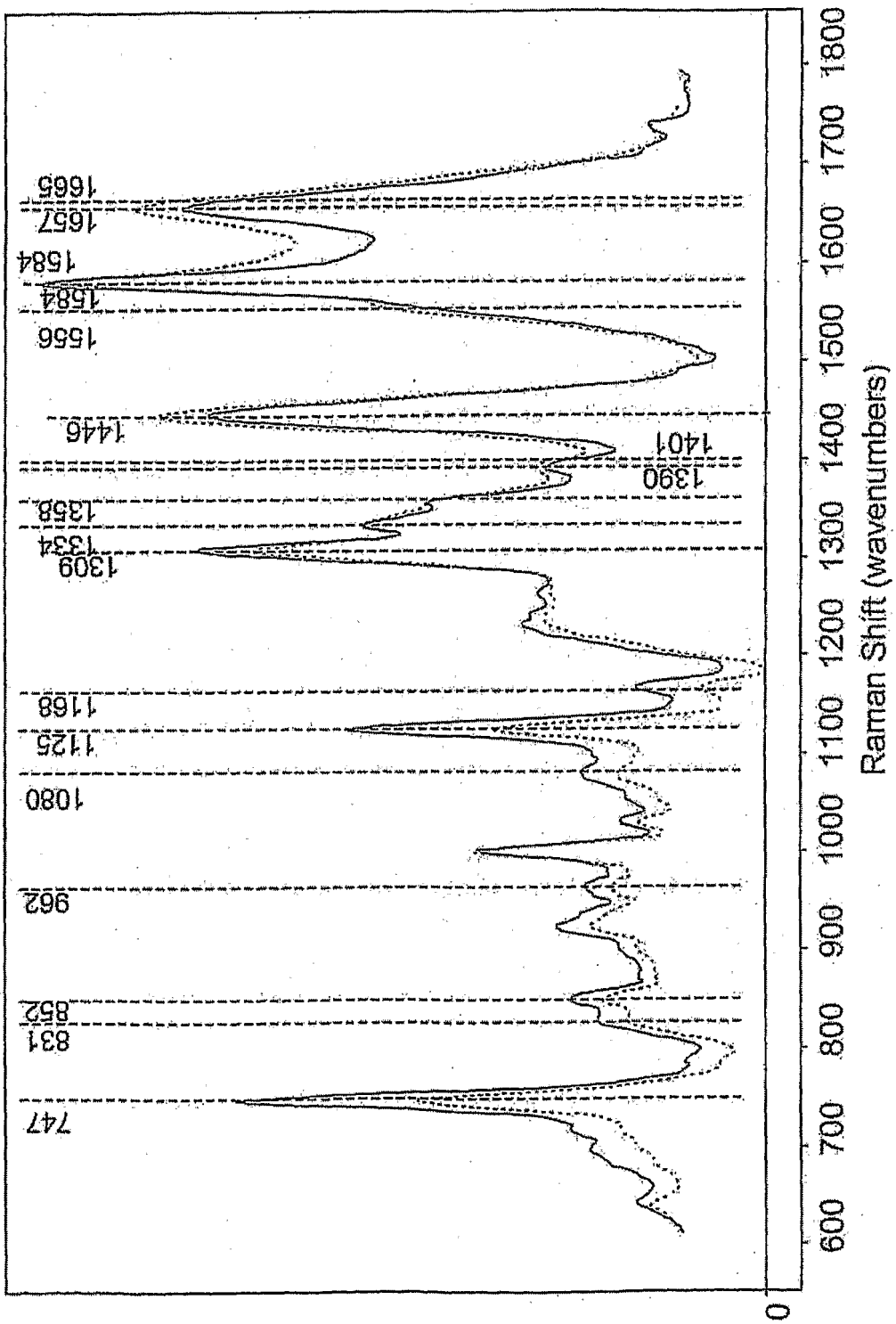
747
831
852
962
1080
1125
1168
1309
1334
1358
1390
1401
1446
1556
1584
1584
1657
1665
0
600
700
800
900
1000
1100
1200
1300
1400
1500
1600
1700
1800
Raman Shift (wavenumbers)

Figure 19

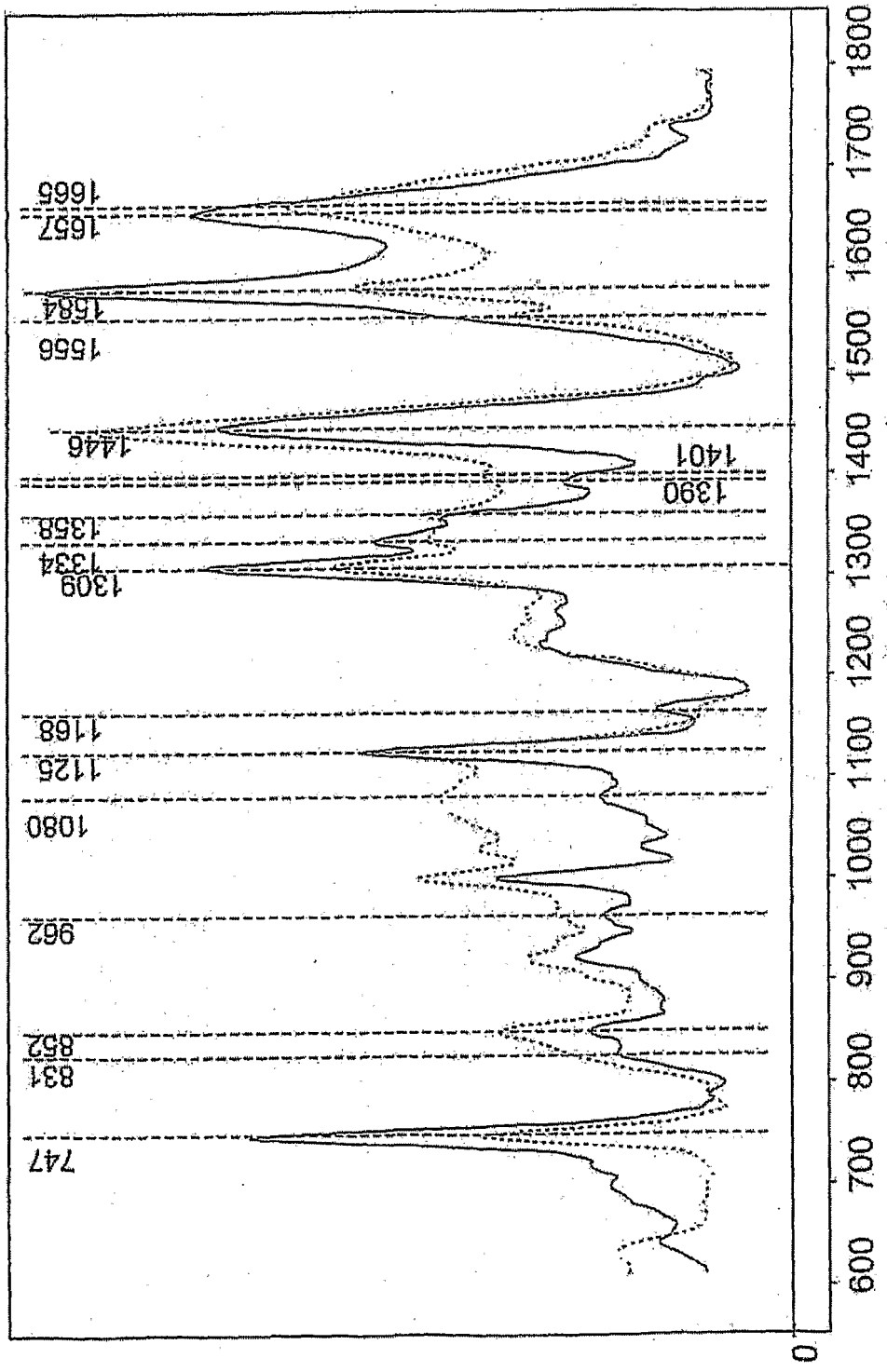
747
831
852
962
1080
1125
1168
1309
1334
1358
1390
1401
1446
1556
1584
1657
1665
0
600
700
800
900
1000
1100
1200
1300
1400
1500
1600
1700
1800
Raman Shift (wavenumbers)

Figure 20

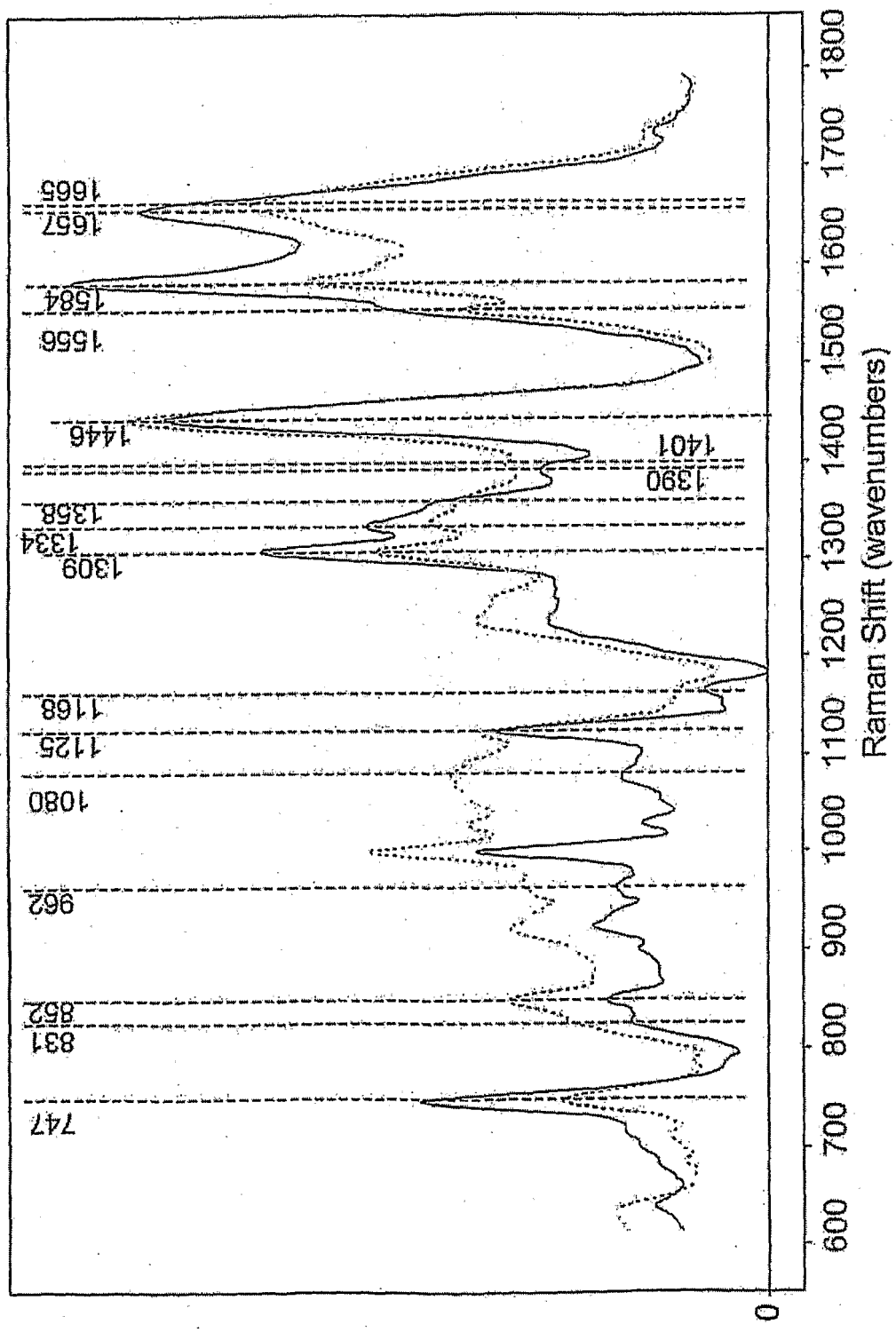
747
831
852
962
1080
1125
1168
1309
1334
1358
1390
1401
1446
1556
1584
1657
1665
0
600
700
800
900
1000
1100
1200
1300
1400
1500
1600
1700
1800
Raman Shift (wavenumbers)

Figure 21

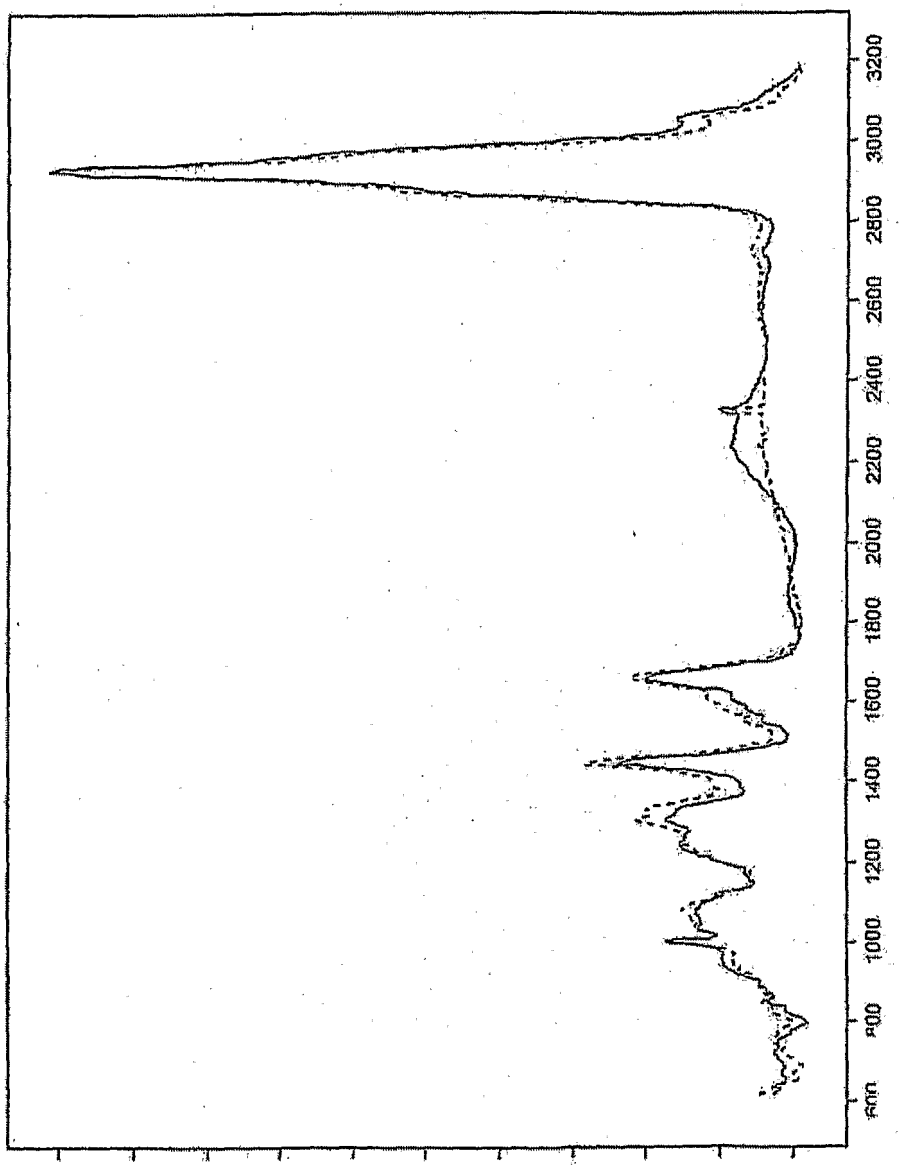
Raman shift (cm-1)
400
800
1000
1200
1400
1600
1800
2000
2200
2400
2600
2800
3000
3200

Figure 22A

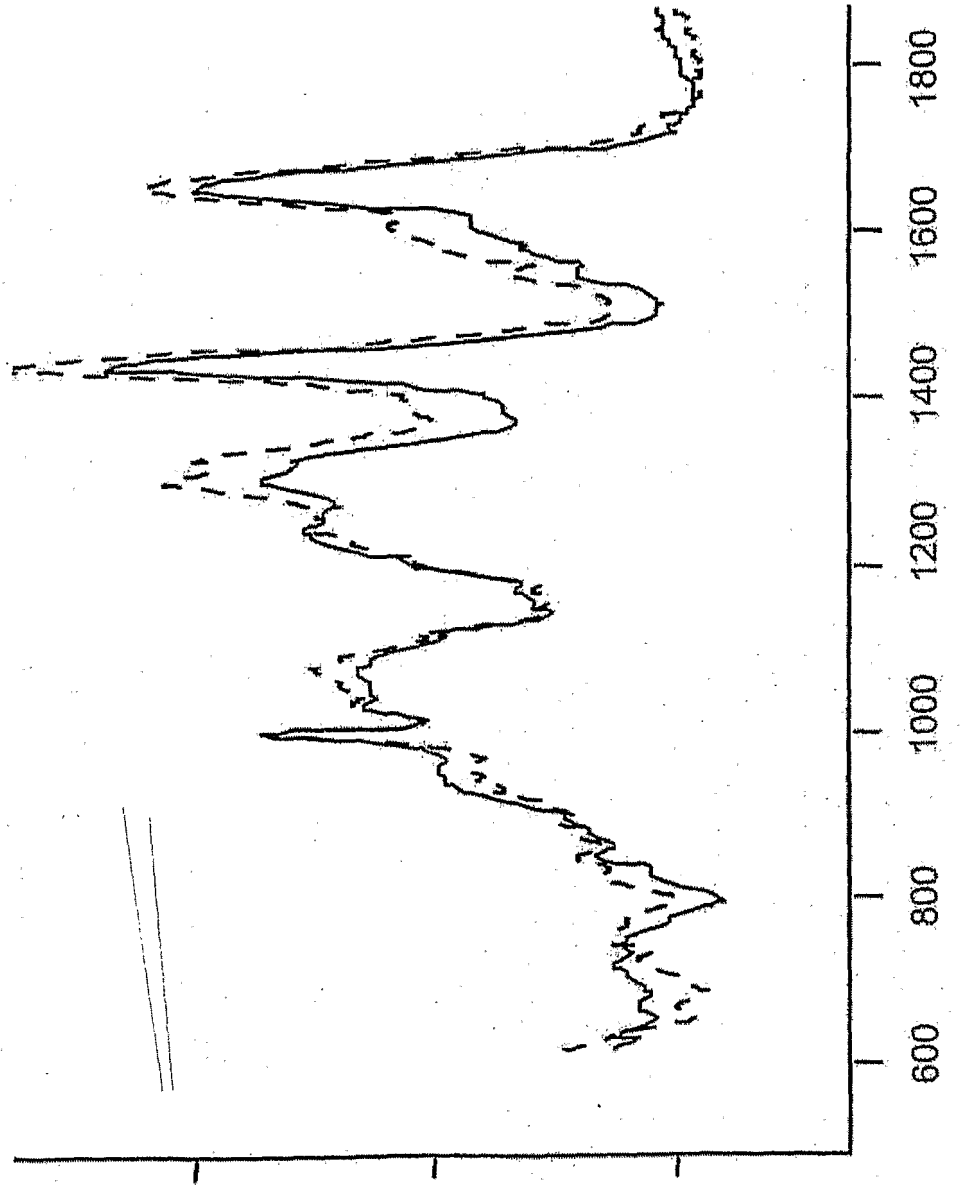

Figure 22B

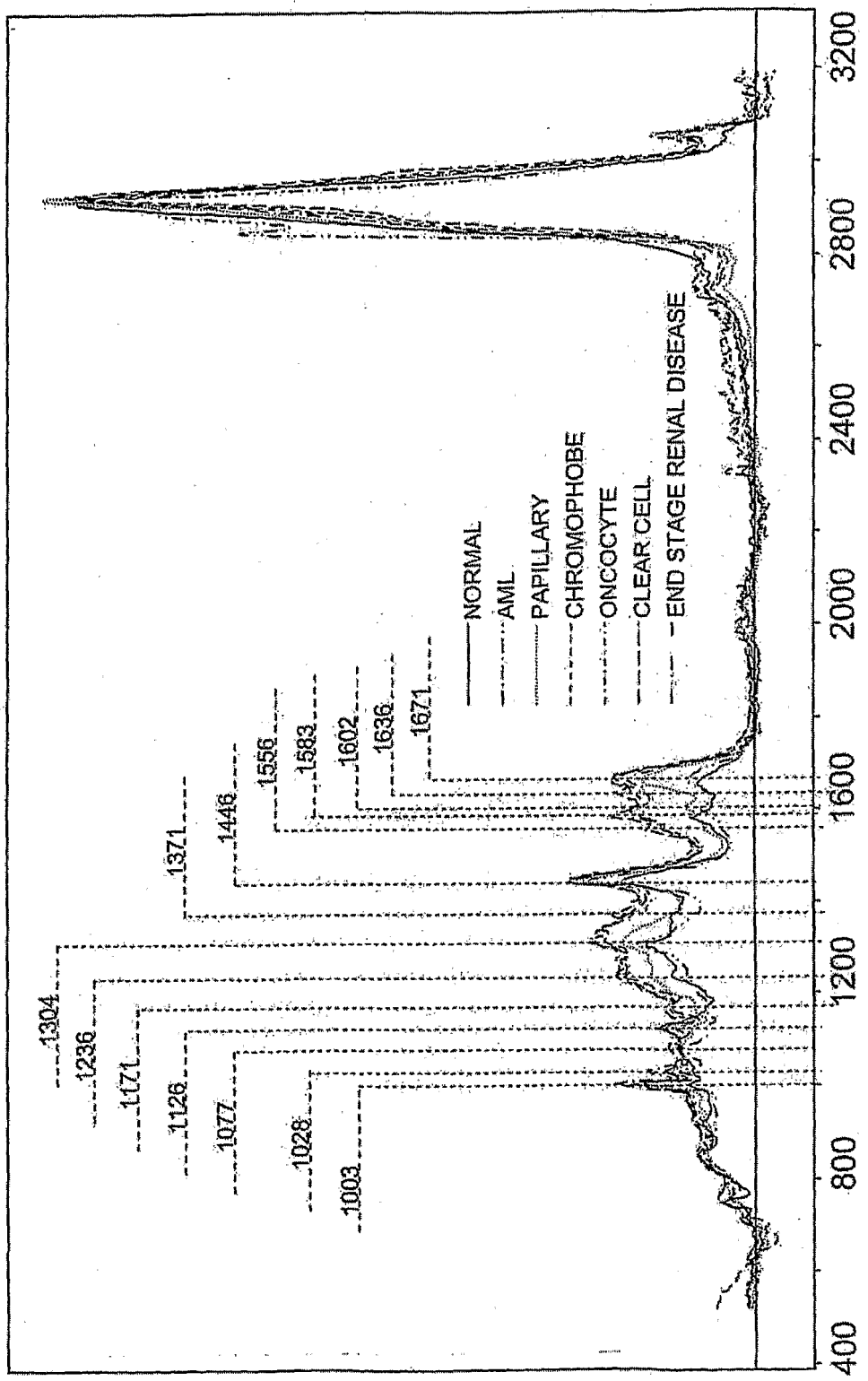
400
800
1200
1600
2000
2400
2800
3200
1304
1236
1171
1126
1077
1028
1003
1371
1446
1556
1583
1602
1636
1671
NORMAL
AML
PAPILLARY
CHROMOPHOBE
ONCOCYTE
CLEAR CELL
END STAGE RENAL DISEASE

Figure 23

专利名称(译)	用于通过拉曼光谱成像进行细胞学分析的系统和方法		
公开(公告)号	EP1945794A2	公开(公告)日	2008-07-23
申请号	EP2006837304	申请日	2006-11-09
申请(专利权)人(译)	CHEMIMAGE CORPORATION		
当前申请(专利权)人(译)	CHEMIMAGE CORPORATION		
[标]发明人	MAIER JOHN S COHEN JEFFREY MCCLELLAND LINDY STEWART SHONA		
发明人	MAIER, JOHN, S. COHEN, JEFFREY MCCLELLAND, LINDY STEWART, SHONA		
IPC分类号	C12Q1/00 C12Q1/70 C12Q1/68 G06F19/00 G01J3/44 C12Q1/28 A61K48/00 C40B30/06 C40B40/08 C40B50/06 G01N21/00 G01N33/53		
CPC分类号	G01N33/5005 G01N15/1459 G01N21/65 G01N33/574 G01N33/57407 G01N2021/656		
优先权	11/269596 2005-11-09 US 60/735062 2005-11-09 US		
外部链接	Espacenet		

摘要(译)

一种差分操纵细胞的方法和系统，其中悬浮在流体中的细胞用基本上单色的光照射。从照射的细胞获得拉曼数据集，其中数据集是疾病状态的特征。评估数据集以识别患病细胞。还获得了经照射的细胞的拉曼化学图像。基于评估和拉曼化学图像，细胞悬浮的流体被不同地操纵。将患病细胞引导至第一位置，并将其他未患病细胞引导至第二位置，作为差异操作的一部分。可以用物理应力，化学应力和生理应力处理患病细胞，然后将其返回到在照射之前从其获得患病细胞的患者。